NUMERICAL SIMULATION OF 3-D TURBULENT FLOW AND HEAT TRANSFER OVER BACKWARD FACING STEP AND THROUGH A RECTANGULAR -DUCT WITH BAFFLES

THESIS SUBMITTED FOR PARTIAL FULFILLMENT OF THE REQUIREMENT FOR AWARDING THE DEGRE OF MASTER IN MECHANICAL ENGINEERING IN FACULTY OF ENGINEERING AND TECHNOLOGY

BY

AFZAL HUSSAIN
Registration No. 140875 of 2017-18
Examination Roll No.: M4MEC19003

Under the Guidance of

Dr. Snehamoy Majumder
Professor
and
Dr. Debasish Roy
Professor
Department of Mechanical Engineering
Jadavpur University

DEPARTMENT OF MECHANICAL ENGINEERING
JADAVPUR UNIVERSITY
KOLKATA -700032
2019

Dedicated To

My Beloved Parents

Brothers

&

Sisters

FACULTY OF ENGINEERING AND TECHNOLOGY
DEPARTMENT OF MECHANICAL ENGINEERING
JADAVPUR UNIVERSITY
KOLKATA

DECLARATION OF ORIGINALITY

AND

COMPLIANCE OF ACADEMIC ETHICS

I hereby declare that this thesis contains a literature survey and original research work, By the undersigned candidate, as part of his Master of Mechanical Engineering course.

All information in this document has been obtained and presented in accordance with academic rules and ethical conduct.

I also declare that, as required by these rules and conduct, I have fully cited and referenced all material and result that are not original to this work.

Name: AFZAL HUSSAIN

Examination Roll No.: M4MEC19003

Thesis Title**: Numerical simulation of 3-D turbulent flow and heat transfer over backward facing step**

And through a rectangular duct with baffles

Signature:

Date:

FACULTY OF ENGINEERING AND TECHNOLOGY

DEPARTMENT OF MECHANICAL ENGINEERING

JADAVPUR UNIVERSITY

KOLKATA

CERTIFICATE OF RECOMMENDATION

We hereby recommend that this thesis under our supervision by Mr. Afzal Hussain, entitled, "NUMERICAL SIMULATION OF 3-D TURBULENT FLOW AND HEAT TRANSFER OVER BACKWARD FACING STEP AND THROUGH A RECTANGULAR DUCT WITH BAFFLES" be accepted in partial fulfilment of the requirements for awarding the degree of Master of Mechanical Engineering under Department of Mechanical Engineering of Jadavpur University.

…… ……..

Dr. Snehamoy Majumder
Thesis Adviser
Department of Mechanical Engineering
Jadavpur University, Kolkata

Dr. Debasish Roy
Thesis Adviser
Department of Mechanical Engineering
Jadavpur University, kolkata

……

Dr. Goutam Majumdar
Professor and Head
Department of Mechanical Engineering
Jadavpur University, Kolkata

……

Prof. Chiranjib Bhattacharjee
Dean
Faculty Council of Engineering and Technology
Jadavpur University, Kolkata

FACULTY OF ENGINEERING AND TECHNOLOGY
DEPARTMENT OF MECHANICAL ENGINEERING
JADAVPUR UNIVERSITY KOLKATA

CERTIFICATE OF APPROVAL

The foregoing thesis entitled "NUMERICAL SIMULATION OF 3-D TURBULENT FLOW AND HEAT TRANSFER OVER BACKWARD FACING STEP AND THROUGH A RECTANGULAR DUCT WITH BAFFLES" is Hereby approved a credible study of Fluid Mechanics and Hydraulics Engineering and presented in a manner satisfactory to warrant its acceptance as a pre-requisite to the degree for which it has been submitted. It is understood that by this approval, the undersigned, do not necessarily endorse or approve the thesis only for the purpose for which it is submitted.

Committee of the final examination for evaluation of the thesis

…….. ……..

…… ……

Signature of Examiners

ACKNOWLEDGMENT

This preface is to express the gratitude of the author to all those individuals who with their Generous co-operation guided him in every aspect to make the thesis work successful.

In presenting this thesis report, the author would like to express his sincere gratitude And indebtedness to his Thesis Advisor **Dr. Snehamoy Majumder**, and **Dr. Debasish Roy** Department of Mechanical Engineering, Jadavpur University, Kolkata for his valuable suggestion And Requisite guidance in various aspects of this project work. It was great pressure for him to Work under his supervision.

The author is thankful to **Prof. Goutam Majumdar**, Head of Mechanical Engineering Department, Jadavpur University and **Prof. Chiranjib Bhattacharjee**, Dean Faculty of Council of Engineering and Technology, Jadavpur University for their support in academic matters. The Author pays his sensible thanks to all the faculties of Fluid Mechanics and Hydraulics specialization For their supporting needs.

Also, the author would like to thank all faculty members and research scholars Associated with the project for their valuable inputs and continued support.

The author would also like to thank all his other lab mates -Saukrit Kumar Chandra, Sohag Sutar and Sobhan Pandit for their co-operation, help, motivation and who supported him in writing, and incented him to strive towards his goal –Aurangzeb Rashid and Sourav Kumar Dey. apart from this, he would also be thankful for his juniors specially Koustav, Sandeep and Anirban.

Lastly, the author would like to thank all who have assisted him in his endeavor.

Date: 22/05/2019

With regards,
Afzal Hussain

Jadavpur University,
Kolkata-700032

ABSTRACT

This study presents the numerical simulations on the turbulent fluid flow and heat transfer characteristics for the rectangular channel over the backward facing step, and with variable baffles heights which are arranged on top and bottom channel walls normal to the direction of flow. Prediction of reattachment length of separated shear layers in a low Reynolds number turbulent flow is a challenging task to evaluate the capabilities of different turbulence model. Physical significances of backward facing step and its industrial applications discussed. To predict the velocity profile, pressure distribution, pressure coefficient, wall shear stress, skin friction coefficient, temperature profile, surface Nusselt number, and turbulence kinetic energy flow of water. The turbulence governing differential equations which describe the flow was approximated by the finite volume method for three-dimensional, with the power-law scheme and the standard k-Ɛ turbulence model associated with the standard wall function to describe the turbulence structure, by using a commercial software package (FLUENT). The velocity and pressure terms of momentum equations are solved by a SIMPLE (semi-implicit method for pressure-linked equation) method. Flow analysis of a backward facing step is carried out at different expansion ratios 1.33,2 and 4. And results are also compared a wide range of Reynolds numbers 66, 660, 6600 and 6.6*10^5. For the study of the duct with baffles, the effect of baffles heights, baffle numbers, baffles arrangement and baffles thickness on the flow and heat transfer characteristics is investigated. The obtained computed results show that the reattachment length increases with an increase in expansion ratio and also with an increase in Reynolds number. The boundary separation and recirculation regions are significantly affected by the height, thickness, and arrangement of baffles plates.

CONTENTS

LIST OF FIGURES

NOMENCLATURE

2-D	Two dimensional
3-D	Three dimensional
t	Time
u, v, and w	velocity component in x, y, and z-direction respectively
$\bar{u}$, $\bar{v}$, and $\bar{w}$	Mean velocity component in x, y, and z-direction respectively
u', v', and w'	Fluctuating velocity component in x, y, and z direction respectively
$\bar{p}$	Modified mean pressure
$\bar{T}$, T'	Mean and fluctuating temperature respectively
σ_t	Turbulent Prandtl number
ϑ , ϑ_t	Kinematic and eddy viscosity respectively
α , α_t	Thermal and eddy thermal diffusivity
$\tau_{xx,}\tau_{xy}, \tau_{xz,}\tau_{yy}, \tau_{yz}\tau_{zz}$	Component of Reynolds stress
k	Turbulent kinetic energy
ϵ	Turbulent dissipation rate
P	Production of turbulent kinetic
C_μ ,$C_{\epsilon 1}$, and $C_{\epsilon 2}$	Model Constants
Re	Reynolds No.
Nu	Nusselt No.
h	Heat transfer coefficient
C_P	Pressure coefficient
D_h	Hydraulic diameter
q''	Heat flux
ρ	Density
∅	Any physical quantities
Γ	Diffusion coefficient
p^* , p'	Guessed pressure and pressure correction
σ_k	Turbulent Prandtl number for k
σ_ϵ	Turbulent Prandtl number for ϵ
S_k, S_ϵ	Source term
ER	Expansion ratio

CHAPTER 1

INTRODUCTION

Chapter 1: Introduction

The topic under investigation is a very important one as flow over a backward facing step forms the basis of many real flow situations. It is often used as test cases for improvement of numerical schemes and is classical in applied aerodynamics. Turbulent reattachment occurs in most of the engineering applications, likes sudden enlargements in pipe and ducts, ignition and stabilization of the flame in scramjet engine, prediction of wall heat transfer in PCB circuits and multiphase flow phenomenon in piston engines. Overall performance of many devices such as diffusers, turbine blades, micro electrical and mechanical devices (MEMS), leading- edge vortex control of aircraft by using MEMS transducers and of aerodynamic bodies is greatly influenced by the flow separation. Experimental data for backward -facing step is present in the literature for a wide range of Reynolds number and at different expansion ratios. The flow separation in ducts with baffles has many engineering applications for example shell- and -tube heat exchangers with baffles, internally cooled turbine blades, cooling panels used in scramjet engine inlet, and air-cooled solar collectors. Augmentation techniques usually employ baffles attached to the heated surface so as to provide an additional heat transfer surface area and to promote turbulence. The flow over baffles has different fluid flow and heat transfer characteristics. The presence of these baffle cause the flow to separate, reattach and create reverse flow. If the baffles are staggered, they will cause the flow to deflect and impinge upon the opposite walls, increasing the washing action. Recently many investigations have been focused on the baffled-walled channel heat exchangers. Most of the study discussed optimal baffle geometry that enhances heat transfer performance for a given pumping power or flow rate. In the experimental efforts, Tanaswa et al.[1] measured the heat transfer coefficient for turbulent flows in a channel with perforated plate arrays mounted on two opposite walls in an in-line fashion by resistance heating method and thermocouple technique. Their results showed that surfaces with perforated plate arrays provided better thermal performances at a constant pumping power than those with slit plate arrays and fence arrays. Cheng and Huang [2] investigated the case where the transverse baffles are not symmetrically placed. Their results have indicated that the relative position of the baffles arrays in an influential factor on the flow field, especially for baffles with large height. Moller et al. [3] experimentally reported velocity and wall- pressure fluctuation in turbulent flow through a simulated tube bank with a square baffle plate arrangement. Habib et al. [4] reported turbulent flow and heat transfer through a duct with baffle plates, he concluded that the heat flux was uniform on the upper and lower walls. The results show that the local and average nusselt numbers increase with an increase in Reynolds numbers. Also, the pressure drop increased as baffle height increases. Demartini et al. [5] used experimental techniques to investigate the pressure drop and streamwise velocity distribution of the turbulent flow with baffles in the channel. Gua and Anand [6] have examined three- dimensional heat transfer in a channel with a single baffle in the entrance region. Founti and Whitelaw [7] used LDA to deduce the velocity field in an axisymmetric heat exchangers with baffles on the shell-side surface. The similar distribution of the mean -flow velocity and turbulence intensity were found after two sets of baffles from the channel entrance. Later Berner et al. [8] Berner et al. [9] obtained experimental

results of mean- velocity and turbulence- distribution in the flow around segmented baffles. Experimental investigation of characteristics of turbulent flow and heat transfer inside the periodic cell formed between segmented baffle staggered in a rectangular duct was studied by Habib et al. [10] the experimental results indicate that the pressure loss increased as the baffle height did. For a given flow rate, local and average heat transfer parameter increases with increasing Reynolds number and baffle height. Numerical prediction of the flow and heat transfer with staggered fins were investigated by Webb and Ramadhayani [11], Kelker and Patankar [12], and Habib et al.[13]. Corrugated walls with or without fins may be used as passages in heat exchangers for the purpose of heat transfer augmentation presented by Amano et al. [14]. Most of the numerical research involving obstructions have been limited to two-dimensional cases. The hydraulic and thermal effects of placing normal baffles inside a three-dimensional channel were studied numerically by Lopez et al.[15]. A numerical investigation of laminar forced convective heat transfer was performed in a three-dimensional channel with baffles in a uniform heat flux was applied to the top and bottom wall, and the side wall was considered adiabatic. They presented that three-dimensional effect on the friction factor of a channel wall with a unity aspect ratio and a blockage ratio of 0.5 increased with an increase in Re. S. V Patankar and EM Sparrow [16] solved numerically the problem of fluid flow and heat transfer in a fully developed heat exchangers. This one was equipped by isothermal plate placed transversely to the direction of flow. They found solid plates caused strong recirculation zones in the flow field. They concluded that nusselt number depends strongly on the Reynolds number, and it is higher in the case of fully developed than that of laminar flow regime. Rajendra et al.[17] conducted an experimental work on the study of heat transfer and friction in a rectangular duct with baffles (solid or perforated) attached to one of the broad walls. Ahmet et al.[18] examined the effect of geometric parameters on the study of turbulent flow passing through a pipe with baffles. The effect of orientation and the distance between nine baffles on the improvement of heat transfer was highlighted in this work. Molki et al. [19] conducted an experimental investigation to evaluate heat transfer and pressure losses in a rectangular channel with baffles. Nasiruddin and Siddiqui [20] studied numerically effects of baffles on forced convection flow in heat exchangers, the effect of size and inclination angle of baffles were detailed. They considered three different arrangement of baffles. They found that increasing the size of the vertical baffle substantially improves the nusselt number. However, the pressure loss is also important. For the case of inclined baffles, they found that the nusselt number is maximum for the angle of inclination directed downstream of the baffle, with a minimum of pressure loss. More recently, Saim et al.[21] presented a numerical study of the dynamic behavior of turbulent air flow in a horizontal channel with transverse baffles. They adopted numerical finite volume method based on the SIMPLE algorithm and chose, the k-Ɛ model for treatment of turbulence. Results obtained for a case of such type, at low Reynolds number, were presented in terms of velocity and temperature fields. They found the existence of a relatively strong recirculation zone near the baffles. The eddy zones are responsible for local variation of nusselts numbers along with the baffles and wall.

CHAPTER 2

LITERATURE REVIEW AND OBJECTIVE OF THE PRESENT WORK

Chapter 2 : Literature Review

R. M. Inman [22] They have done an analysis to estimate convection heat transfer to slug flow in a rectangular channel with a uniform heat source in the field for an understanding of turbulent liquid metal heat transfer in rectangular channels with heat generation in the fluid stream. The results are applied in the thermal entrance as well as in the fully developed region and used for estimating local heat transfer characteristics when the Peclet number is approximately 100.

B. E. Launder *et al*. [23] Presents the outcome of experimental research on turbulence induced secondary flows in a square section ducts. The main emphasis of the experiments has been on the measurement of the secondary flows in a duct with an equally roughed surface.The resultant profiles for smooth and rough surfaces are the same, within the precision of measurement.

A. Melling *et al.* [24] They have done a detailed experimental study of developing turbulent flow in a rectangular duct was made using a laser-Doppler anemometer. The contours of axial mean velocity turbulence intensity were measured in the developing flow. The symmetry of the present flow seems to be better than that of previous measurements and the range of measurements is more extensive and the laser-Doppler anemometer has a potential advantage in the measurement of secondary velocity.

A. O. Demuren *et al* [25] They have done experiments on and calculations methods for flow in straight non-circular ducts involving turbulence-driven secondary motion is reviewed. The resulting set of equations is solved with a forward-marching numerical procedure for three-dimensional shear layers. The main features of the mean flow and turbulence quantities are stimulated realistically by the model proposed by the Naot and Rodi(1982).

J. P. Doormaal *et al* [26] Used a SIMPLE method of Patankar and Spalding to solve the problems regarding incompressible flows. This paper shows several modifications to the method which helps to simplify its implementation and reduce solution costs.

M. Molki [27] In his experiment investigated the heat transfer in rectangular ducts with repeated baffle blockages. The arrangements of the baffles are kept in a staggered fashion with fixed axial spacing. The presence of baffles enhances the heat transfer coefficients which are evaluated in the periodic fully developed and entrance region of the duct. At the end, the experimental data is used to obtain the thermal performance of the duct.

Ravi K. *et al.* [28] Analysed the fully developed flow in a straight duct of the square cross section by using the LES technique based upon the mixed spectral finite difference method of Reynolds number 360. This study predicts the existence of secondary flows and it is observed that the Reynolds normal and shear stresses equally contribute to the production of mean streamwise vorticity.

Z. Yang *et al.* [29] Used the $\kappa-\varepsilon$ model for near- wall turbulent flows. In this model, the eddy viscosity is characterized by a turbulent time scale and turbulent velocity scale respectively. The damping function in eddy viscosity is the function of $R_y = K^{1/2}\frac{y}{\nu}$ instead of y^+ though the same model constants are adopted as standard $\kappa-\varepsilon$ model.

A. Husser *et al.* [30] In a study with a time splitting method by using numerical approach to integrate the three-dimensional, incompressible Navier-stokes equations using spectral/high-order finite difference discretization on a staggered mesh; results from the presents study furnish the details of the corner effects and near- wall effects in this complex turbulent flows.

David C. Wilcox [31] Compared between the low Reynolds number $\kappa-\varepsilon$ model and $\kappa-\omega$ model for high Reynolds number, incompressible, turbulent boundary layers with favorable, zero and adverse pressure gradient respectively. The k-ε model is demonstrated to be inconsistent with the well-established physical structure of the turbulent boundary layer, and low Reynolds number corrections cannot remove the inconsistency. By comparison, the k-ω model proves to be more accurate for all the tests conducted.

Sixin Fan *et al.* [32] Proposed a low Reynolds number $\kappa-\varepsilon$ model suitable for the region near to the wall for unsteady turbulent boundary layers where the flow changes rapidly. In this article, the improvement of low-Reynolds number $\kappa-\varepsilon$ model has been done. The present model has the correct characteristics of behavior at the near wall region. The near wall and low-Reynolds-number are expressed as a function of local turbulent Reynolds number. The turbulence model has been valid for unsteady turbulent boundary layers with and without adverse pressure gradients. This model predicts the unsteady near wall flow and unsteady skin friction for different conditions.

F. R. Menter [33] Proposed two equations Eddy-Viscosity Turbulence Models with an engineering perspective. The first model is the baseline (BSL) model, which utilizes the original $\kappa-\omega$ model of Wiclox on the inner region of the boundary layer. It has a performance similar to the Wilcox model. The second model results from a modification to the definition of the eddy-viscosity in the BSL model. The new model is called the shear-stress transport model. The present model has been found to predict the boundary layer characteristics with much improvement, particularly with the adverse pressure gradient.

Tsan-Hsing Shih [34] Proposed new k-ε eddy viscosity model with a new model for the dissipation equation. The new eddy viscosity formation depends on the realizability constraints where the new model dissipation rate depends on the dynamic equation of the mean square vortices fluctuation. It is found that the present model performs well for a variety of flows like rotating homogeneous shear flows, boundary-free shear flows, including a mixing layer, planar and round jets, etc. The results obtained from this model are also included for comparison. This

experiment has shown that the present model is a more improve model than standard k-ε eddy viscosity model.

Andrew T. Thies *et al*[35] has demonstrated that the use of a new set of empirical constants in the $\kappa-\varepsilon$ model together with the Pope and Sarkar corrections can provide accurate jet flow, particularly in the Mach number range from 0.4 to 2 and jet temperature ratio of 1.0 to 4.0 respectively. The promising aspects of this work are that the empirical relations can be used both for the axisymmetric and asymmetric conditions with higher accuracy.

S. Ekkad *et al*. [36] in their experimental study shown the detailed Nusselt number distributions in case of a two-pass square channel with one ribbed wall sprayed with thermo- chromic liquid crystals. Results are found for a particular range of Reynolds number from 6000 to 60000 respectively.

A. Murata *et al.* [37] performed an experimental study to investigate the effects of angled rib turbulators on the heat transfer of an orthogonally rotating square duct by varying the Reynolds number from 10,000 to 20,000. In this case, the higher heat transfer removal has been observed for the case of 60º angled rib.

Akira Murata *et a.l* [38] in their numerical work used second- order finite difference method. The Reynolds numbers were 350 and 50 respectively for turbulent and laminar cases respectively. The results of this comparison have shown the clear differences in the heat transfer distribution. The reason is that the higher momentum fluid of the turbulent is more distributed than laminar fluid.

K. A. M. Moinuddin *et al* [39] performed an experimental study of the development of the turbulent boundary layers along a stream wise chine will be presented. A recent study along a right-angled stream wise edge was given by Panchapakesan and Joubert(1988 and 1999). By alternating the tunnel side walls quasi- symmetry was achieved and the measurement indicates the symmetry about the bisector with a maximum deviation of 5 percent.

Hongyi *et al.* [40] analyzed the fully developed turbulent flow in a straight square annular duct is simulated using large eddy simulation(LES) and a grid refinement study is carried out using $130\times66\times6$ (0.57 million) and $130\times130\times130$ (2.2 million).The result exhibits the distinctive secondary flow of Prandtl second kind, which consists of a chain of counter-rotating vortex pairs around both convex and concave 90º corners in the annular duct.

P. R. Chandra *et al.* [41] have done an experimental study over heat transfer and friction behaviors in rectangular channels with a varying number of ribbed walls for different Reynolds number ranging from 10,000 to 80,000. The results of this investigation are used in different application of turbulent internal channel flows.

S. W. Chang *et al.* [42] In their paper have shown results related to an experimental study related to the heat transfer in a radially rotating square duct with two opposite walls fitted by transverse ribs. The experimental results illustrate the individual and interactive effects of Coriolis and centripetal buoyancy force of each rotating rib surface. Based on experimental data a co-relation has been developed to permit the evaluation of interactive effects of rib flows, Coriolis force and centripetal buoyancy on heat transfer.

Kang-Hoon Ko *et al.* [43] have conducted experiment to measure the average heat transfer coefficients in a uniformly heated rectangular channel. Heat transfer coefficient, pressure loss is obtained for different types of porous medium with different geometrical conditions and Reynolds number varying from 20,000 to 50,000 respectively. This experiment gives more accurate result compared to heat transfer in a straight channel with no baffles in comparison to other earlier works.

Xiang-Zhe CUI *et al*. [44] estimated the effects of mixing vane shape on the flow structure and heat transfer in the downstream of mixing vane in a sub channel of the fuel assembly. The Standard k-ε model has been used here and periodic and symmetric boundary conditions are used. The result with three turbulence models is compared with experimental data by keeping flow blockage ratio constant and by varying the twist angel of the mixing vane.

C. M. Winkler *et al.* [45] Analysed the preferential concentration of dense particles in a downward fully developed turbulent square duct flow at Re=360.Two- way coupling and particle coupling are not considered. The variation in preferential concentration with cross-sectional location is also studied. Particles are seen to accumulate in regions of higher velocity change; the tendency of particles to accumulate in regions of high vorticity increases with response time near the wall.

Rajendra Karwa *et al*. [46] studied experimentally the heat transfer enhancement in an asymmetrically heated rectangular duct with the presence of perforated baffles. The duct width to height ratio considered is 7.77; while the baffle pitch to height ratio is 29 and the baffle height to duct ratio is 0.495 respectively. The Reynolds number considered from 2850 to 11500. It has been observed that the Nusselt number enhances by 73.7-82.7% higher than that for the smooth duct. The friction factor for the solid baffles is found to be 9.6-11.1 times of the smooth duct.

Lei Wang *et al.* [47] in a study analyzed the turbulent heat transfer and friction with continuous and truncated ribs experimentally by varying the Reynolds number ranging from 8,000 to 20,000 and liquid crystal thermography is used to demonstrate the detailed distribution of heat transfer coefficient between a pair of ribs.

Hussien Al-Bakhit *et al.* [48] In their study considering a parallel flow heat exchanger, numerically simulated to determine the impact of different parameters on the performance and the accuracy of constant heat transfer coefficient assumption. It is seen that there is a significant

change in the overall heat transfer coefficient in the developing region and the three-dimensional heat transfer in the heat exchanger wall must be included in the analysis.

Chu-Wei Lin [49] in his experimental study investigates the local heat transfer in a rectangular channel with a baffle of pores and different heights. The flow geometry is like the backward facing step. He has presented a wide spectrum of results varying different parameters like the Reynolds number, the non-dimensional axial length to present the distribution of Nusselt number.

Gaurav Sharma *et al.*[50] done some analysis with the aim to investigate the role of the secondary flows in the transport and dispersion of particles in a square duct flow, by the numerical simulation of square duct flow of Re,= 300. It was found that lateral mixing is enhanced for passive tracers and higher inertia particles tend to mix more efficiently in the streamwise direction due to the near wall accumulation and passive tracers tend to remain within the secondary swirling flows.

M. Uhlmann *et al.* [51] done a direct numerical simulation of turbulent flow in a straight square duct was performed in order to determine the minimal requirements for self-sustaining turbulence. We present a characterization of the flow state at marginal Reynolds numbers. It is shown that in the regime of marginal Reynolds number buffer-layer coherent structure play a crucial role in the appearance of the secondary flow of Prandtl's second kind.

Abraham J. P. *et al*. [52] numerically predicted the breakdown of laminar pipe flow into transitional intermittency condition. It was observed that two types of fully developed flows are possible by the process of transitional intermittency. The first possibility is a fully developed intermittency flow while the second possibility is the fully developed turbulent flow which can exist theoretically. The velocity distribution has been found to be asymmetric signifying the complexities generated out of the transitional state of the flow.

Gustavo Adolfo Ronceros Rivas *et al*. [53] present results of a numerical investigation of fully developed turbulent flow in a square-duct using two anisotropic turbulence models. For the results produced by RSM was used a CFD commercial package. Comparison among the result produced by two turbulence models and experimental data is done, as well as an analysis of performance for the secondary flow streamlines, axial velocity, the contour map of Reynolds normal and shear stress.

H. Gnanga *et al.* [54] They have done an analysis with the aim of this note is an evaluation of a cubic eddy viscosity turbulent model. The study is carried out in a square duct. The comparison of the modified model results with DNS and LES simulation shows good agreements; in particular, the mean secondary velocity and the mean streamwise vorticity are well predicted.

Z. Zuo-jin [55] Presents the direct numerical simulation results of the turbulent flow in a straight square duct at a Reynolds number of 600 based on the duct width and the mean wall shear

velocity. The result indicates that it is reasonable to neglect the sub-grid scale models in this spatial resolutions level for the for the duct flow at a particular Reynolds number.

M. Fair weather *et al.* [56] Conducted particle dispersion in a square duct flow is studied using large eddy simulation combined with Lagrangian particle tracking under the condition of one-way coupling. The flow has bulk Re=250k and the results obtained for the fluid phase show good agreement with experimental data. It is seen that for the largest particle, the secondary flows contribute to particle concentration in the corner of the dark floor.

Zuo zin Zhu *et al.* [57] In their paper presented the large eddy simulation(LES) results of turbulent heat and fluid flows in a straight square duct (SSD) at Reynolds number ranging from 10^4 to 10^6.The result shows that the LES results is better than the DNS results. The LES results can explain why DNS is applicable to the problem at a moderate Re, and revealed that largest relative deviation of overall mean Nusselt number is less than 10% as compared to existing experimental correlations.

Pongjet Promvonge *et al.* [58] In a numerical experiment investigated the heat transfer characteristics of turbulent square duct flow through inline V-shapes discrete ribs. The isothermal condition is maintained to the upper and lower duct walls and the two side walls are insulated. This experiment is based on the finite volume method with the SIMPLE algorithm. Air is taking as a working fluid whose flow rate in terms of Reynolds number ranging from 10,000 to 25,000.

Ahmed M. Bagabir*et al*. [59] He has conducted a numerical investigation to examine turbulent flow and heat transfer characteristics in a three dimensional ribbed square channels. The governing equations are discretized by the second order upwind differencing scheme, decoupling with the SIMPLE (semi-implicit method for pressure linked equations) algorithm of S. V. Patankar [47]. The fluid flow and heat transfer characteristics are presented for the Reynolds number based on the channel hydraulic diameter ranging from 10^4 to 4×10^4. Rib arrays of 45º V-shaped are mounted in inline. The performance of these ribs is also compared with the 90º transverse ribs.

Hamidou Benzenine *et al*. [60] They numerically analyzed the steady turbulent forced convection flow in a two-dimensional horizontal rectangular cross section channel with isothermal walls and with two and three transverse wavy baffles. The governing equations are solved using the finite volume method by using the SIMPLE algorithm with the realizable $\kappa-\varepsilon$ model. The working fluid is the air and the Reynolds numbers considered from 5,000 to 20,000. In this analysis the distributions of friction factors and Nusselt number for different conditions have been presented.

Benoumessad Kamel *et al*. [61] They investigated open channel flow or river flow by using a 3-D non-linear $\kappa-\varepsilon$ turbulence model in cylindrical coordinates in order to calculate the complex boundary channel flow. The SIMPLE algorithm is used to acquire the coupling of velocity and

pressure. This study also shows that 3D non-linear k-ε turbulence model can be used for analyzing the flow structure in an open channel flow. The novelty of this model is that it can be used in actual river flow and wetland problems encountered in practice.

H. Zhang *et al.* [62] They have provided available information by conducting several Direst numerical simulation (DNS) on turbulent duct flow at Re=300;600;900 and 1200.A quantitative comparison has been done between current and previous DNS results. At last the mean flow and turbulence statistics at higher res were presented and the effect of Res on the mean flow and flow dynamics was discussed.

Hamidou Benzenine *et al.* [63] They studied numerically the behavior of a two-dimensional turbulent flow of air in a rectangular pipe with three flat or corrugated baffles. In this study, the dynamic and thermal behavior of the flow considering the turbulence intensity, the ratios of the friction coefficients and the Nusselt number and thermal expansion coefficients respectively for different geometries over a range of Reynolds number varying from 5000 to 20000 have been examined.

Branislav D. Stankovic *et al.* [64] They done fundamentally significant experimental and theoretical studies for mathematical modeling and numerical computations of this flow configuration areanalyzed. Optimal choice of the turbulence model and the key facts are obtained through the examination of physical mechanisms that generate secondary flow.

A. Vidal *et al*. [65] They have done the direct numerical simulation of fully developed turbulent flow through a straight duct with increasing corner rounding radius r were performed to study the influence of corner geometry of secondary flow. It is seen that the high-speed streaks are preferentially located near the transition between the straight and curved surface.

S. K. Bose *et al* [66] They have done a number of experiments on the turbulence structure and consequent geometrical structures of the flow. In this paper, it is shown that the vertical motion in a cell is kinematically analogous to the torsion problem of the prismatic isotropic electric beam. Based on experimental results the patch vortex in a cell is modeled to have an elliptic shape with the major axis thrust towards a corner of the duct.

Hamidou Benzenine *et al*.[67] They Analyzed the turbulent flow of air in a duct of rectangular section provided with baffles. The low Reynolds number based $\kappa-\varepsilon$ turbulence has been considered. The velocity and pressure term of momentum equations are solved by the SIMPLE algorithm. The main feature of the study is that the recirculation bubble size is strongly affected by the presence of the baffles.

Donald M. Kuchn [68] They have done experimental investigation on the effects of adverse pressure gradient on the incompressible reattaching flow over a rearward-facing step turbulent flow.

David M. Driver and H. lee Seegmiller [69] They have done an experiment on for an incompressible turbulent flow over a rearward facing step in a diverging channel .and obtained mean velocities, Reynolds stresses, and triple products that were measured by a laser doppler velocimeter.

S. Thangam and C. G. Speziale [70] They have presented detailed calculation that strongly indicates that the standard k-epsilon model-when modified with an independently calibrated anisotropic eddy viscosity-can yield. Surprisingly good predictions for the back-step problem.

Nobuhide Kasagi and AKI. Matsunage [71] They have done detailed turbulent flow measurements using a three-dimensional particle-tracking velocimeter, for a plane channel with a one-sided 50% abrupt expansion, which acted as a backward-facing step. The turbulent channel flow reached a fully developed state wall upstream of the step. The Reynolds number based on the upstream centerline velocity and the step height was 55540.

Niclas Tylli, Lambros Kaiktsis and Inerchen [72] They have presented an experimental and numerical result of the three-dimensional laminar flow over a backward-facing step with an expansion ratio of 2 and downstream aspect ratio of 20. Experimental result for transitional and turbulent flow are also reported.

Tatiana G. Elizarova, Eugene V. Shilnikov, Regine Weber, Jacques Hureau [73] They have presented the results of an experimental and numerical investigation of turbulent flow over a backward-facing step in a channel. Experimental data are visualized using a particle image velocimeter (PIV) device. As a mathematical model, they used quasi-hydrodynamic (QHD) equations.

Karel Kozel, Per R Londa and Jaromir Prihoda [74] They have done numerical modeling of flow through the 2-dimensional and 3-dimensional backward-facing step. In laminar case, they have applied for several higher order upwind and central discretization and compared numerical results with measurement. The turbulent regime is considered in 2D as well as 3D and the influence of secondary flow is obtained. Different modification of low Reynolds number two equation turbulence models and an explicit algebraic Reynolds model (EARSM) are considered.

T. P. Chiang and Tony W. H. Sheu [75] They have performed numerical simulation of Navier-Stokes equations for incompressible Navier-Stokes flow inside a channel. The flow field under investigation was characterized as a having a backward-facing step, with an expansion ratio y=H/h=1.9423, over which fully developed channel flow is suddenly expanded into the channel with a channel width B, to upstream channel height h, ratio B/h=2,4,6 and 10. Numerical solutions for this backward-facing step problem were obtained on the basis of expansion ratios and Reynolds numbers considered as, Re=100,389,800.

Z. F. Tian, J. Y. Tu and G. H. Yeoh [76] They have investigated the physical characteristics of dilute gas-particle flows over a backward-facing step geometry. An investigation is performed to access the performance of two computational approaches -the Lagrangian particle-tracking mode and Eulerian two-fluid model to predict the particle phase flow parameter under the influence of

different particle inertia. A Particle with the corresponding diameter of 1 mu and 70 mu are simulated under the flow condition of two Reynolds numbers based on the step height Re=15000 and Re=64000.

Anwar-ul-Haque, Fareed Ahmad, Shunsuke Yamada and Sajid Raza Chaudhry [77] They have done the prediction of reattachment length of separated shear layers in low Reynolds number turbulent flow in a challenging task to evaluate the capabilities of different turbulence models, especially for MEMS applications. The Physical significance of the backward-facing step and its industrial applications discussed. Flow analysis of backward facing step in 2D as well as in 3D were carried out by using the finite volume method. Incompressible segregated scheme with a SIMPLE algorithm for pressure velocity coupling. Although the recirculation created by the backward- facing step is predicted by all turbulence models but epsilon-based turbulence models under-predict the reattachment length of flow whereas shear stress turbulence model accurately predict the flow reattachment.

K. Sengupta, K. K. Q. Zhang and F. Mashayek [78] They performed a direct numerical simulation study to investigate the effect of compressibility on the flow over a backward-facing step. A spectral multidomain method is used for simulating the compressible flow at Reynolds number of 3000 over an open backward-facing step. The role of compressibility in the sub-sonic regime is studied by simulating the flow at different free-stream mach numbers.

Ajay Pratap Singh, Akshoy Ranjan Paul, Pritanshu Ranjan [79] Computational investigation are carried out on flow through a channel having a single backward-facing step. The effect of step angle and expansion ratio on separation length is studied and compared with experimental results. The step angle considered are 15,30,45 and 90. Whereas the expansion ratios considered as 1.48 and 2.0.a 2-Dimensional, segregated, normalized group (RNG) K-EPSILON turbulence model has been chosen for CFD simulations. The analysis of the results showed that with the increase in step angle and expansion ratio, the reattachment length increases. Effects of Reynolds number is also studies by varying it over a range 15000 to 64000 and it is also shows that the reattachment length increases with an increase of the Reynolds number.

Noral wadic. Sidik, Javad Ghaderian, Sakeineh Sadeghhipour [80] They have used the effectiveness of the lattice Boltzmann equation as a computational tool for performing large-eddy simulation of turbulent flow. Three-dimensional turbulent flow over a backward-facing step was considered for this investigation.

Yanhua Wu, Huiying reu, Hui tang [81] Their work characterizes the impact of the realistic roughness due to deposition of foreign material on the turbulent flows at surface transition from elevated rough wall to smooth wall high resolution PIV measurement were performed in the stream wise wall normal x-y planes at two different span-wise positions in both smooth and rough backward-facing step flows. The experiment conditions were set at a Reynolds number

3450 based on the free stream velocity U and the mean step height h, expansion ratio of 1.01, and the ratio of incoming boundary layer thickness to the step height d/h of 8.

S. Bayraktar [82] They have obtained result from 3-dimensional incompressible flow over the backward-facing step in a rectangular duct using realizable k-epsilon model are reported. Effects of step inclination angle have been investigated for B=30,45,90. While upper wall of duct kept parallel to the bottom wall and then rose to, A =6. Reynolds number based on free stream velocity and step height is examined by varying its magnitude in the range of 15000-64000. Simulated results are presented for revealing the general flow features and reattachment length after a successful validation with the experimental data of Driver and Seegmiller [83]. It is found that turbulence kinetic energy increased suddenly after the step for both straight and raised upper walls and reaches its maximum at x/h=5. The size of reattachment length increases with step inclination angle i.e. maximum reattachment length occurs at 90. For both straight and raised upper wall. It is seen that raising the upper wall leads to longer reattachment length.

Michal A. Kopera, Robert M kerr, Hugh m. Blackburn and Dwight Barkley [84] They had simulated turbulent flow in a channel with a sudden expansion using the incompressible Navier-Stokes equations. The objective is to provide statistical data on the dynamical properties of flow over a backward-facing step that could be used to improve turbulence modeling. The expansion ratio is E=2.0 and the Reynolds number, based on the step height and mean inlet velocity, is Re=9000.

Benjamin A Toms [85] They have studied large-eddy simulation of turbulent flow over a backward-facing step, to test the influence of grid resolution, inlet turbulence, wall boundary treatment, and eddy viscosity models. The computational results are validated with experimental data. A grid resolution with 10 cells spanning the step height adequately models the flow, although a doubling of resolution results in the realizable of smaller scale kinematic features. The inlet turbulence conditions are determined to be the most significant contributor to downstream flow evolution. Reattachment length is found to be strongly dependent on the magnitude of the inlet root mean square velocity. The choice of the eddy viscosity model is found to have negligible influence, while the no-slip condition and the LES log-low-based wall function performed similarly for the given flow.

Hui Hyun Choi, Van Thinh Nguyen, John Nguyen [86] Their studies were based on open source CFD package open FOAM. they carried out a number of numerical simulations using Reynolds averaged Navier-Stokes (RANS) and large eddy simulation approaches the numerical investigation has been implemented for various step angles (10,15,20,25,30,45 and 90), different comparisons of the flow and reattachment lengths between the numerical results and the observations shows very good agreement, the results obtained from LES show a better agreement with the observation than the result obtained from the RANS model.

OBJECTIVE OF THE PRESENT WORK

The present study will present the method and the results of a numerical simulation of 3-D rectangular section over backward facing step for different expansion ratios and also for a wide range of Reynolds number. A second objective is the numerical simulation 3-D rectangular section with obstruction plates of different heights, arrangement, and thickness.

CHAPTER 3

MATHEMATICAL FORMULATION

Chapter 3: Mathematical formulation

The differential equations governing the turbulent incompressible fluid motion has been represented in this chapter. Subsequently, numerical modeling for the present work has also been described.

Numerical analysis in fluid dynamics involves a mathematical representation of the physical problem for which the solution is sought. Essentially they are the conservation laws of mass, momentum, and energy respectively. Following the continuum approach, the governing equations are generated in the form of partial differential equations (PDE). The conservation equation for the mass is reffered to as a continuity equation while the same for the momentum equation is known as the Navier-Stokes equation. Similarly equations following conservation of energy expressed in terms of temperature.

3.1 PROBLEM DESCRIPTION

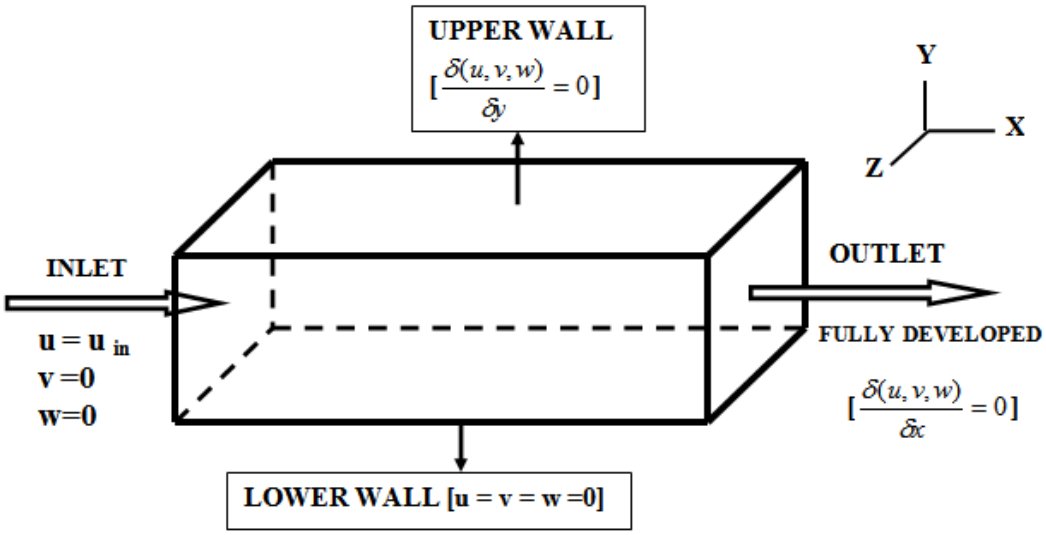

Figure 3.1. Physical geometry and flow configuration of the horizontal

Rectangular Duct

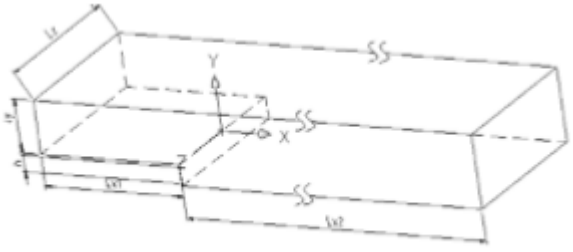

Figure 3.2. Computational domain of the backward-facing step

3.2 BOUNDARY CONDITIONS

3.2. 1Velocity boundary condition

In inlet boundary conditions, the distribution of all flow variables needs to be specified at inlet boundaries mainly flow velocity. This type of boundary conditions is common and specified mostly where the inlet flow velocity is known. And in outlet boundary conditions, the distribution of all flow variables needs to be specified at outlet boundaries mainly flow velocity. This can be thought of as a conjunction to inlet boundary condition. This type of boundary conditions is common and specified mostly where outlet velocity is known. The flow attains a fully developed state where no change occurs in the flow direction when the outlet is selected far away from the geometrical disturbances. In such region, an outlet could be outlined and the gradient of all variables could be equated to zero in the flow direction except pressure.

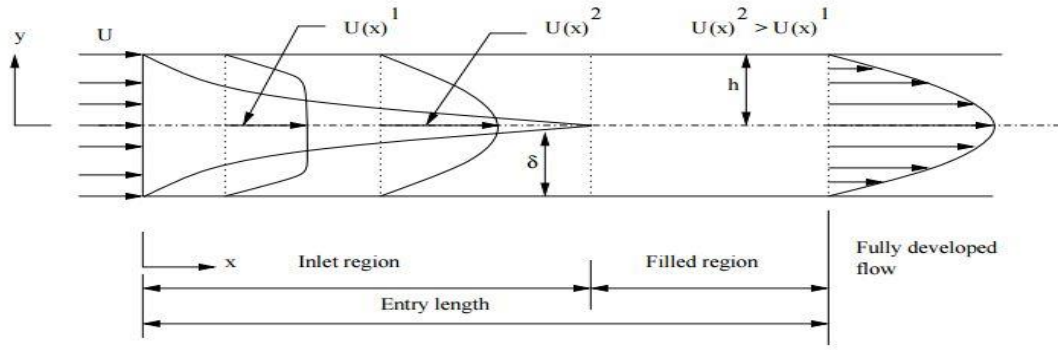

Figure 3.3. Developing velocity profile along streamwise x-axis

1) At y=o, u=0
2) At y=δ, u=U
3) At y=δ, $\frac{\partial u}{\partial y}$=0

3.2.2 Thermal boundary condition

1) The wall temperature remains constant around the periphery and along the length of the duct. In this case, the temperature gradient in the direction of flow, $\frac{\partial T}{\partial x}$, is variable over the cross section at a given axial position.

2) The wall temperature is constant around the periphery of the duct but varies along the length in a manner such that the heat input per length is constant. In this case the quantity, $\frac{\partial T}{\partial x}$, is constant when the tumperature pfofile becomes fully developed.

3) The heat flux is constant in both the peripheral and flow direction. Here, again the quantity, $\frac{\partial T}{\partial x}$, is constant.

3.2.3 Wall boundary conditions

The most common boundary that comes upon in confined fluid flow problems is the wall. This is commonly known as no-slip boundary condition and this is the appropriate conditions for the velocity components at the wall. The normal component could be set to zero straightaway while the tangential component is set to the velocity of the wall.

$$V_{normal} = 0 \text{ and } V_{tangential} = V_{wall}$$

Heat transfer through the wall can be specified or if the walls are considered adiabatic, then the heat transfer across the wall is set to zero.

$$Q_{adiabatic\ wall} = 0$$

3.2.4 Pressure boundary condition

This type of boundary condition is used where boundary values of pressure are known and the exact details of the flow distribution are unknown. This includes pressure inlet and outlet conditions mainly. Typical examples that utilize this boundary condition include buoyancy-driven flows, internal flows with multiple outlets, free surface flows and external flows around objects. An example can be of flow outlet into an atmosphere where pressure is atmospheric.

3.3 Assumptions

These assumptions are made for the subsequent analysis:

1) The fluid is viscous and incompressible.

2) The flow is study and turbulent.

3) The geometry is 3-D rectangular with rectangular solid baffles on the top and bottom walls.

4) Uniform -inlet, no-slip wall boundary condition.

3.4 Governing equations

3.4.1 Continuity equations

$$\frac{\partial \bar{u}}{\partial x} + \frac{\partial \bar{v}}{\partial Y} + \frac{\partial \bar{w}}{\partial z} = 0 \qquad 3.1$$

And $\frac{\partial u'}{\partial x} + \frac{\partial v'}{\partial y} + \frac{\partial w'}{\partial z} = 0$ 3.2

3.4.2 Reynolds Averaged Navier-Stokes equations:

X-Direction Equation

$$\frac{\partial \bar{u}}{\partial t} + \bar{u}\frac{\partial \bar{u}}{\partial x} + \bar{v}\frac{\partial \bar{u}}{\partial y} + \bar{w}\frac{\partial \bar{u}}{\partial z} = -\frac{\partial \bar{p}}{\partial x} + \vartheta\left(\frac{\partial^2 \bar{u}}{\partial x^2} + \frac{\partial^2 \bar{u}}{\partial y^2} + \frac{\partial^2 \bar{u}}{\partial z^2}\right) - \frac{\partial \tau_{xx}}{\partial x} - \frac{\partial \tau_{yx}}{\partial y} - \frac{\partial \tau_{zx}}{\partial z} \quad 3.3$$

Y-Direction Equation

$$\frac{\partial \bar{v}}{\partial t} + \bar{u}\frac{\partial \bar{v}}{\partial x} + \bar{v}\frac{\partial \bar{v}}{\partial y} + \bar{w}\frac{\partial \bar{v}}{\partial z} = -\frac{\partial \bar{p}}{\partial y} + \vartheta\left(\frac{\partial^2 \bar{v}}{\partial x^2} + \frac{\partial^2 \bar{v}}{\partial y^2} + \frac{\partial^2 \bar{v}}{\partial z^2}\right) - \frac{\partial \tau_{xy}}{\partial x} - \frac{\partial \tau_{yy}}{\partial y} - \frac{\partial \tau_{zy}}{\partial z} \quad 3.4$$

Z-Direction Equation

$$\frac{\partial \bar{w}}{\partial t} + \bar{u}\frac{\partial \bar{w}}{\partial x} + \bar{v}\frac{\partial \bar{w}}{\partial y} + \bar{w}\frac{\partial \bar{w}}{\partial z} = -\frac{\partial \bar{p}}{\partial z} + \vartheta\left(\frac{\partial^2 \bar{w}}{\partial x^2} + \frac{\partial^2 \bar{w}}{\partial y^2} + \frac{\partial^2 \bar{w}}{\partial z^2}\right) - \frac{\partial \tau_{xz}}{\partial x} - \frac{\partial \tau_{yz}}{\partial y} - \frac{\partial \tau_{zz}}{\partial z} \quad 3.5$$

3.4.3 Energy equation

$$\frac{\partial \bar{T}}{\partial t} + \bar{u_\iota}\frac{\partial \bar{T}}{\partial x_i} = \frac{\partial}{\partial x_i}\left[\alpha\frac{\partial \bar{T}}{\partial x_i} - \overline{u_\iota' T'}\right] \quad 3.6$$

With

$$-\overline{u_\iota' T'} = \alpha_t \frac{\partial \bar{T}}{\partial x_i} \quad 3.7$$

$$\alpha_t = \vartheta_t / \sigma_t \quad 3.8$$

Where σ_t is turbulent prandtl number, $\bar{u}, \bar{v}$ *and* $\bar{w}$ are the mean velocity components and u', v' *and* w' are the fluctuating velocity component in the X, Y and Z -directions respectively. $\bar{p}$ is the modified mean pressure; $\bar{T}$ is mean temperature; T' is fluctuating temperature; $\tau_{xx}, \tau_{xy}, \tau_{xz}, \tau_{yy}, \tau_{yz}, \tau_{zz}$ are the component of Reynolds Stress Tensor; ϑ is the kinematic viscosity; ϑ_t is the eddy viscosity; α is the thermal diffusivity and $\alpha_t$is eddy thermal diffusivity.

Now here as the number of unknown is more than the number of equations, "the problem is indeterminate", one needs to close the problem to obtain a solution, for that common turbulence model are classified on the basis of the number of additional transport equations that need to be solved along with RANS Equations.

3.4.4 MODEL EQUATIONS

Here we used Standard K-∈ model to solve these problems along with Continuity equation, RANS Equations, and Energy equation.

In the standard K-∈ model with isotropic eddy-viscosity, the Reynolds Stress Tensor takes the form:-

$$\tau_{ij}=\overline{u_i' u_j'} = \frac{2}{3} k\delta_{ij} - \vartheta_t \left(\frac{\partial \overline{u_i}}{\partial x_j} + \frac{\partial \overline{u_j}}{\partial x_i}\right) \qquad 3.9$$

Where k is the turbulent kinetic energy (TKE) and is defined as;-

$$\text{TKE=K}=\frac{1}{2}\tau_{ii} = \frac{1}{2}\overline{u_i' u_i'} = \frac{1}{2}\left(\overline{u'u'} + \overline{v'v'} + \overline{w'w'}\right) \qquad 3.10$$

The model equation for turbulent kinetic energy, k is

$$\frac{\partial k}{\partial t} + \overline{u_i}\frac{\partial k}{\partial x_j} = \frac{\partial}{\partial x_j}\left[\frac{\vartheta_t}{\sigma_k}\frac{\partial k}{\partial x_j}\right] + P - \in \qquad 3.11$$

The model equation for turbulent dissipation, ∈ is

$$\frac{\partial \in}{\partial t} + \overline{u_j}\frac{\partial \in}{\partial x_j} = \frac{\partial}{\partial x_j}\left[\frac{\vartheta_t}{\sigma_\epsilon}\frac{\partial \epsilon}{\partial x_j}\right] + C_{\in 1}\frac{P\in}{K} - C_{\in 2}\frac{\in^2}{K} \qquad 3.12$$

The production of turbulent kinetic, P is

$$P = -\tau_{ij}\frac{\partial \overline{u_i}}{\partial x_k} \qquad 3.13$$

The entire system of the equation can be closed if σ_t is known and ϑ_t is determined correctly. The turbulent viscosity, ϑ_t can be related to turbulent kinetic energy k and its dissipation rate, ∈ in the following way

$$\vartheta_t = C_\mu \frac{K^2}{\in} \qquad 3.14$$

The quantity C_μ is a model constant to be determined accurately for a specific flow. the kinetic energy k and its dissipation rate ∈ are evaluated at each point in the domain from their governing differential equations.

The standard value of all the model constant as fitted with benchmark experiments are (Lunder and Sharma)C_μ=0.09, $C_{\epsilon 1}$=1.44, $C_{\epsilon 2}$ = 1.92, σ_K= 1, σ_ϵ =1.3.

3.4.5 DATA REDUCTION

The objective of data reduction is to calculate the average Nusselt number and Reynolds number. The hydraulic diameter, D_h is chosen as the characteristic dimension.

$$\mathrm{Re} = \frac{UD_h}{\vartheta} \qquad 3.15$$

$$\mathrm{Nu} = \frac{hD_h}{k} \qquad 3.16$$

Here k is thermal conductivity of flowing fluid.

For rectangular cross-section duct, hydraulic diameter, D_h, is obtained from the following equation.

$$D_h = \frac{4A}{P} \qquad 3.17$$

Where A is cross-section area and P is a wetted perimeter

The average convective heat transfer coefficient of the water flow in the duct is obtained cengel[] as follows.

$$\mathrm{h} = \frac{q''}{(T_w - T_b)} \qquad 3.18$$

also, all fluid properties in the duct are evaluated at the bulk temperature $T_b = {(T_{bi} + T_{bo})}/{2}$

CHAPTER 4

SOLUTION METHODOLOGY

CHAPTER 4 : SOLUTION METHODOLOGY

4.1 Numerical algorithm

The mathematical models described above consist of a set of differential equations subject to appropriate boundary conditions. To provide the algebraic form of the governing equations, a fully staggered grid system have been adopted for the velocity components and the scalar variable and these equations were discredited using a control volume formulation. The numerical solution in present work is accomplished by using Semi-implicit method for pressure linked equation revised (SIMPLER) and power-law scheme proposed by Patankar [].

4.2 Control volume formulation:

In the control volume formulation, the calculation domain is divided into a number of non-overlapping control volumes surrounding each grid point. The differential equation is integrated over each control volume. Piecewise profiles expressing the variation of the variable between the grid points are used to evaluate the required integrals.

The most attractive feature of the control volume is that the resulting solution would imply that the integral conservation of quantities such as mass, momentum is exactly satisfied over any group of control volumes, and, of course, over the whole domain. These characteristics exist for any number of grid points. Thus even the coarse grid solution exhibits exact integral balance.

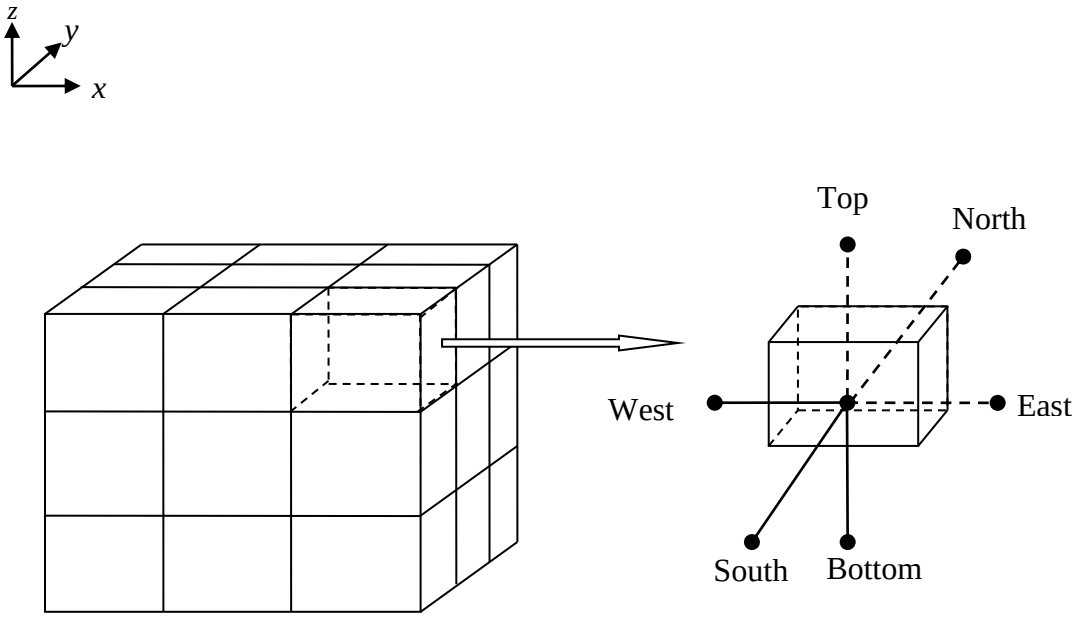

Figure 4.1. Control volume formulation

4.3 The power law model

The power law model as described by patankar has been used for the discretization of the flow governing equations in the present study. The power-law differentiating scheme is a more accurate approximation to the exact solution of the conduction-diffusion equation and produces a better result than the hybrid scheme by Patankar[].

$$\frac{\partial}{\partial t}(\rho\,\phi) + \text{div}\,(\rho\,\phi\,u) = \text{div}\,(\Gamma\,\text{grad}\,\phi) + S_{\phi} \qquad 4.1$$

The above equation is called the transport equation for property ϕ, indicating the velocity field or any other physical quantities related to the problem concerned. It highlights the various transport process i.e. the rate of change term and convective term on the left-hand side and the diffusion term (Γ – diffusion coefficient) and the source term respectively on the right-hand side.

4.4 The staggered grid

To avoid discrepancies related to source pressure term and velocities in momentum equations, staggered grid arrangement has been considered. In the staggered grid, the velocity components are calculated for the points lies on the faces on the control volumes. Thus x-direction velocity u is calculated at the faces that are normal to the x-direction. The main grid point is shown by small circles fig.4.2. The dashed lines indicate the control volume faces. The location for u lies on the x-direction. The link joining two adjacent main grid points. Whether u location is exactly mid way between the grid points depends upon how the control volumes are defined. u location must lie on the control volume face, irrespective of whether the latter happens to be mid way between the grid points. Similarly, v and w can be calculated.

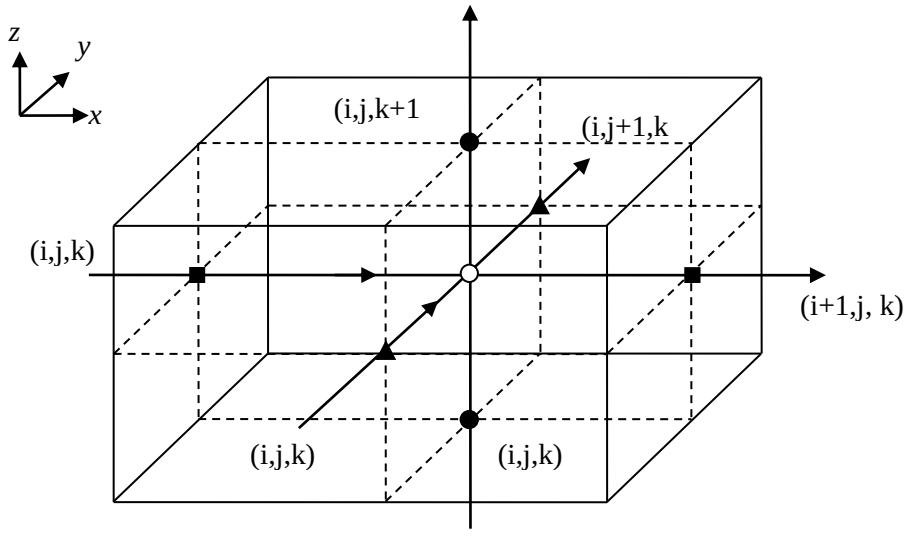

Figure 4.2. Staggered grid arrangements in three dimensions

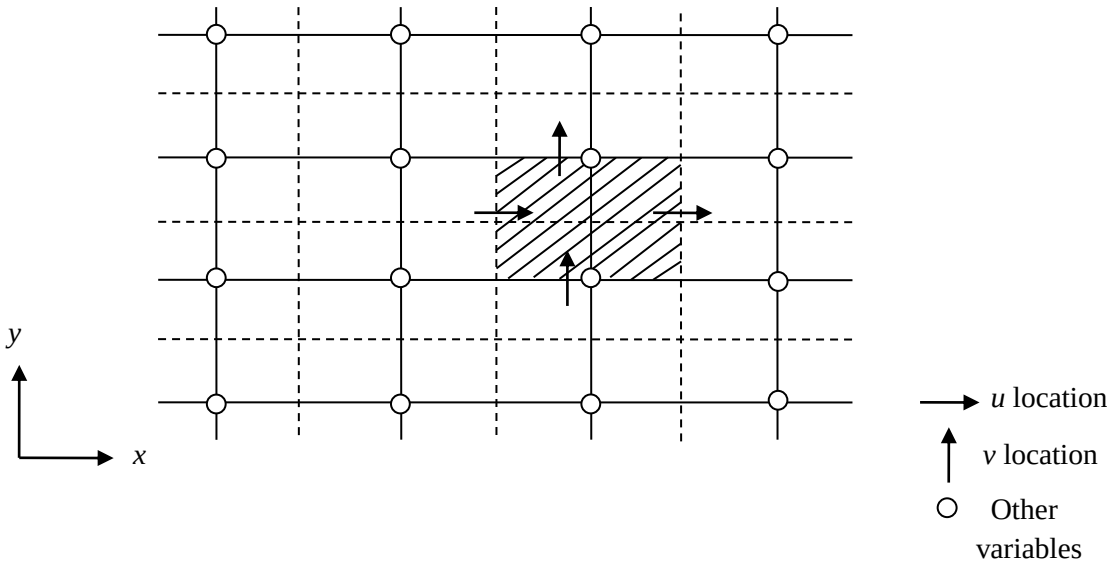

Figure 4.3. the Staggered grid in two dimensions

4.5 Simple algorithm

A staggered control volume for the x-momentum equation is shown in fig. (4.4) if the attention has been focused on the locations for u only, there is nothing unusual about this control volume. Its faces lie between the point e and corresponding locations for the neighbor u's. the control volume is staggered in relation to the normal control volume around the main grid point p. the staggering is in the x-direction only, such that the faces normal to the direction pass through the main grid points P and E. the difference $p_P - p_E$ can be used to calculate the pressure forces acting on the control volume for the velocity u.

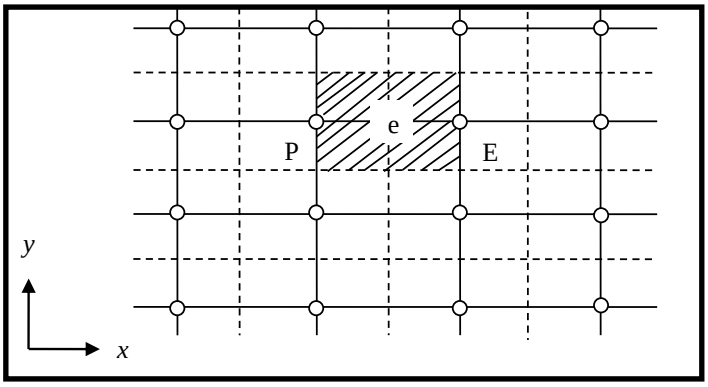

Figure 4.4. Control volume for u

The calculation of the diffusion coefficient and mass flow rate at the faces of u control volume shown in fig. (4.2) would require an appropriate interpolation. The resulting discretization equation can be written as,

$a_e u_e = \Sigma a_{nb} u_{nb} + (p_P - p_E) A_e$ 4.2

Here the number of neighbor term will depend on the dimentionality of the problem. For two dimensional situations, four u neighbors are shown outside the control volume and for three-dimensional cases; six neighbors would be included. The neighbor coefficient a_{nb} account for the combined covection-diffusion influence at the control volume faces. The term $(p_P - p_E) A_e$ is the pressure force acting on the u control volume, A_e being the area on which the pressure difference acts. For two dimensions, A_e will be Δy X1, while for the three dimensional case $A_e$will stand for $\Delta y \Delta z$.

The momentum equation for the other direction is handled in a similar manner. Equation 4.3 below shows the control volume for the y-direction momentum equation; it is staggered *in the y-direction. The discretization equation for v_n can be seen to be,*

$a_n v_n = \Sigma a_{nb} v_{nb} + b + (p_P - p_N) A_n$ 4.3

Where, $(p_P - p_N) A_n$ is the appropriate pressure force. For the three dimensional case, a similar *equation for the velocity component w can be written.*

The momentum equation can be solved only when the pressure field is given or is somehow estimated. Unless the correct pressure field is employed, the resulting velocity field will not satisfy the continuity equation. Such an imperfect velocity field based on a guessed pressure field p^* will be denoted by u^*, v^*, w^*. These starred velocity field will result from the solution of the following discretization equations.

$a_e u_e^* = \Sigma\, a_{nb} u_{nb}^* + b + (p_P^* - p_E^*) A_e$ 4.4

$a_n v_n^* = \Sigma\, a_{nb} v_{nb}^* + b + (p_P^* - p_N^*) A_n$ 4.5

$a_t w_t^* = \Sigma\, a_{nb} w_{nb}^* + b + (p_P^* - p_T^*) A_t$ 4.6

In these equations, the velocity component and pressure have been given the superscript *. The location t, can be noted, lies on the z-direction gridline between the grid points P and T.

4.6 The pressure and velocity corrections:

Our aim is to improve the guessed pressure p^* such that the resulting starred velocity field will progressively get closer to stisfying the continuity equation. The correct pressure p is obtained from,

$p = p^* + p'$ 4.7

where, p' will be called pressure correction. The corresponding velocity corrections u', v', w' can be introduced in a similar manner:

u = u^* + u' 4.8

v = v^* + v' 4.9

w = w^* + w' 4.10

so we get,

$a_e u'_e = \Sigma\ a_{nb} u'_{nb}$ + b + $(p^*_P - p'_E)\ A_e$ 4.11

Neglecting the term $\Sigma a_{nb} u'_{nb}$ from the above equation 4.11 we get,

$a_e u'_e = (p^*_P - p'_E)\ A_e$ 4.12

Or,

$u'_e = (p^*_P - p'_E)\ d_e$ 4.13

Where,

$d_e = \frac{A_e}{a_e}$ 4.14

Equation 4.2 will be called the velocity correction formula. It can be written as,

$u_e = u^*_e + (p'_P - p'_E)\ d_e$ 4.15

This shows how the starred velocity u^*_e is to be corrected in response to the pressure correction to produce u_e.

The corrections formula for the velocity components in other directions can be written similarly:

$v_n = v^*_n + (p'_P - p'_N)\ d_n$ 4.16

$w_t = w^*_t + (p'_P - p'_T)\ d_t$ 4.17

4.7 The pressure correction equation

We shall now turn the continuity into an equation for the pressure correction. For the purpose of this derivation, we shall assume that the density ρ does not directly depend on pressure. The derivation is given here for the three-dimensional situation. The continuity equation is,

$\frac{\partial \rho}{\partial t} + \frac{\partial (\rho u)}{\partial x} + \frac{\partial (\rho v)}{\partial y} + \frac{\partial (\rho w)}{\partial z} = 0$ 4.18

Now, it will be integrated over the shaded control volume shown in fig. 4.1 for the integration of the term $\frac{\partial \rho}{\partial t}$, it is assumed that ρ_P prevails over the control volume. Also a velocity component such as u_e located on a control volume face will be supposed to govern the mass flow rate for the whole face. In conformity with the fully implicit practice, the new value of valocity and density (i.e. those at time t+Δt) will be assumed to prevail over the time step; the old density ρ_P° (i.e. the one at a time t) will appear only through the term $\frac{\partial \rho}{\partial t}$.

With this dicision, the integrated form of continuity equation 4.18 becomes,

$$\frac{(\rho_P-\rho_P^{\circ})\Delta x\Delta y\Delta z}{\Delta t} + ((\rho u)_e\text{-}(\rho u)_w)\Delta y\Delta z + ((\rho v)_n\text{-}(\rho v)_s)\Delta z\Delta x + ((\rho w)_t\text{-}(\rho w)_b)\Delta x\Delta y = 0 \qquad 4.19$$

Now substituting all the velocity components, the expression given by the velocity correction formula we obtain, after rearrangement, the following discretization equation for p':

$$a_P p'_P = a_E p'_E + a_W p'_W + a_N p'_N + a_S p'_S + a_T p'_T + a_B p'_B + b \qquad 4.20$$

Where,

$$a_E = \rho_e d_e \Delta y \Delta z \qquad 4.21$$

$$a_W = \rho_w d_w \Delta y \Delta z \qquad 4.22$$

$$a_N = \rho_{nd_n} \Delta z \Delta x \qquad 4.23$$

$$a_S = \rho_s d_s \Delta z \Delta x \qquad 4.24$$

$$a_T = \rho_t d_t \Delta x \Delta y \qquad 4.25$$

$$a_B = \rho_b d_b \Delta x \Delta y \qquad 4.26$$

$$a_P = a_E + a_W + a_N + a_S + a_T + a_B \qquad 4.27$$

$$b = \frac{(\rho_P^0-\rho_P)\Delta x\Delta y\Delta z}{\Delta t} + ((\rho u^*)_w\text{-}(\rho u^*)_e)\Delta y\Delta z + ((\rho v^*)_s\text{-}(\rho v^*)_n)\Delta z\Delta x + ((\rho w^*)_b\text{-}(\rho w^*)_t)\Delta x\Delta y \qquad 4.28$$

Since the value of the density ρ will normally be available only at the main grid points,

The interface densities such as ρ_e may be calculated by any convenient interpolation. Whatever the method of interpolation, the value of ρ_e must be consistantly used for the two control volumes to which the interface belongs.

It can be seen from the equation (4.28) that the term b in the pressure correction equation is essentially the left- hand side of the discredited continuity equation (4.19) evaluated in terms of starred velocity. If b is zero, it means that the starred velocities, in conjunctions with the available value of $(\rho_P^{\circ} - \rho_P)$, do satisfy the continuity equation, and no pressure correction is needed. The term b thus represents a 'mass source', which the pressure correction must annihilate.

The pressure correction equation derived as above is prone to divergence unless some under-relaxation are used. We under relax u^* ,v^* and w^*while solving the momentum equations (with the relaxation factor α, set equal to about 0.5); further we add only a fraction of p' to p^* in other words we employ,

p= $p^* + \alpha_P p'$ 4.29

With α_P set equal to 0.8. The task of equation (4.29) is to calculate p, which will be used as p^* in the new iteration. The value of relaxation factors that are mentioned here, namely α=0.5 and α_P=0.8, have been found to satisfactory in a large number of fluid flow computations.

4.8 SIMPLE ALGORITHM

The **SIMPLE** stands for Semi- implicit Method or Pressure Linked Equations.

The sequences of operation are

1) Start with a guessed pressure field, p^*

2) Solve the momentum equations such as equations (4.4) to (4.6)to obtain u^*, v^* and w^*.

3) Solve the p' equation.

4) Calculate p from equation (4.7) by adding p' to p^*.

5) Calculate u, v, and w from their starred values using the velocity correction formulas (4.15)-(4.19)

6) Solve the discretization equation for other ϕ's (such as temperature).

7) Treat the corrected pressure p to new guessed pressure p^*.

8) Repeat the steps from step 2 till the conserved solution is obtained.

4.9 SIMPLER ALGORITHM

The **SIMPLER** stands for "Semi-Implicit Method or Pressure Linked Equation Revised". This method is an improved version of SIMPLE. The steps for calculation are as follows.

Start with a guessed velocity field.

Calculate the coefficient of momentum equations. Hence, calculate the pseudo velocities û $v\hat{}\ and$ ŵ by using the value of neighbour velocities u_{nb}.

$$u\hat{}_e=\frac{\sum a_{nb}u_{nb+b}}{a_e} \qquad 4.30$$

$$v\hat{}_n=\frac{\sum a_{nb}v_{nb}+b}{a_n} \qquad 4.31$$

$$w\hat{}_t=\frac{\sum a_{nb}w_{nb}+b}{a_t} \qquad 4.32$$

Calculate the coefficient of pressure equation and solve it to obtain the pressure field.

$$a_P p_{P=} a_E p_{E+} a_W p_{W+} a_N p_N + a_S p_S + a_T p_T + a_B p_B + b \qquad 4.33$$

Where $a_E, a_W, a_N, a_S, a_T, a_B, a_P$, b are as given in equations (4.21)-(4.33).

Treating this field as p^*, solve the momentum equation to obtain $u^*, v^*\ and\ w^*$.

$$a_e u_e^* = \sum a_{nb} u_{nb}^* + \text{b} + (p_P^* - p_E^*)A_e \qquad 4.34$$

$$a_n v_n^* = \sum a_{nb} v_{nb}^* + \text{b} + (p_P^* - p_N^*)A_n \qquad 4.35$$

$$a_t w_t^* = \sum a_{nb} w_{nb}^* + b + (p_P^* - p_T^*)A_t \qquad 4.36$$

Calculate the mass source term b, and hence solve the p' equation.

Correct the velocity field but do not correct the pressure.

$$u_e = u_e^* + d_e(p'_P - p'_E) \qquad 4.37$$

$$v_n = v_n^* + d_n(p'_P - p'_N) \qquad 4.38$$

$$w_t = w_t^* + d_t(p'_P - p'_T) \qquad 4.39$$

CHAPTER 5

RESULTS AND DISCUSSION

CHAPTER 5: RESULTS AND DISCUSSION

In this chapter we discussed the computational results of the problem for a different case. First of all, we discussed simulation results of the duct with a backward-facing step for different step height. then we will discuss the results for the duct with different obstruction height and of different arrangements

5.1 BACKWARD FACING STEP

In this case, we had a rectangular duct height of 0.1 m, and three step heights 0.025m, 0.05m and 0.075m with Reynolds number of flow 6.6*10^5. And studied the effect of step height on reattachment length, turbulent kinetic energy, pressure coefficient, skin friction coefficient and also studied their variation at Reynolds numbers 66, 660, 6600, and 6.6*10^5 for step height 0.05m.

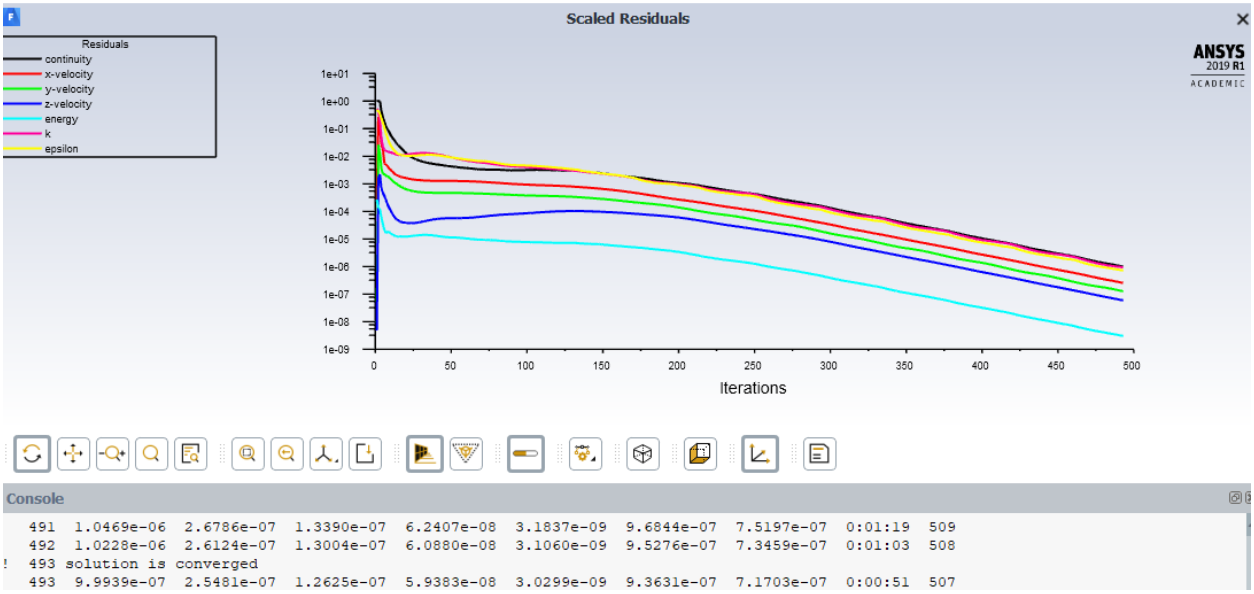

Figure 5.1. Residuals of mass, momentum, energy, turbulent kinetic energy, and dissipation rate

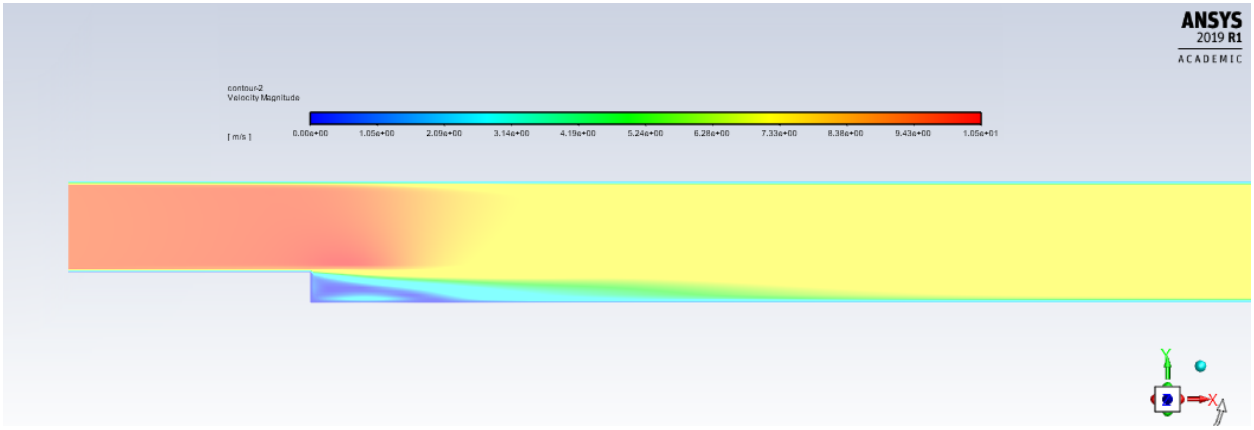

(a) ER=1.33

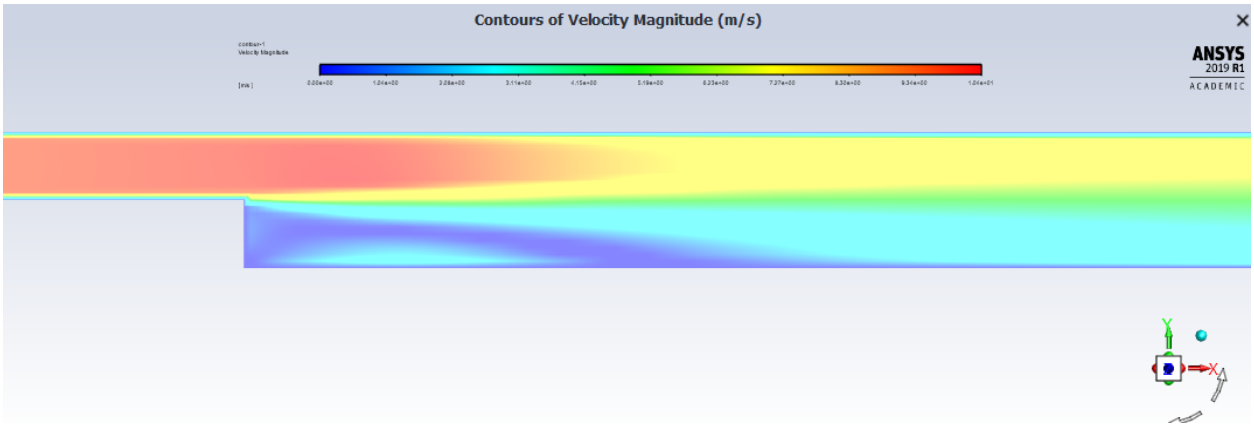

(b) ER=2

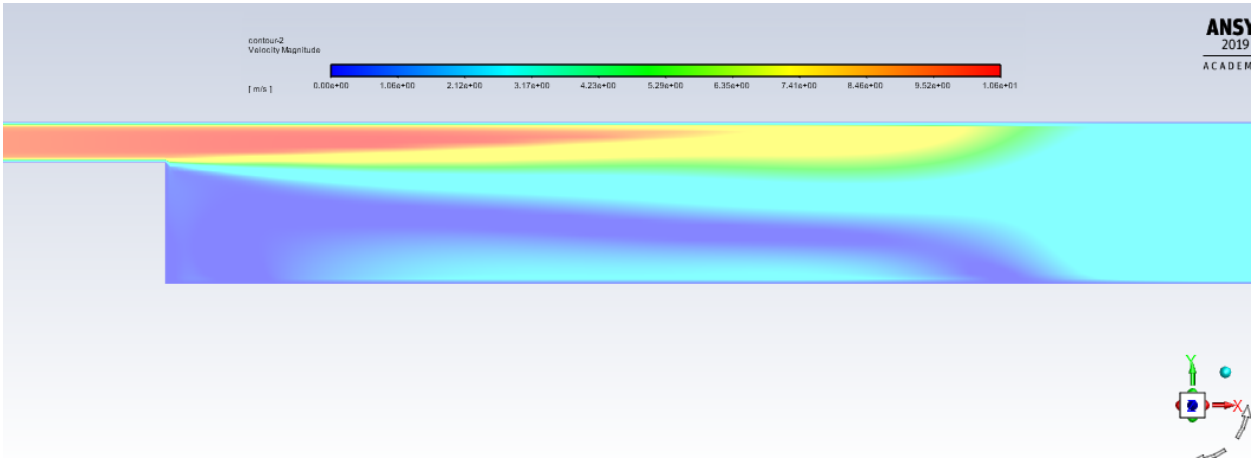

(c) ER=4

Figure 5.2. Effect of step height on reattachment length and velocity magnitude

Figure (5.2) demonstrate that with an increase in step height reattachment length increases.

Re-attachment length is a commonly used parameter to determine the ability of a turbulence model to correctly simulate the flow over backward facing step. A key measure of the computational accuracy of any numerical scheme is the prediction of the reattachment point. this parameter is the distance from the step to the position on the wall, at the bottom of the channel, at which the velocity along the channel becomes positive.

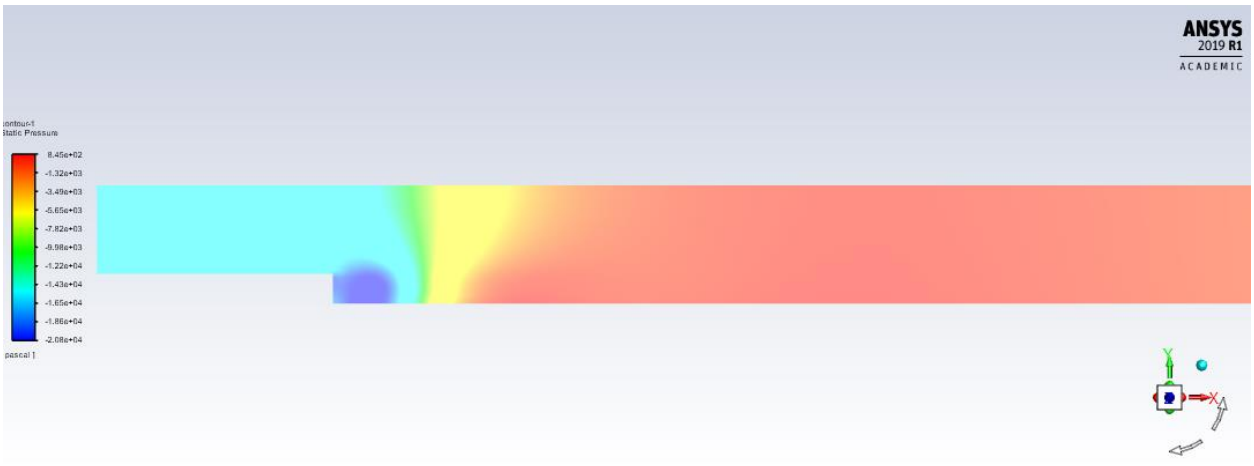

(a) ER=1.33

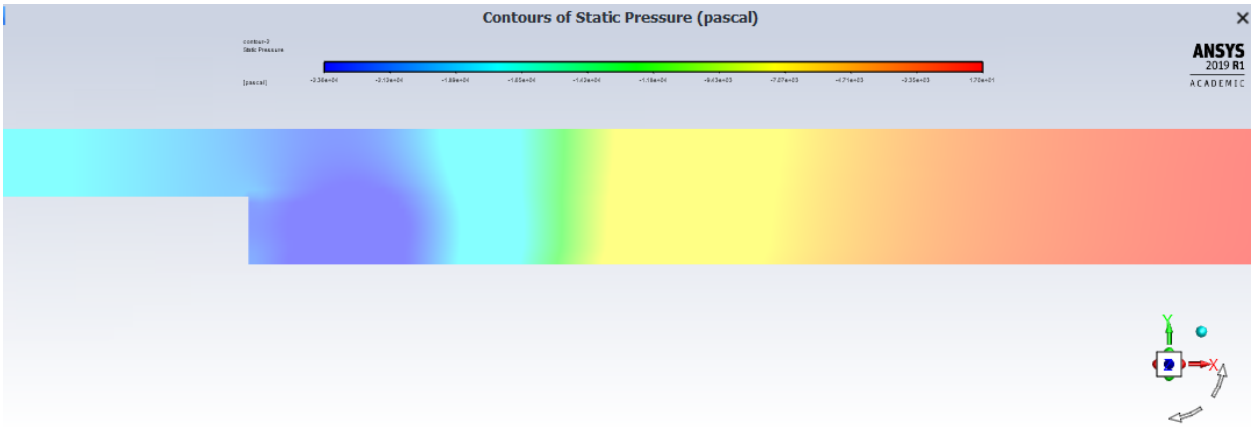

(b) ER=2

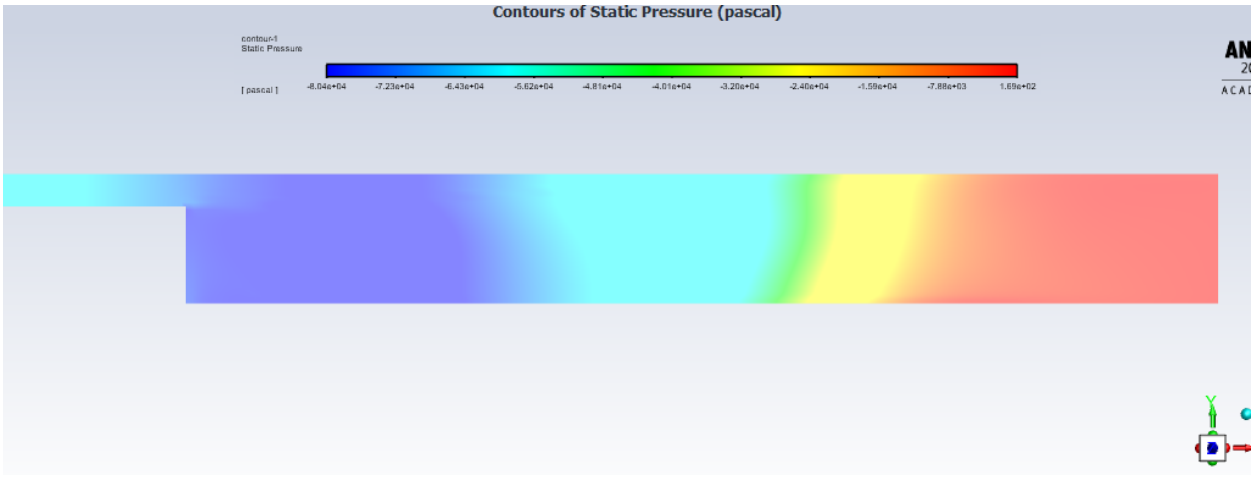

(c) ER=4

Figure 5.3. Effect of ER on static gauge pressure

Figure (5.3), demonstrate that increase in ER results in a roughly smooth gradual change in static gauge pressure. The Figure shows at lower ER pressure abruptly changes near step height region. And with an increase in ER pressure leads to change smoothly.

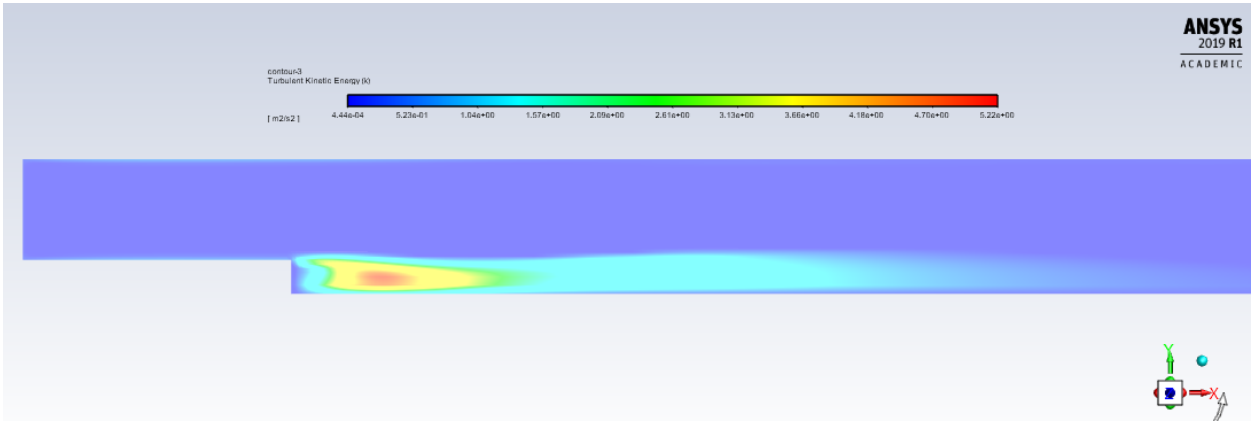

(a) ER=1.33

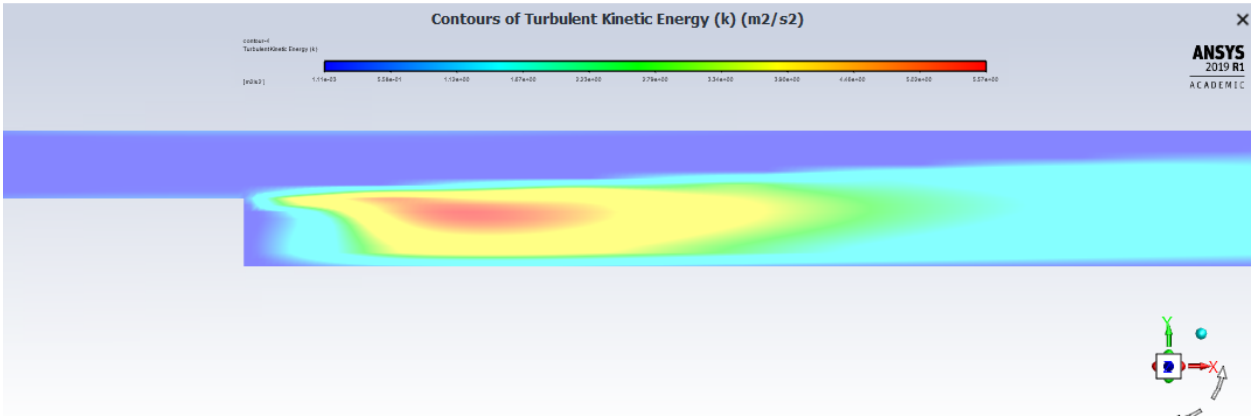

(b) ER=2

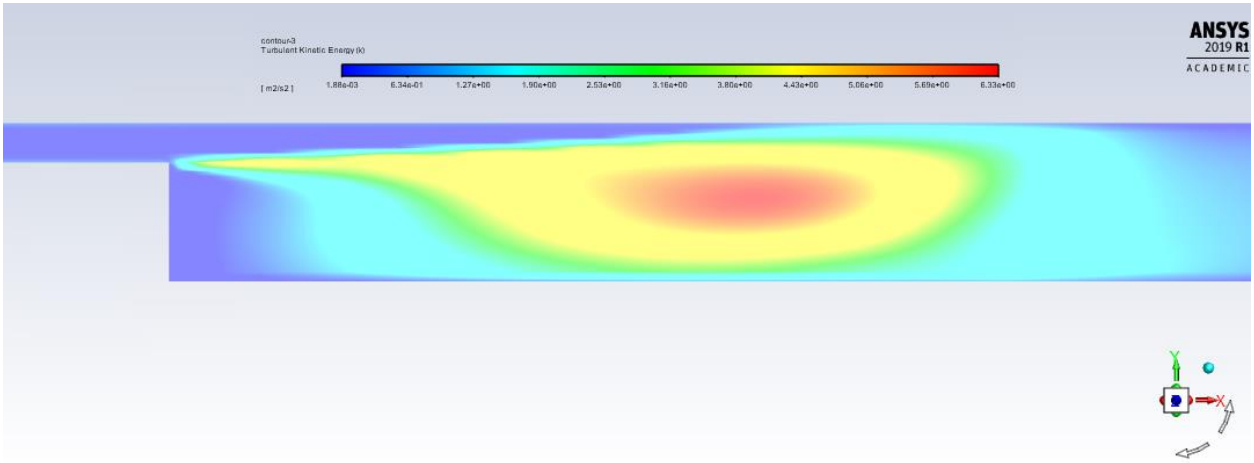

(c) ER=4

Figure 5.4. Effect of step height on turbulent kinetic energy

Figure (5.4), demonstrate that with an increase in ER turbulent kinetic energy in the region downstream of flow just after step height increase. At low ER turbulence kinetic energy in the region just after step height is more but is less strong. With an increase in ER turbulent kinetic energy in the region just after the step height is less but after that it spread more strongly as compared to low ER.

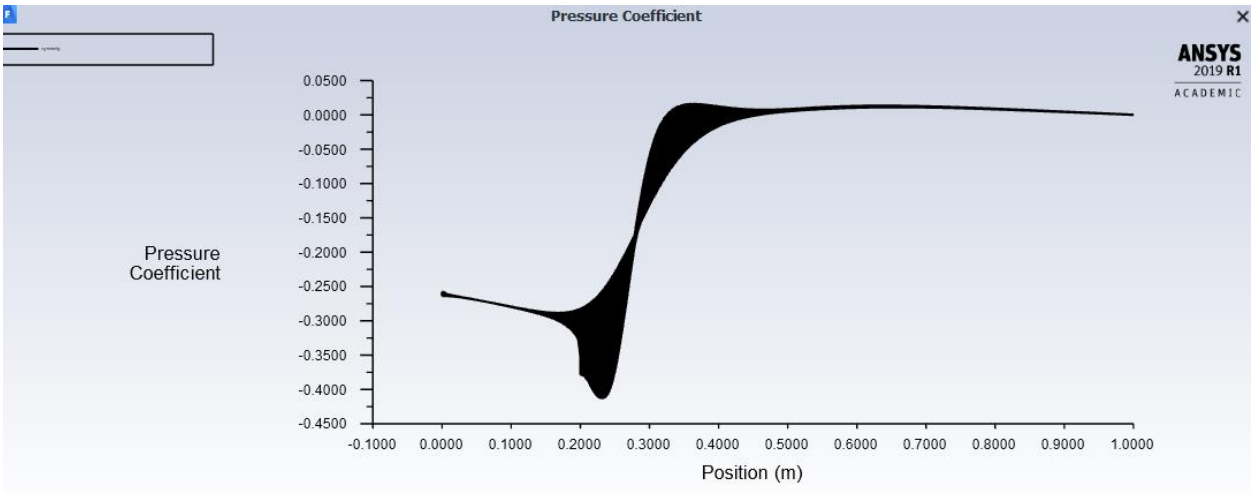

(a) ER=1.33

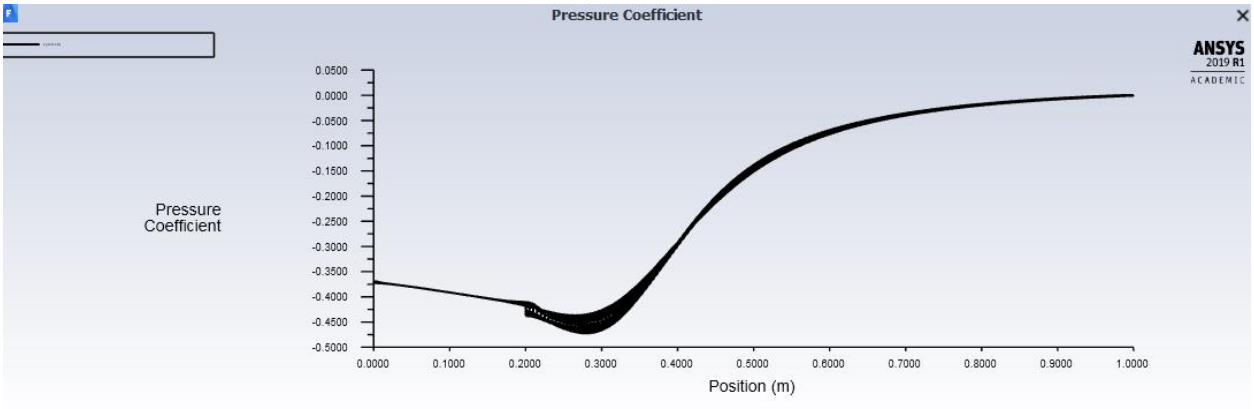

(b) ER=2

Figure (5.5), shows at a lower ER pressure coefficient abruptly changes near step height region. And with an increase in ER pressure coefficient leads to change smoothly.

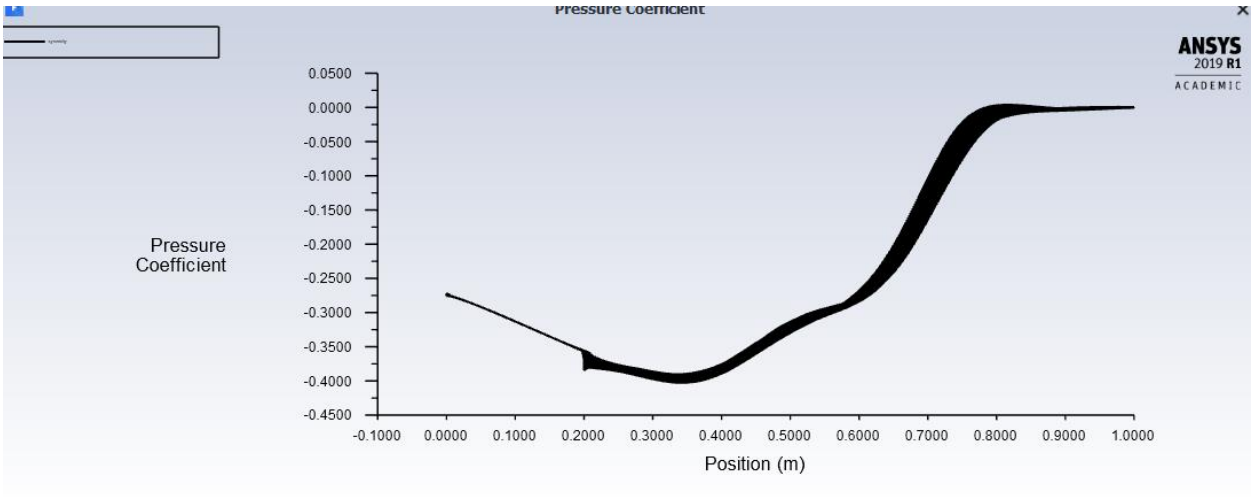

(c) ER=4

Figure 5.5. Effect of ER on pressure coefficient

The variation of ER influences not only the velocity field but also the pressure distribution in the whole domain investigated. To represent the pressure field in dimensionless form, a pressure coefficient is defined as:-

$$C_P = \frac{(p - p_{atm})}{\frac{\rho U_\infty^2}{2}}$$

Where p is the static pressure and p_{atm} is the atmospheric pressure. Figure (5.5), shows the variation of pressure coefficient. The pressure coefficient changes smoothly with an increase in ER near the step.

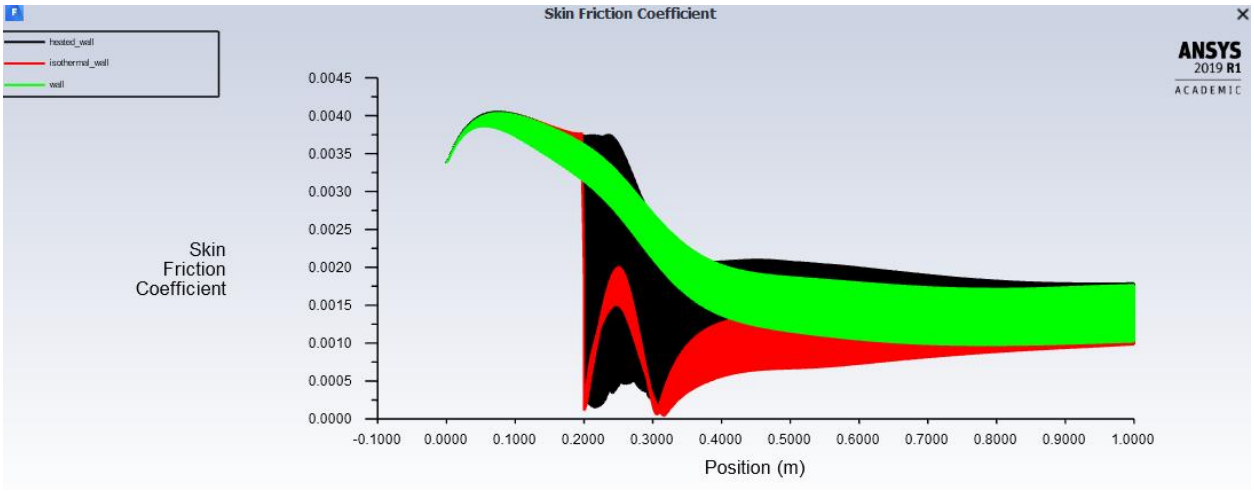

(a) ER= 1.33

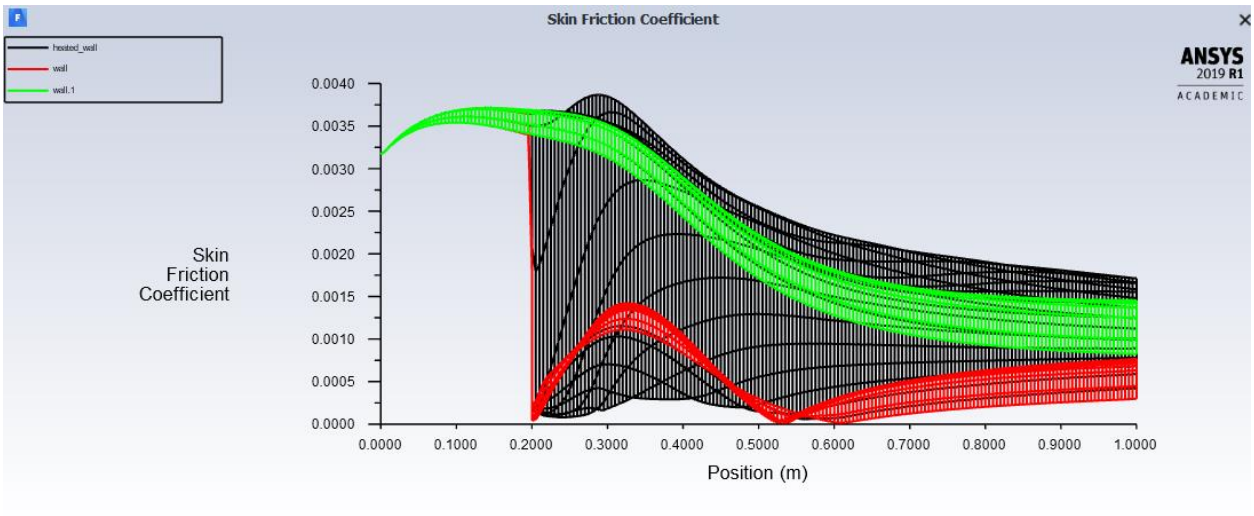

(b) ER=2

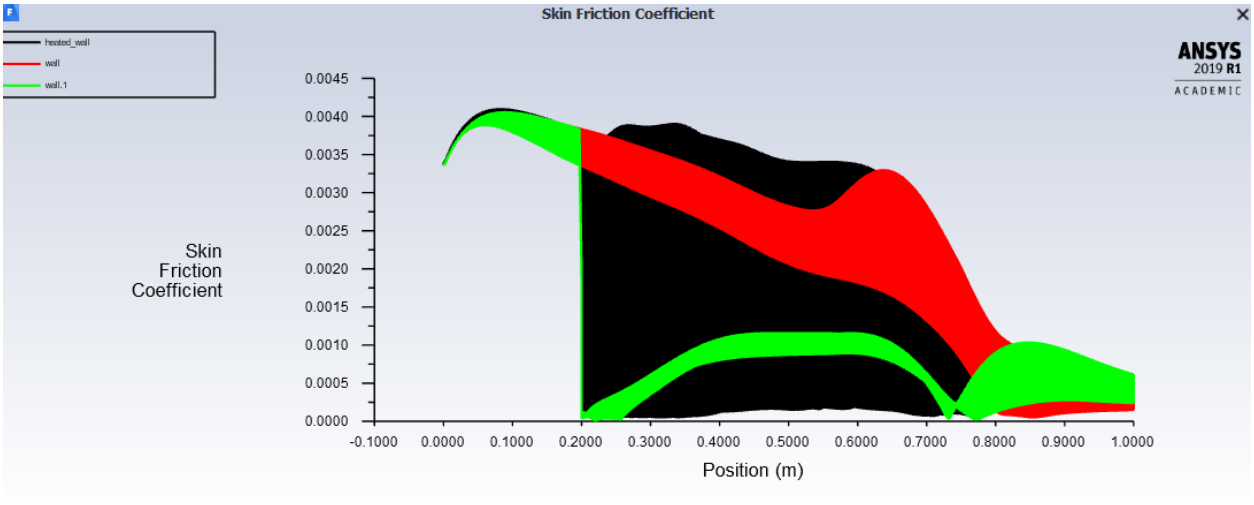

(c) ER=4

Figure 5.6. Effect of ER side bottom ant top wall skin friction coefficient

Figure (5.6) shows that with an increase in step height skin friction coefficient on the bottom wall decreases after step height in downstream of the flow.

The skin friction coefficient is defined as

$$C_f = \frac{\tau_w}{\frac{1}{2}\rho U_\circ^2}$$

Where, $\tau_w = \mu \frac{\partial \bar{u}}{\partial y}\Big|_{y=0}$

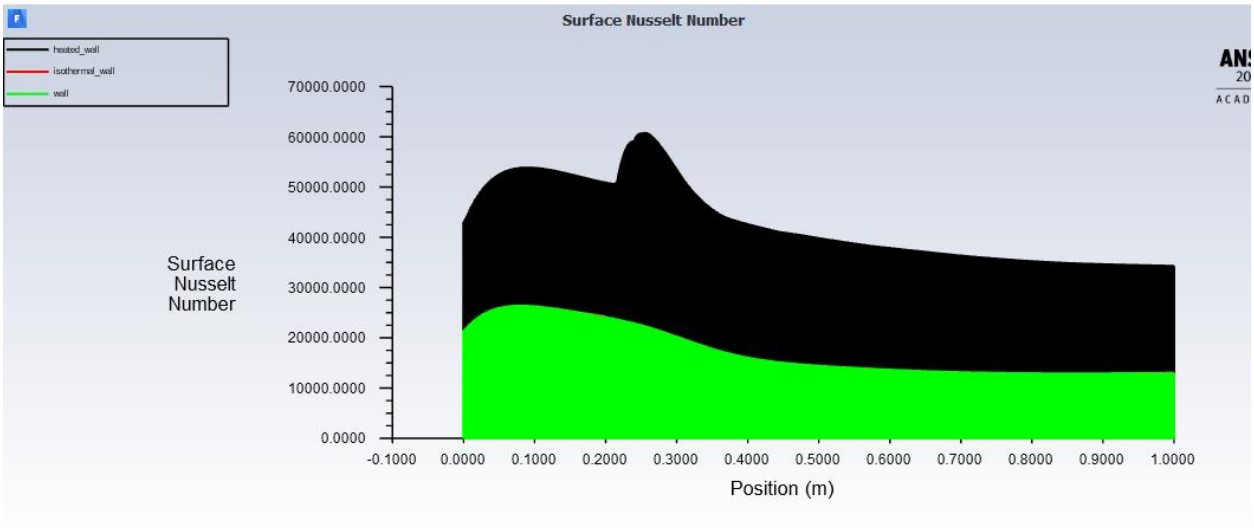

(a) ER=1.33

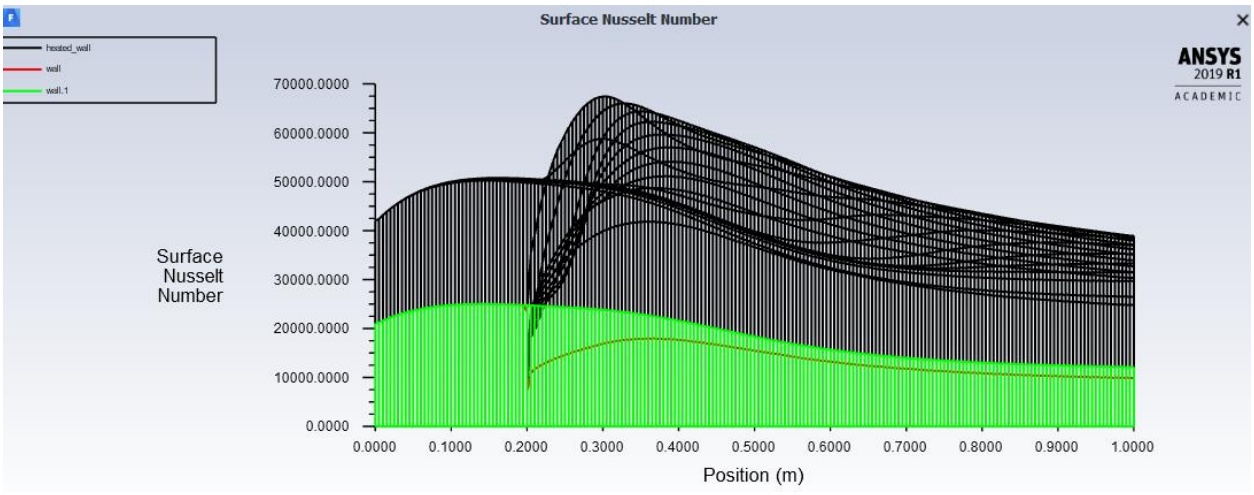

(b) ER=2

Figure (5.6) shows that skin friction coefficient decreases at the outlet with the increase in ER and the curve of skin friction coefficient in the region just after step height in inverted U-shape. With an increase in ER pick value is decreases. Figure (5.7) shows with an increase in ER Nusselt number in the region after step height increases slightly.

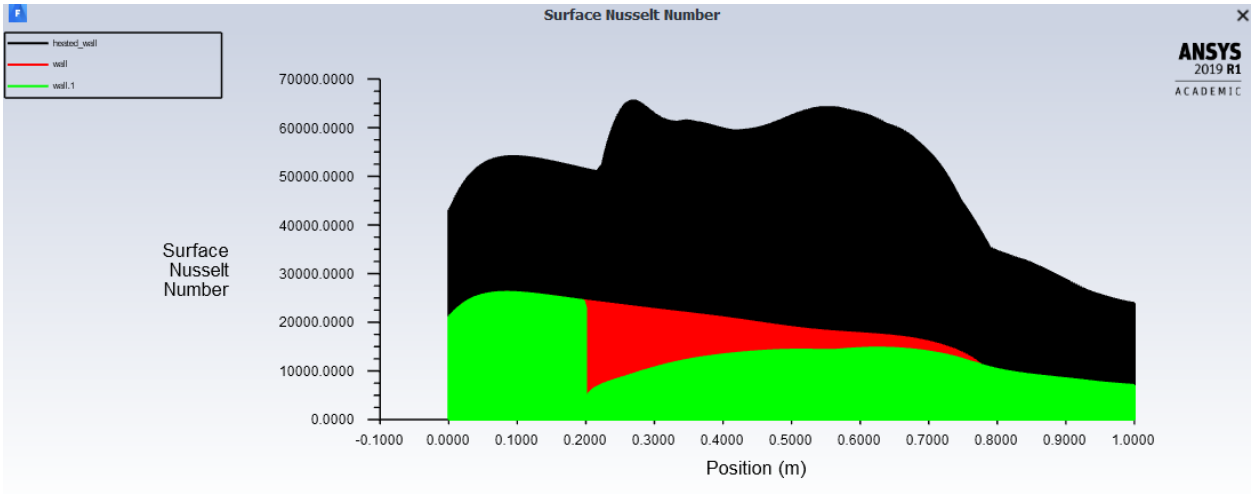

(c) ER=4

Figure 5.7. Effect of ER on surface Nusselt number

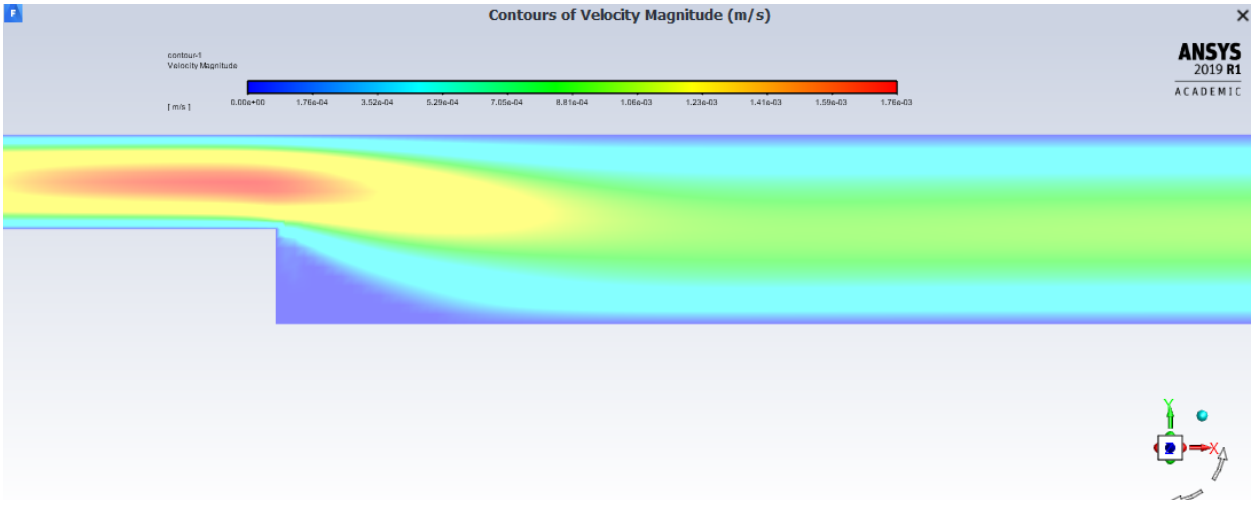

(a) Re= 66

Figure (5.8) shows with an increase in Reynolds number velocity magnitude in the region at the upper wall increases. And the recirculation region increases.

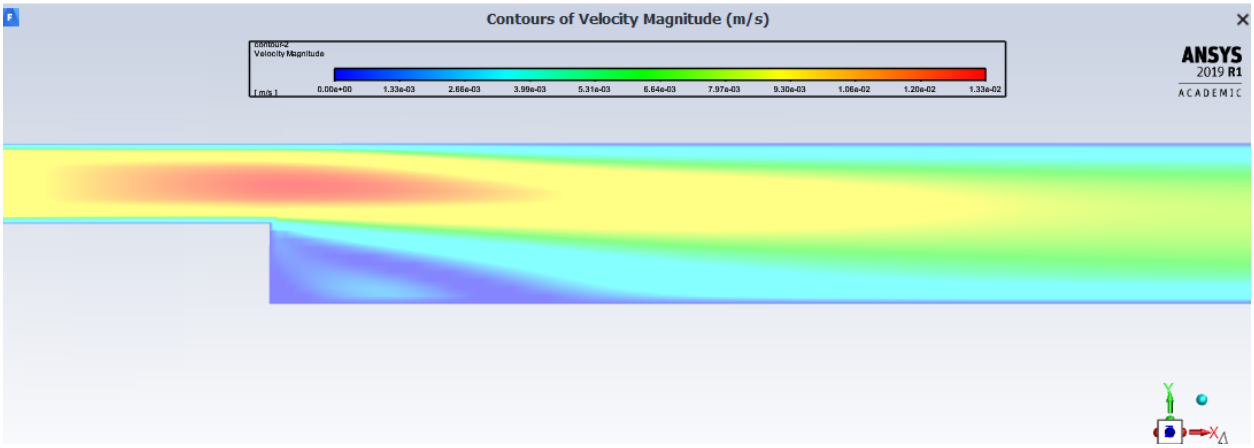

(b) Re= 660

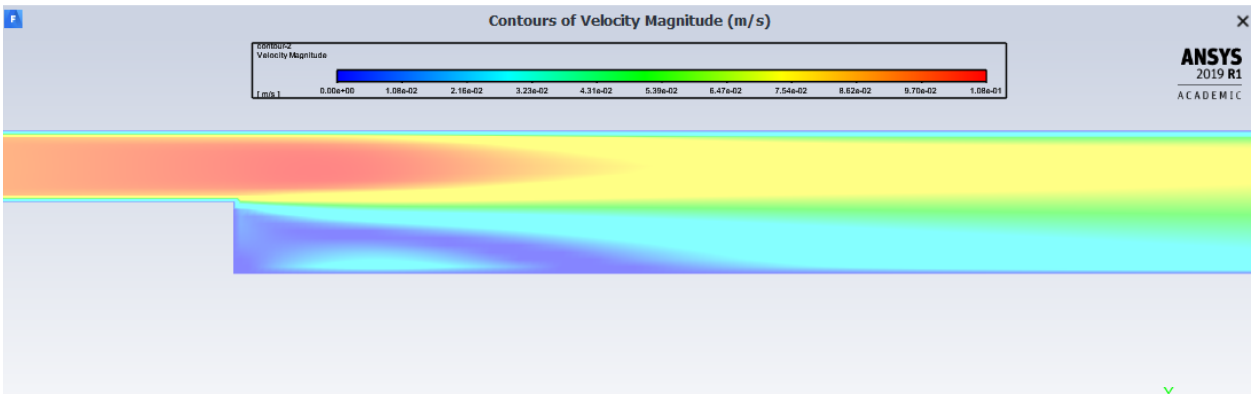

(c) Re=6600

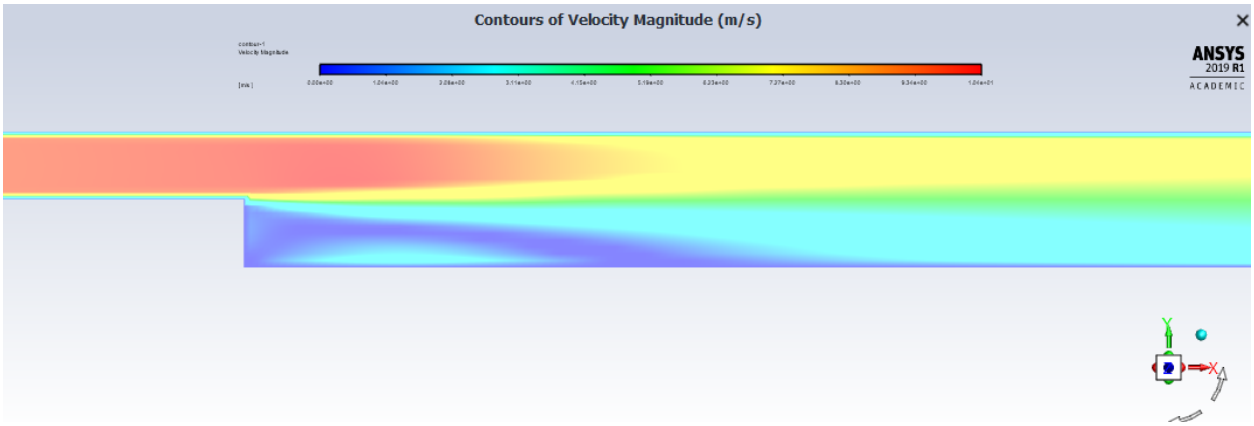

(d) Re=6.6*10^5

Figure 5.8. Effect of Reynolds number on reattachment length and velocity magnitude

Figure (5.8), demonstrate that reattachment length increases with increase in Reynolds number.

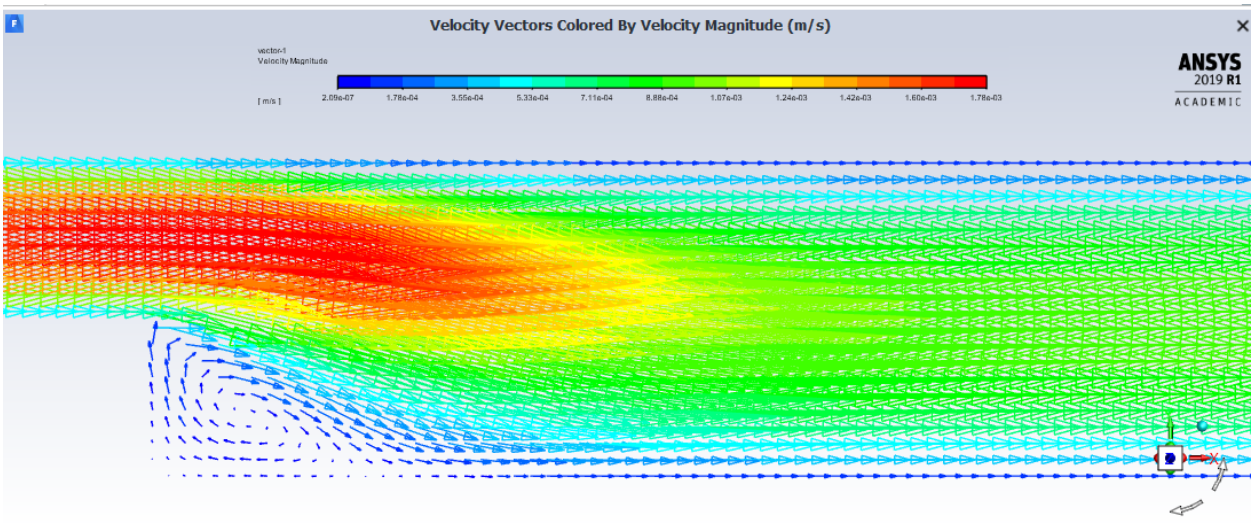

(a) Re= 66

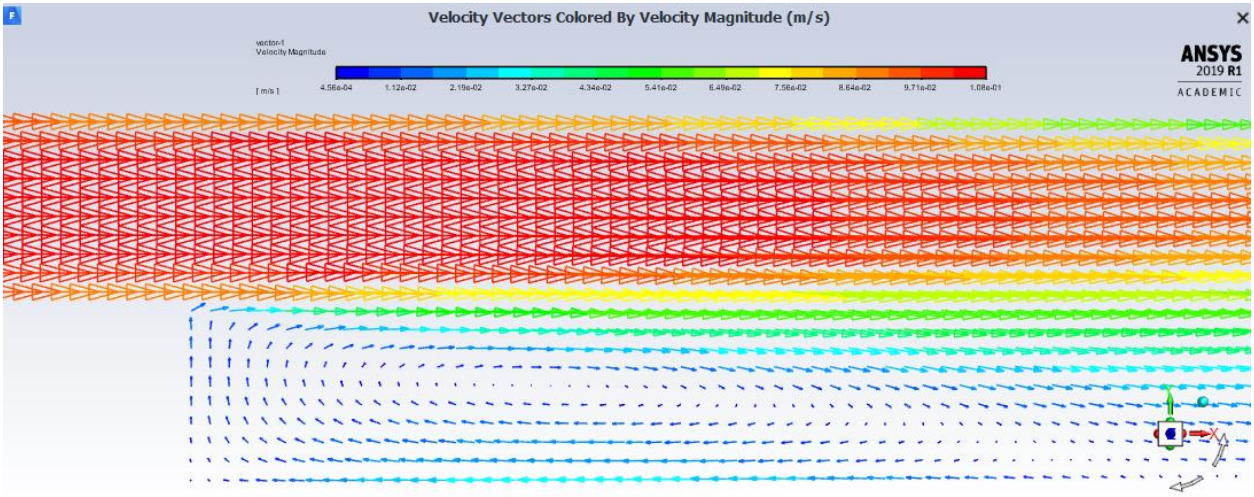

(b) Re= 660

Figure (5.9), demonstrate that the increase in Reynolds number leads to larger recirculation region. But at law Reynolds number stronger recirculation region is obtained. Higher velocity is in the region just above the step height.

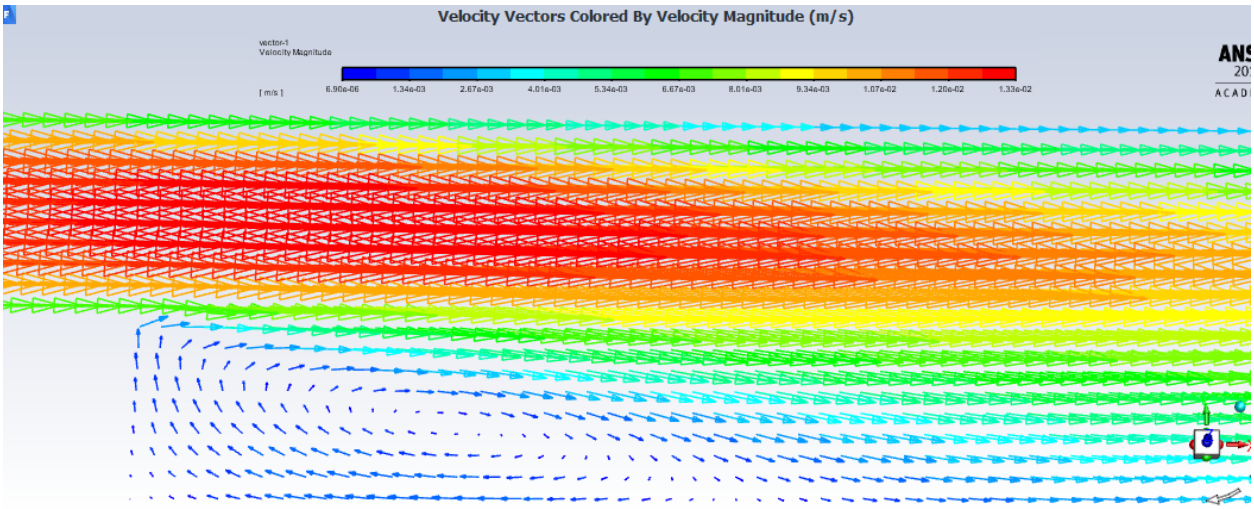

(c) Re=6600

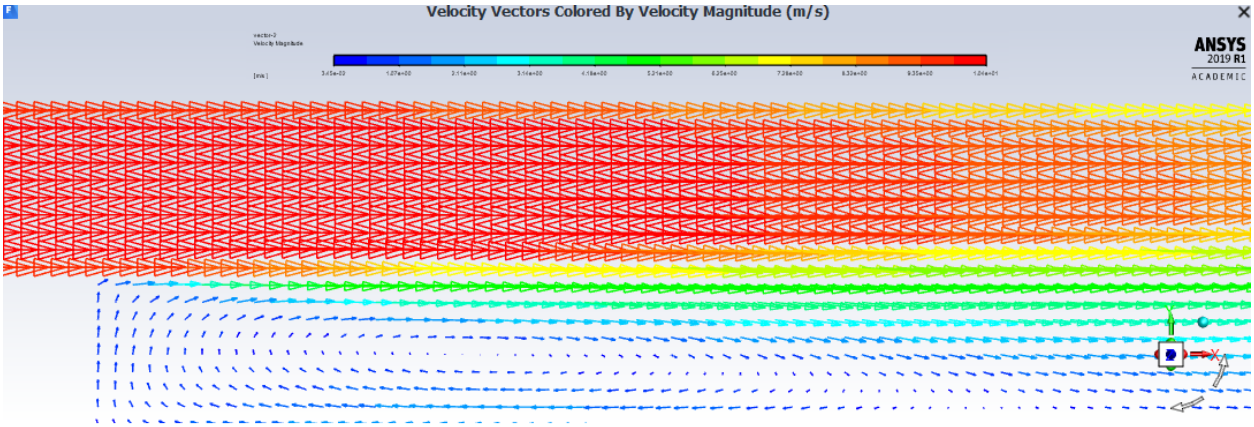

(d) Re=6.6*10^5

Figure 5.9. Effect of Reynolds number on recirculation zone (velocity vector near step height)

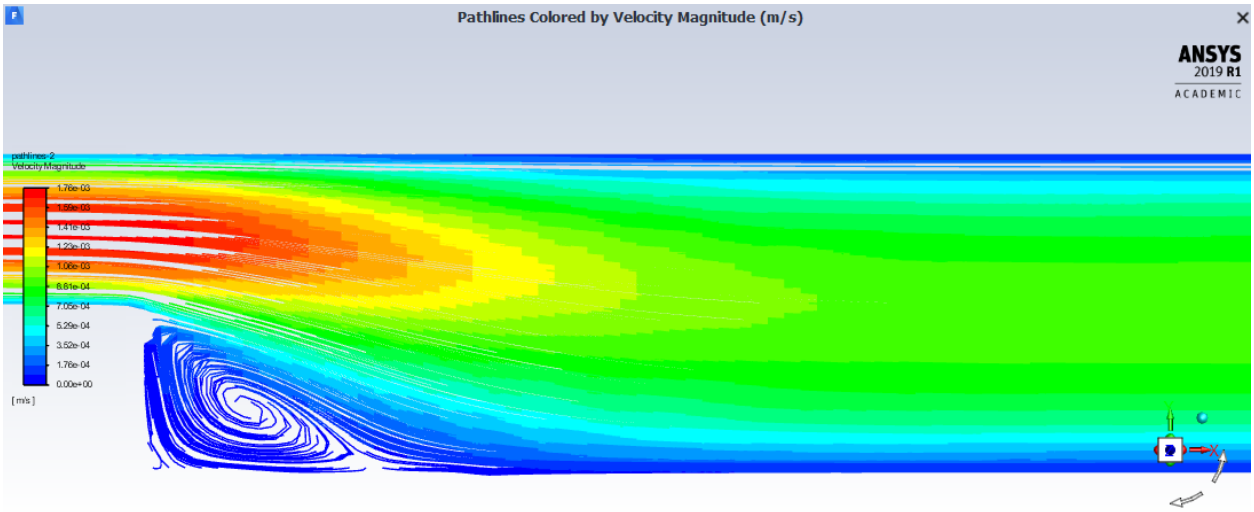

(a) Re=66

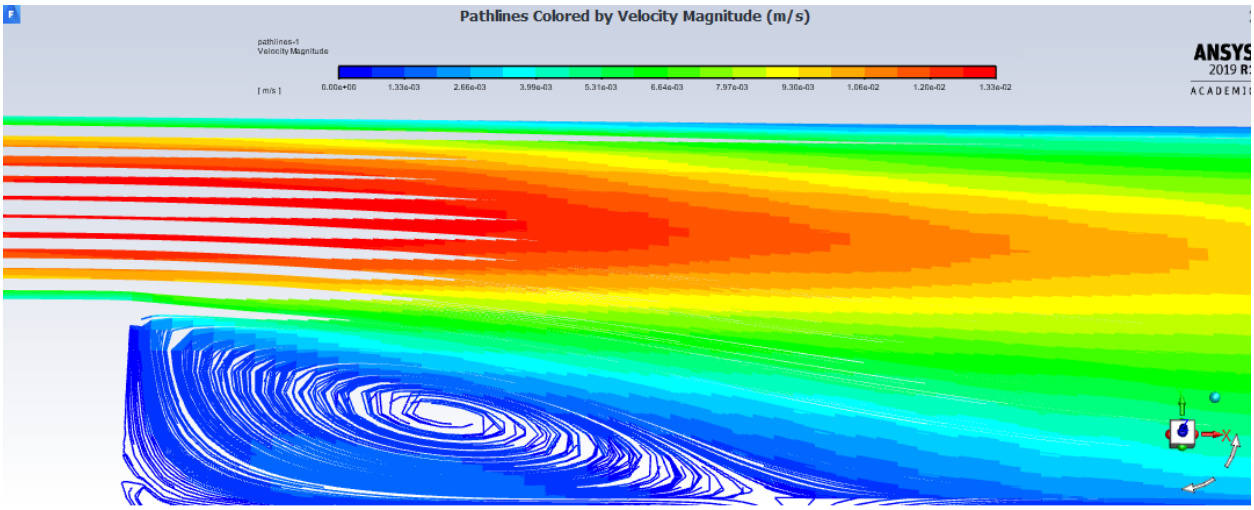

(b) Re=660

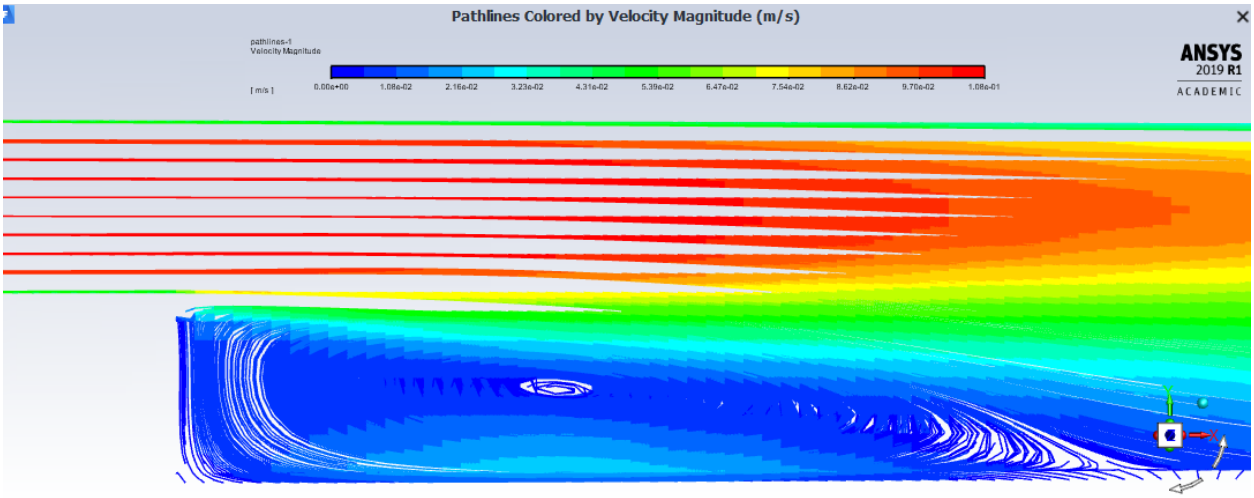

(c) Re=6600

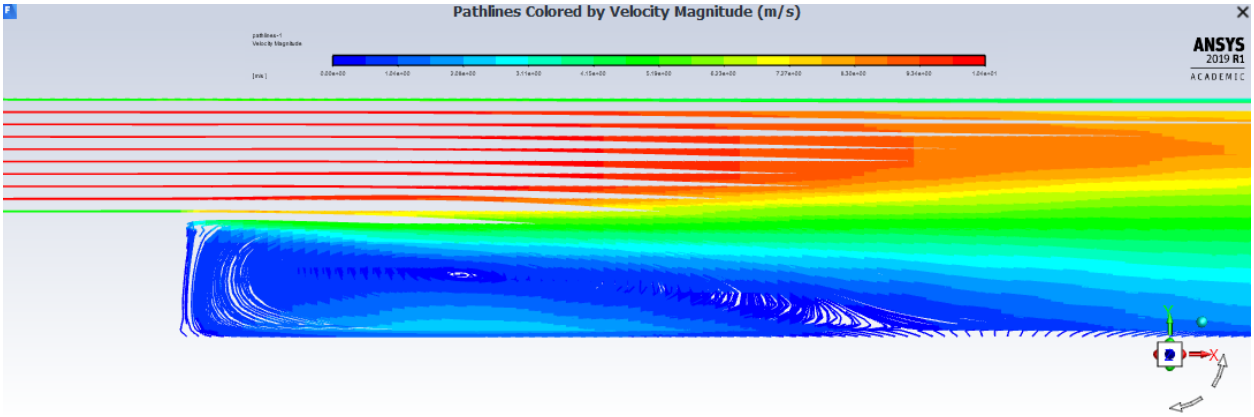

(d) Re=6.6*10^5

Figure 5.10. Effect of Reynolds number on streamline

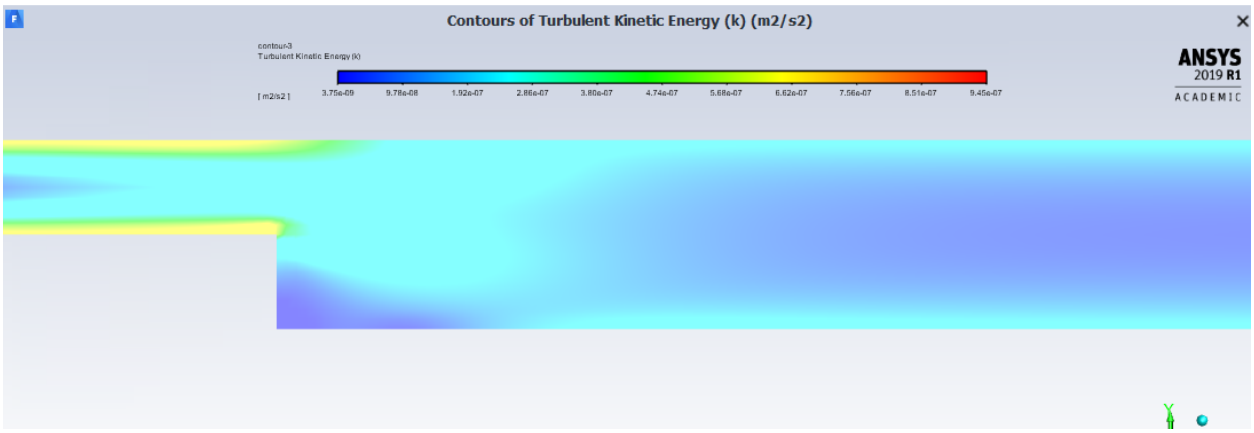

(a) Re=66

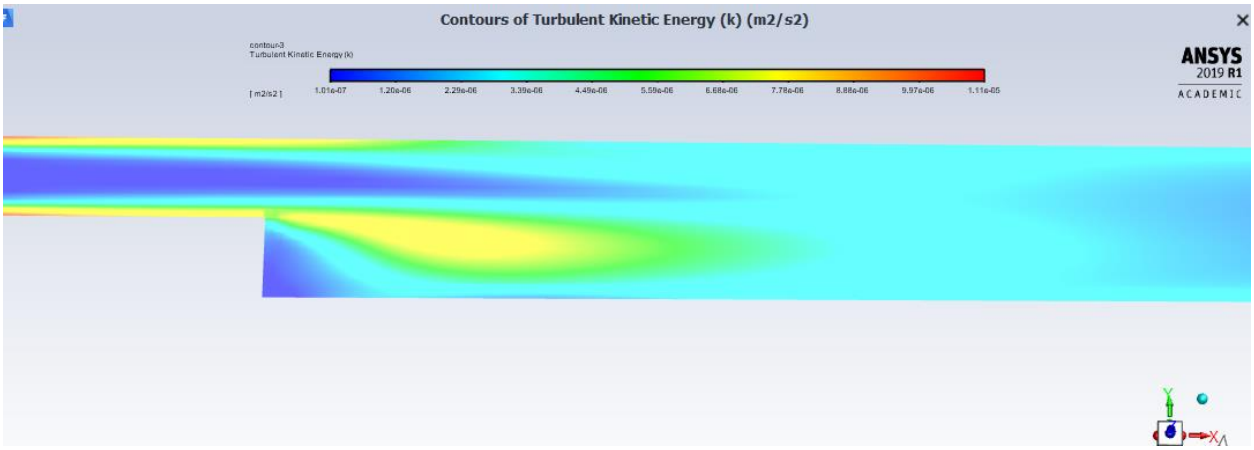

(b) Re=660

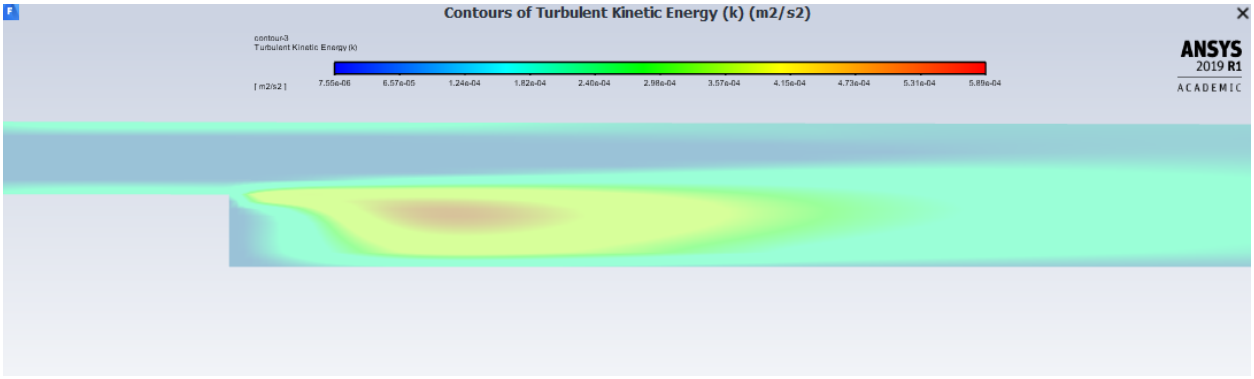

(c) Re= 6600

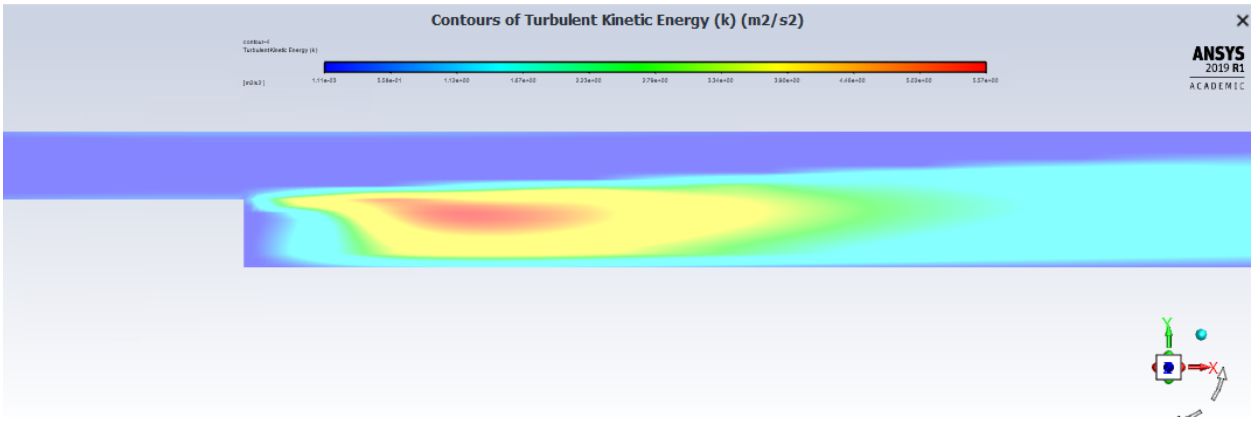

(d) Re=6.6*10^5

Figure 5.11. effect of Reynolds number on turbulence kinetic energy

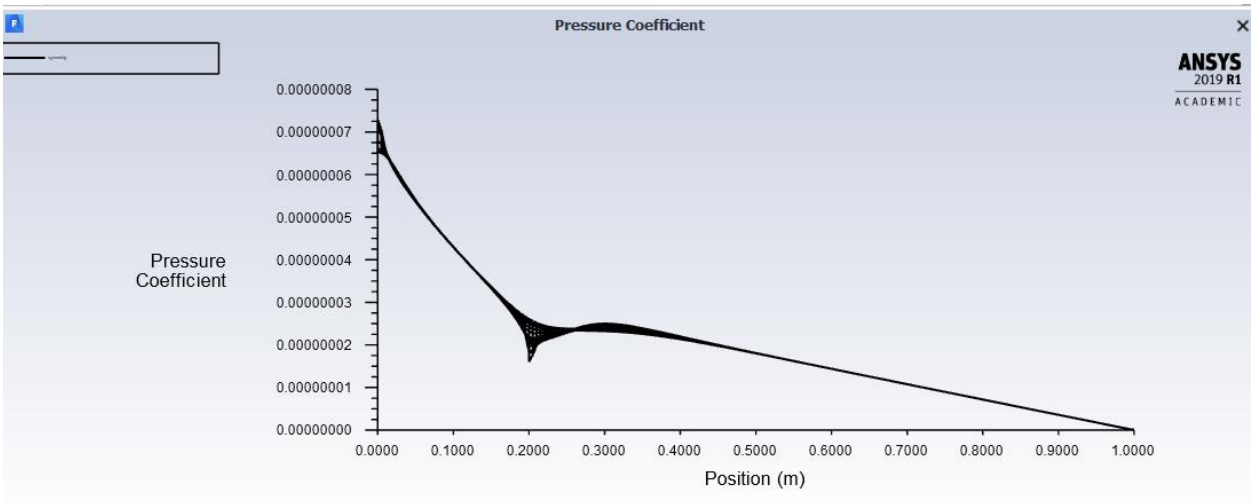

(a) Re=66

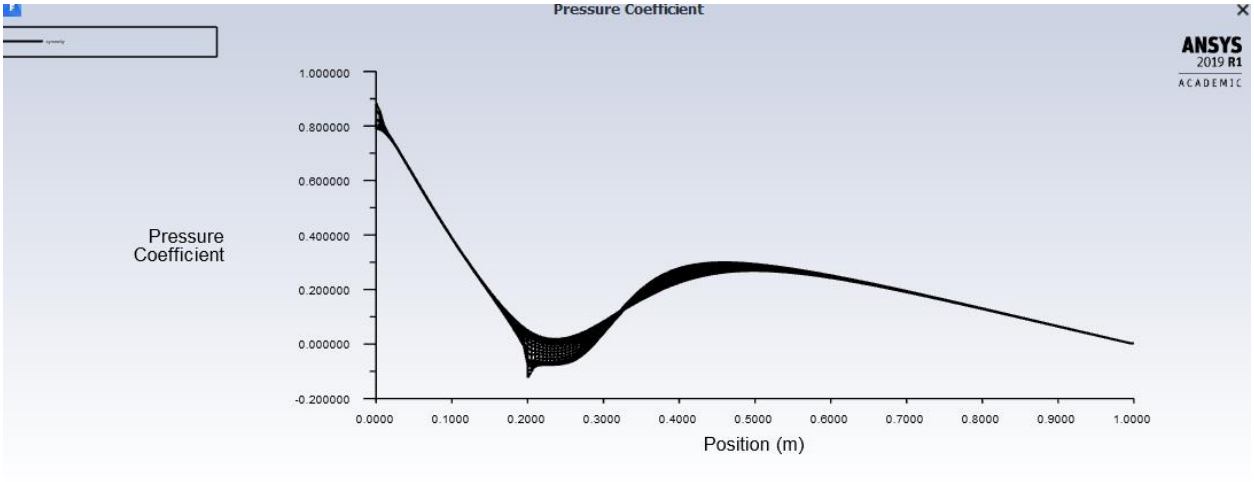

(b) Re=660

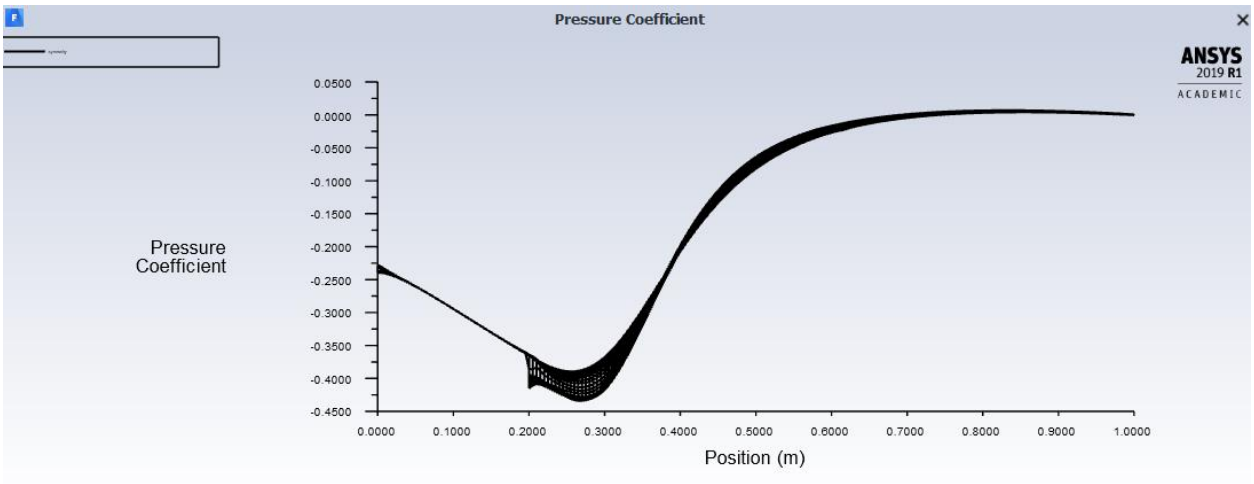

(c) Re=6600

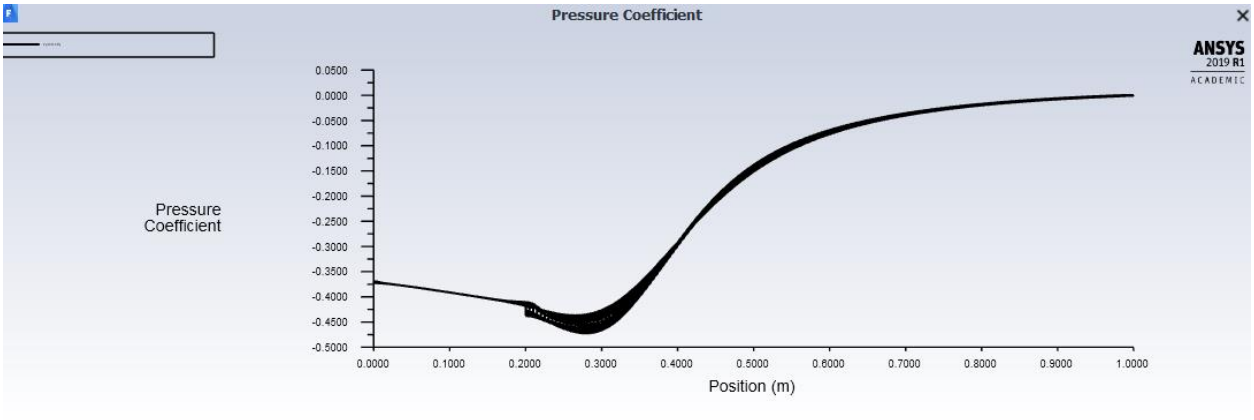

(d) Re=6.6*10^6

Figure 5.12. Effect of Reynolds number on pressure coefficient

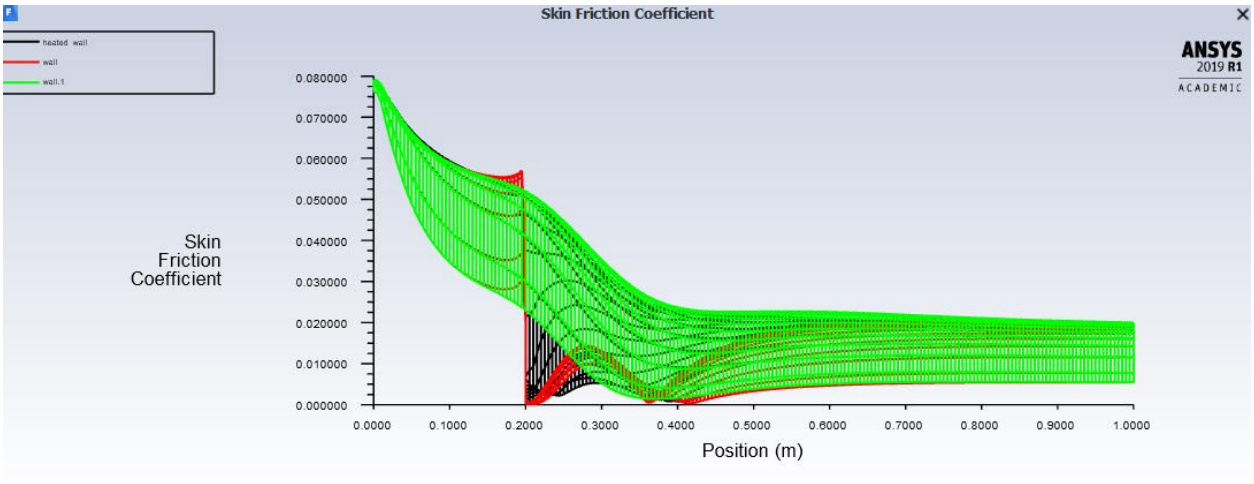

(a) Re=66

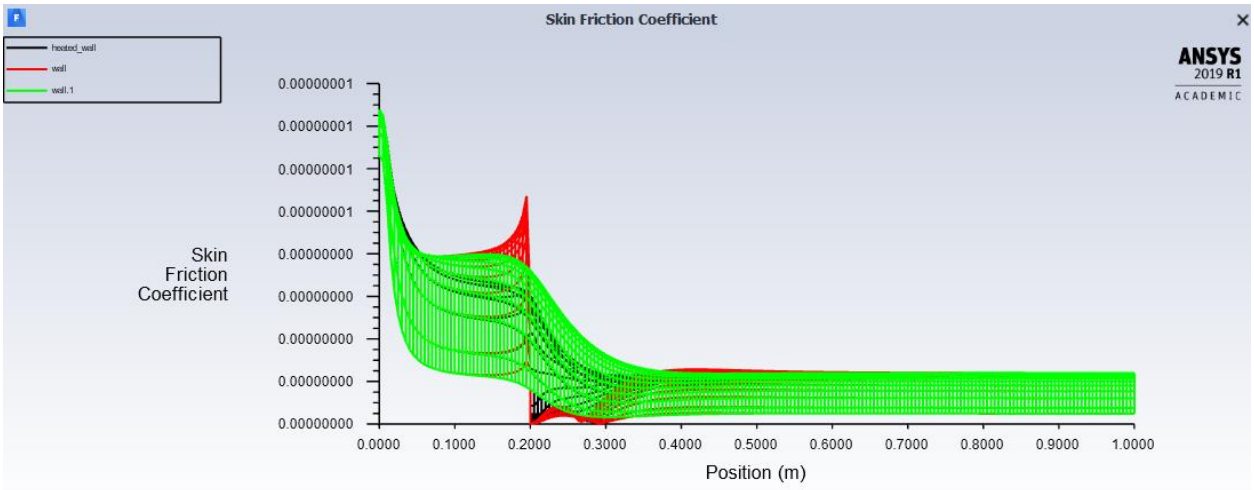

(b) Re=660

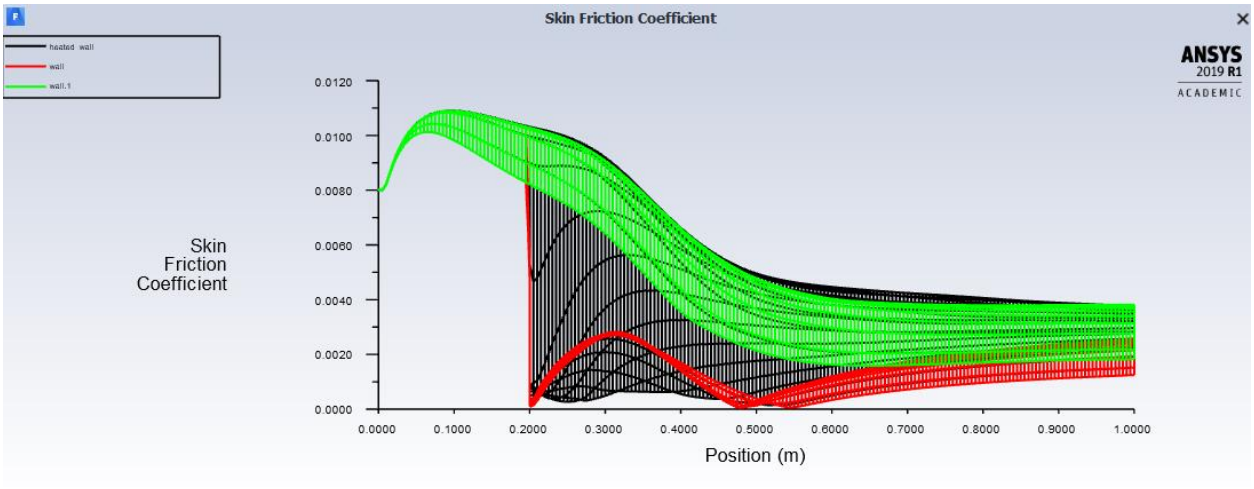

(c) Re=6600

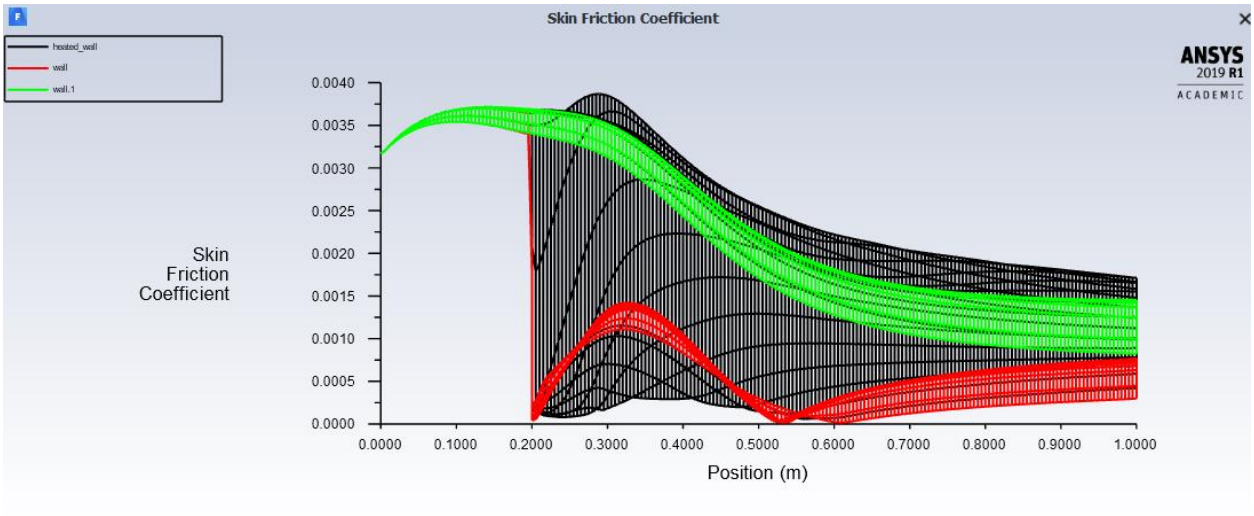

(d) Re=6.6*10^5

Figure 5.13. Effect of Reynolds number on skin friction coefficient

5.2 DUCT WITH DIFFERENT OBSTRUCTION HEIGHTS AND ARRANGEMENTS

Computational results of the velocity vectors and the streamline for staggered and inline baffles plates are found in fig.(5.14)

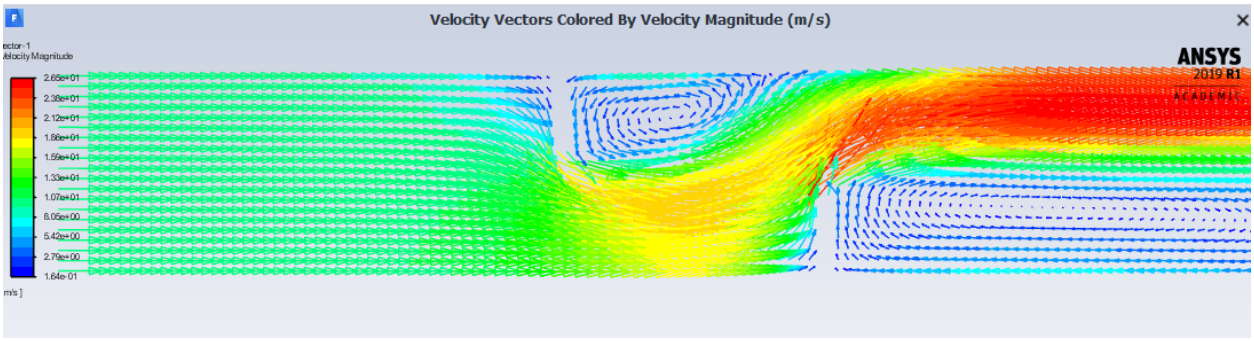

(a)

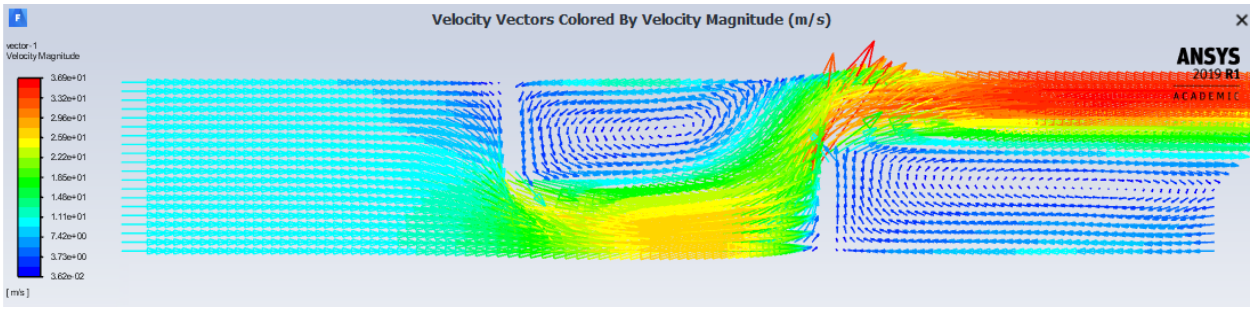

(b)

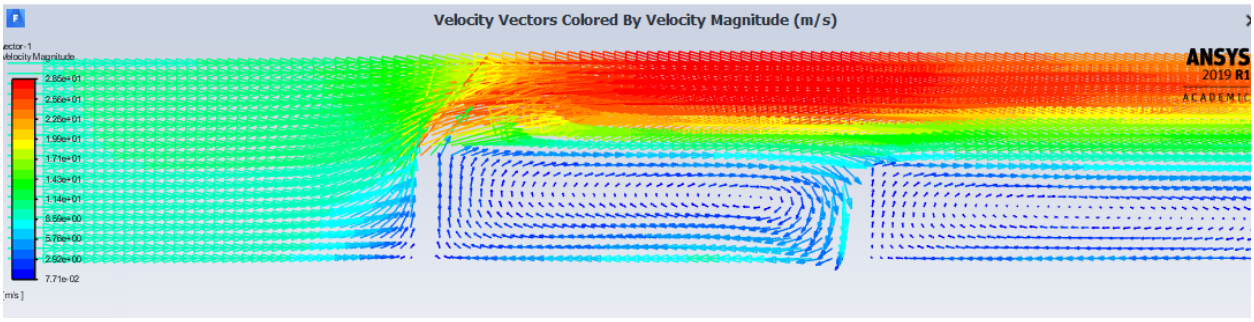

(c)

Figure 5.14. Effect of baffle plates arrangement of velocity field distribution

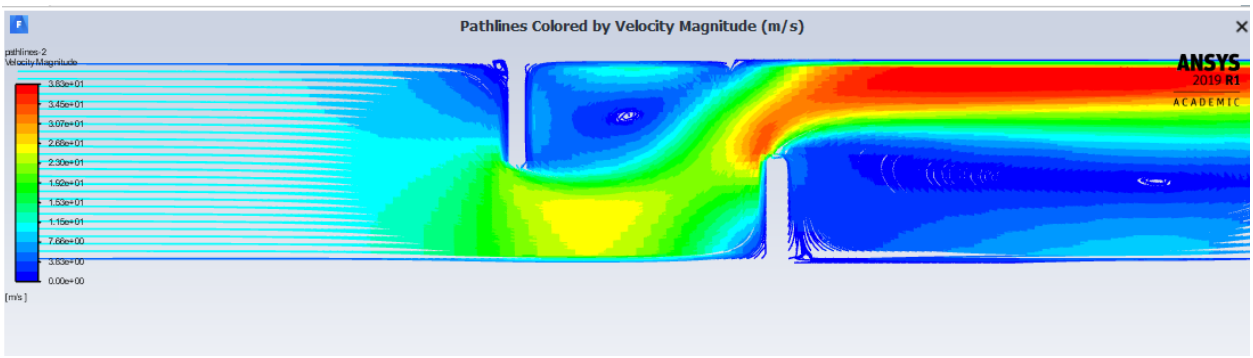

(a)

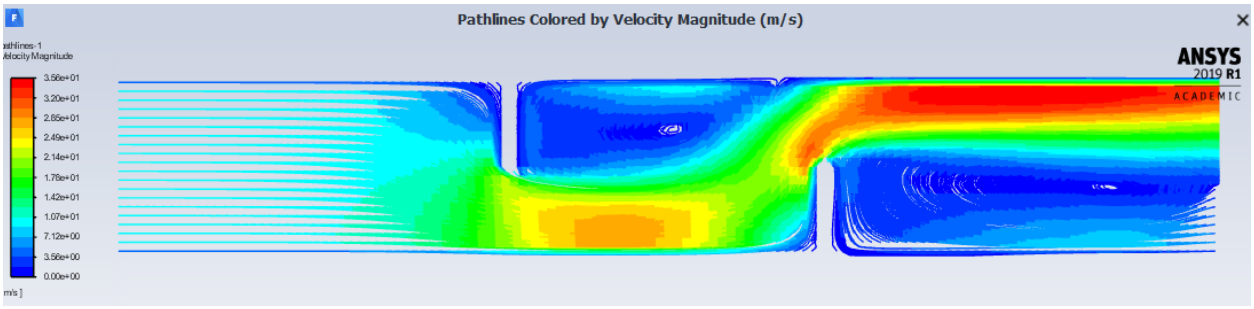

(b)

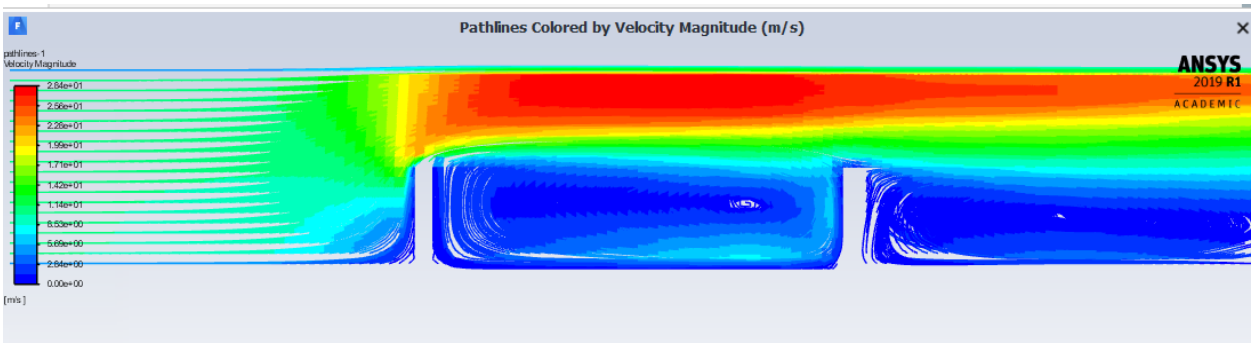

(c)

Figure 5.15. Streamline with baffle plates arrangement

It is evident there is a separation of the boundary layer, just close the upstream of the baffle and a recirculation zone behind the baffles plate. The figure shows that the spacing between the plate affected the recirculation region length as depicted in case (a) and (b). The spacing between the baffles in case (b) is large and the recirculation is increased. The arrangement of the case (a) and case (b) is called a staggered. Also, the figure shows that the flow between the baffle is accelerated and the value of the velocity are high at the upper part of the duct. In case (c), the baffle plates are in a line arrangement. The recirculation region is less compared with the case (b)

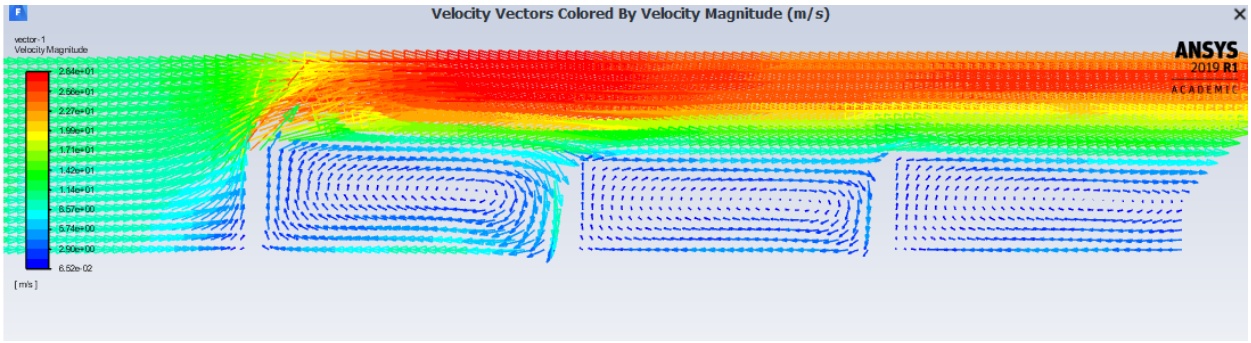

(a)

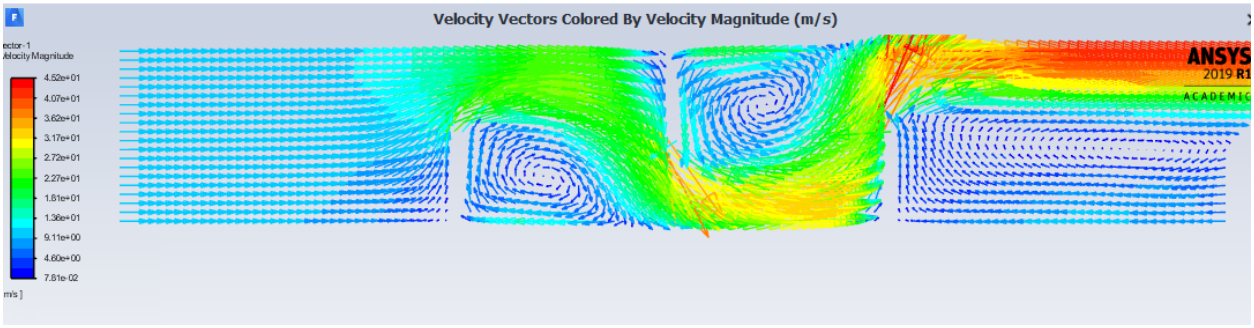

(b)

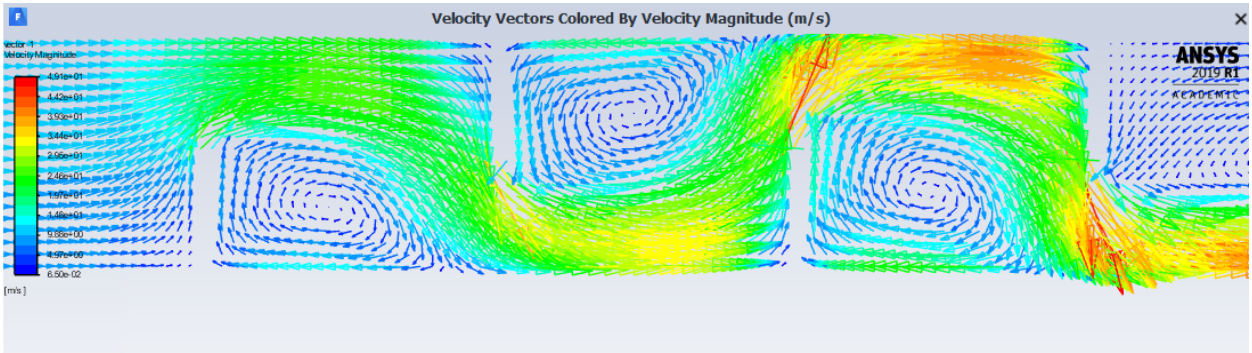

(c)

Figure 5.16. Effect of number of baffle plates on the velocity field distribution

This fig (5.16), demonstrates the effect of increasing the number of the baffles on the velocity field distribution. It is clear that in the inline arrangement, case (a), the increase of the number of baffles increases the recirculation region, especially down stream the second and third baffle. When the number of baffles in the staggered state is increased, the recirculation regions and separation of the boundary layer is increases for the three baffle plates and decreased for the fourth one as in case (b) and (c).

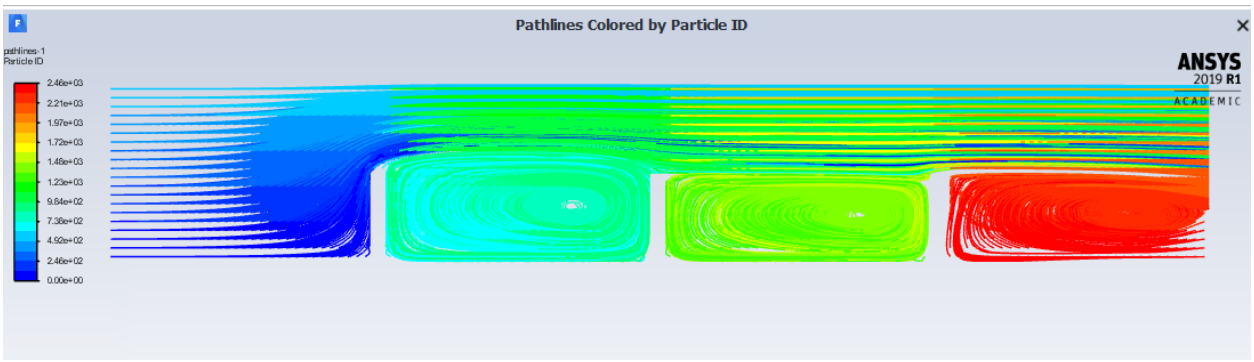

(a)

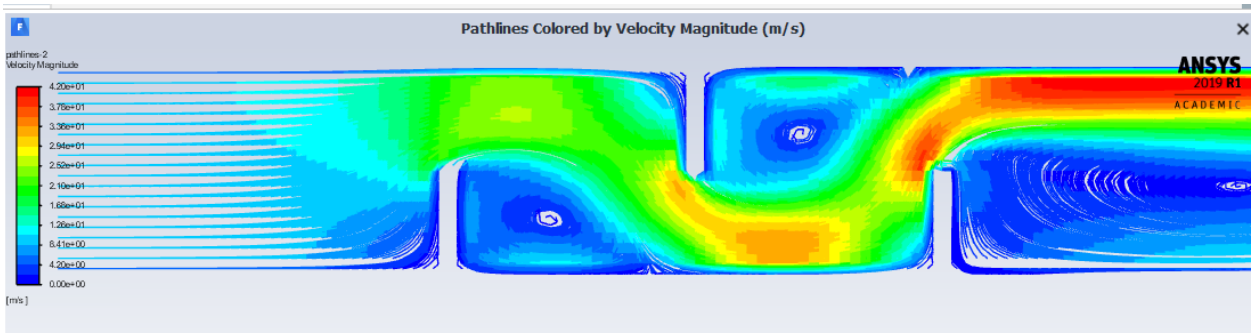

(b)

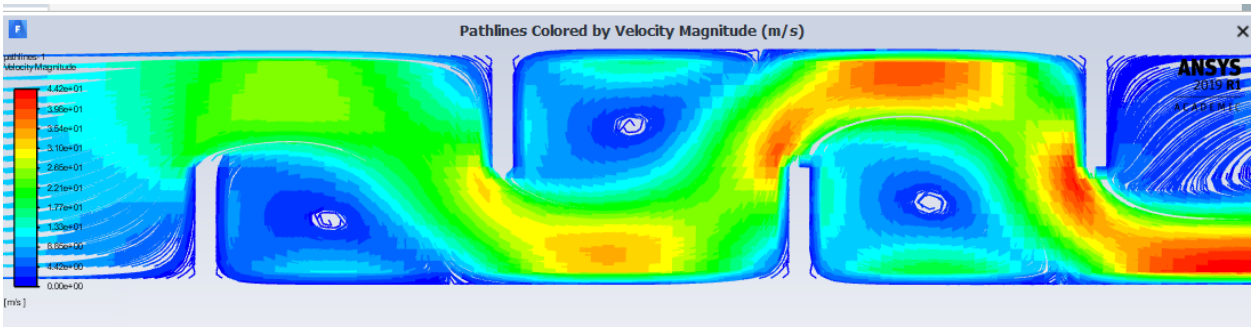

(c)

Figure 5.17. Streamlines with different numbers and locations of baffle plates

Fig.(5.17), shows that stream lines are deflected just close to the baffles and a recirculation occurs down stream of the baffle.

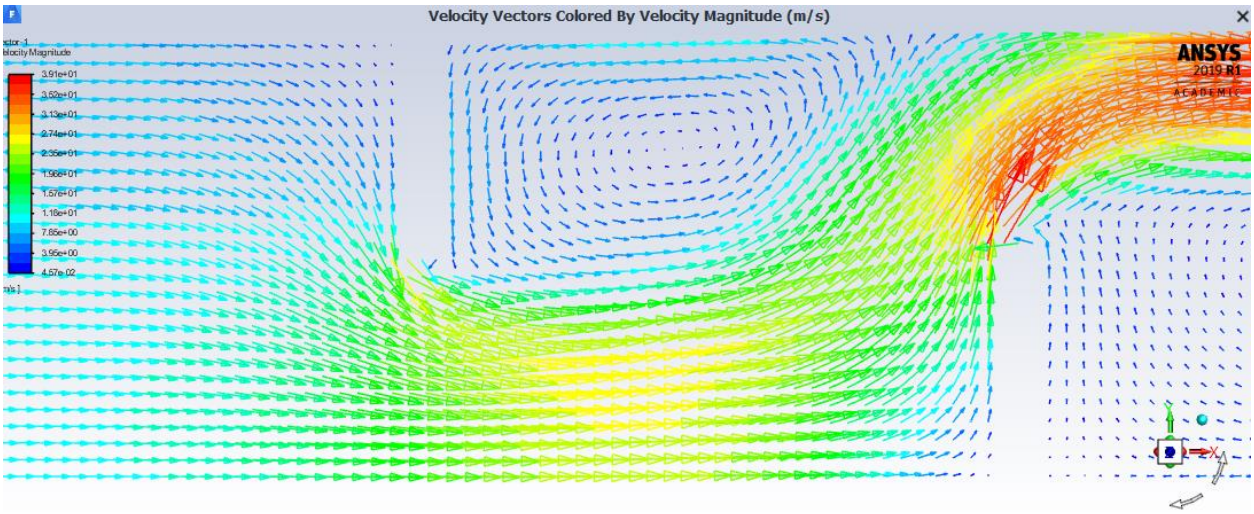

(a)

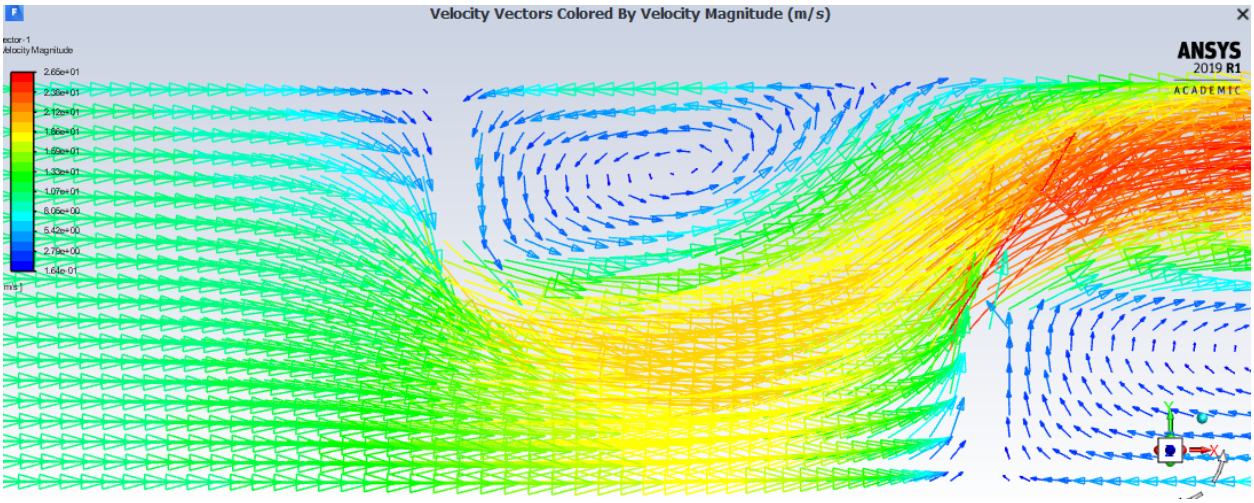

(b)

Figure 5.18. Effect of baffle plate height on the flow field

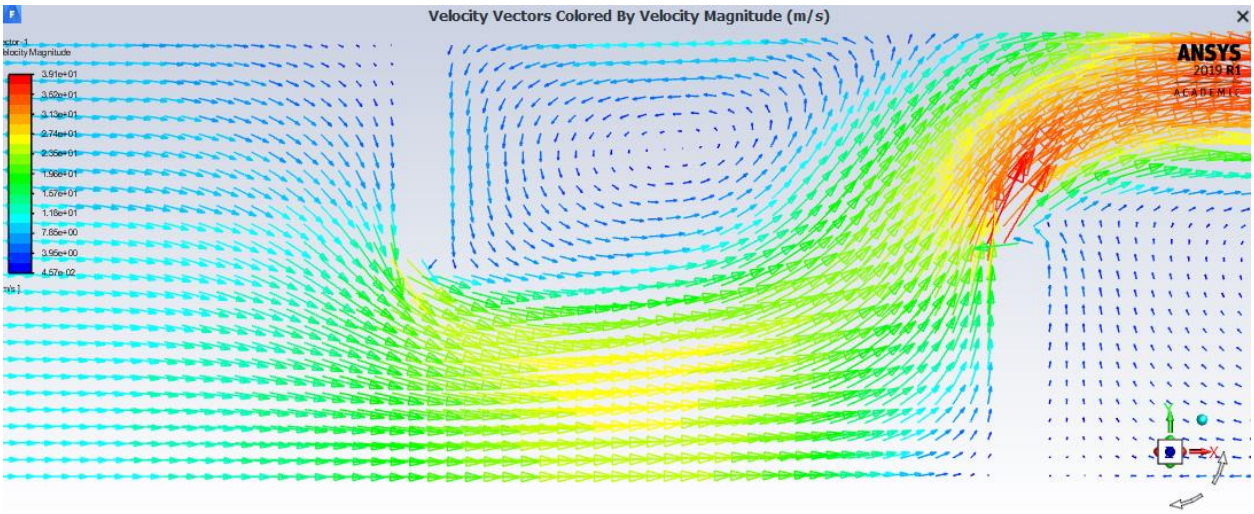

(a)

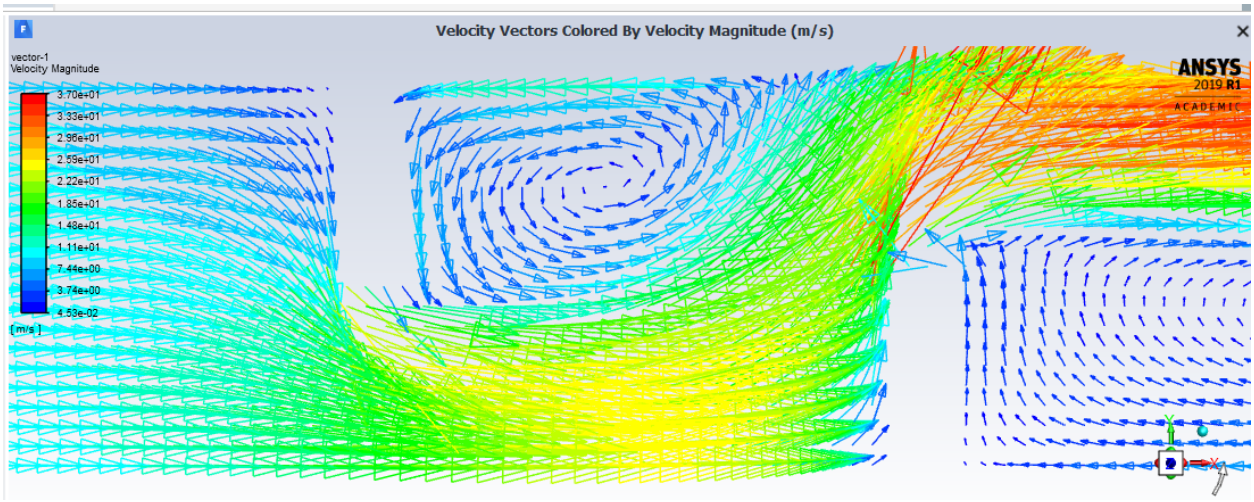

(b)

Figure 5.19. Effect of baffle plate width on flow field

The separation of the boundary layer and recirculation regions are strongly effected with the thickness of the baffle and baffle height as depicted in fig.(5.18) and fig.(5.19). figure(5.18), shows the influence of baffle height on the boundary layer separation regions both in inline and staggered arrangement. It is evident that recirculation regions are decreases with the decrease of baffle height. The acceleration of the flow is decreased, hence the value of the velocity is less because the contraction area is large. Figure(5.19), exhibits the effect of baffle thickness on the flow field distribution both mentioned arrangement. as the case (b) shows, recirculation becomes stronger when the baffle thickness increased. However, the value of velocity in the upper wall is less than in case (a), when the thickness is decreased, the separation of the boundary layer and recirculation region is decreased.

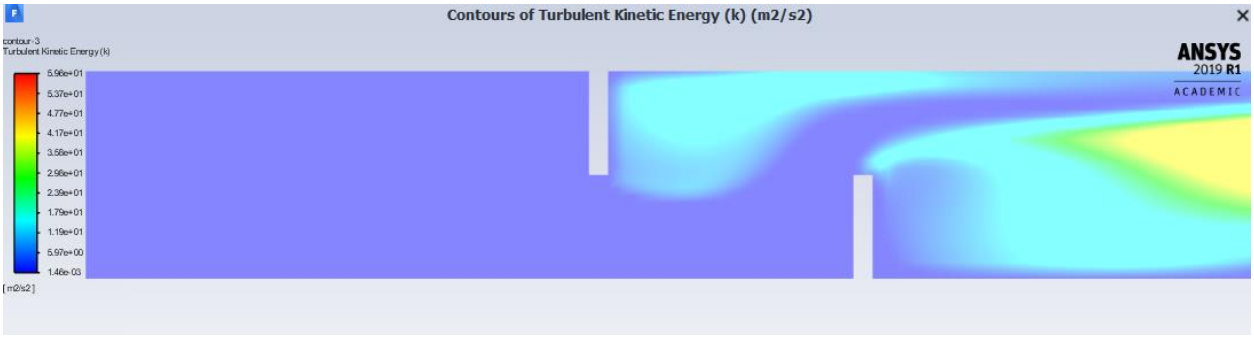
Contours of Turbulent Kinetic Energy (k) (m2/s2)
contour-3
Turbulent Kinetic Energy (k)
5.96e+01
5.37e+01
4.77e+01
4.17e+01
3.58e+01
2.98e+01
2.39e+01
1.79e+01
1.19e+01
5.97e+00
1.46e-03
[m2/s2]
ANSYS
2019 R1
ACADEMIC

(a)

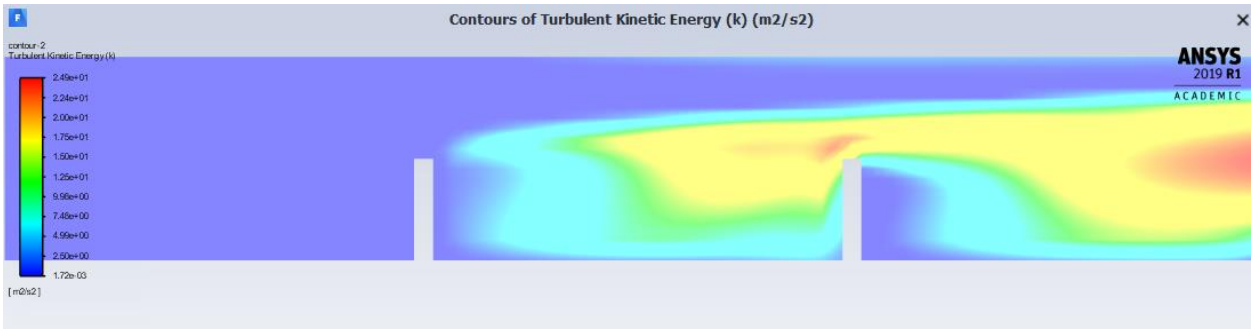
Contours of Turbulent Kinetic Energy (k) (m2/s2)
contour-2
Turbulent Kinetic Energy (k)
2.49e+01
2.24e+01
2.00e+01
1.75e+01
1.50e+01
1.25e+01
9.96e+00
7.48e+00
4.99e+00
2.50e+00
1.72e-03
[m2/s2]
ANSYS
2019 R1
ACADEMIC

(b)

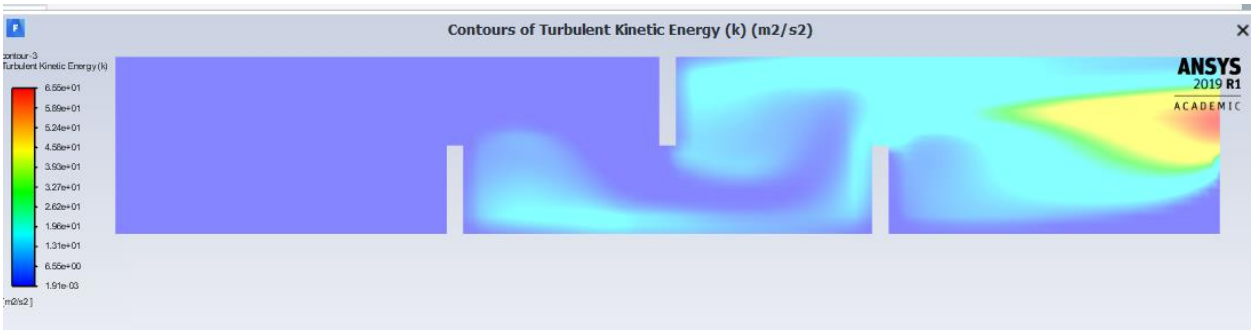
Contours of Turbulent Kinetic Energy (k) (m2/s2)
contour-3
Turbulent Kinetic Energy (k)
6.55e+01
5.89e+01
5.24e+01
4.58e+01
3.93e+01
3.27e+01
2.62e+01
1.96e+01
1.31e+01
6.55e+00
1.91e-03
[m2/s2]
ANSYS
2019 R1
ACADEMIC

(c)

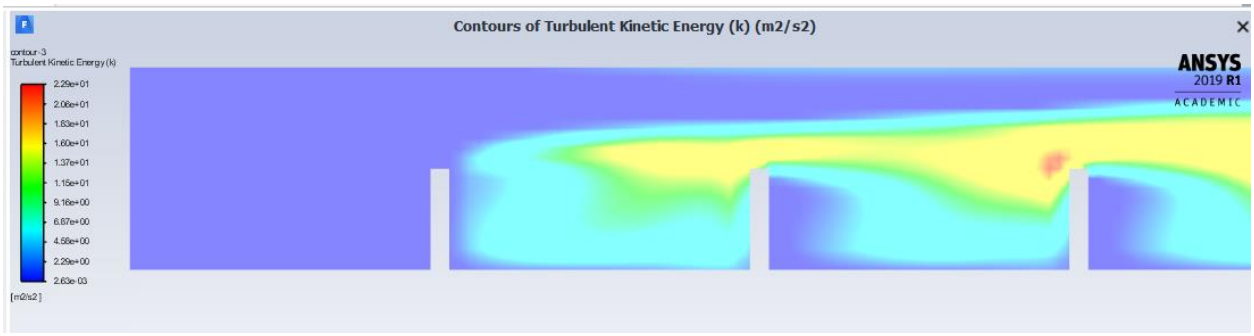
Contours of Turbulent Kinetic Energy (k) (m2/s2)
contour-3
Turbulent Kinetic Energy (k)
2.29e+01
2.06e+01
1.83e+01
1.60e+01
1.37e+01
1.15e+01
9.16e+00
6.87e+00
4.58e+00
2.29e+00
2.63e-03
[m2/s2]
ANSYS
2019 R1
ACADEMIC

(d)

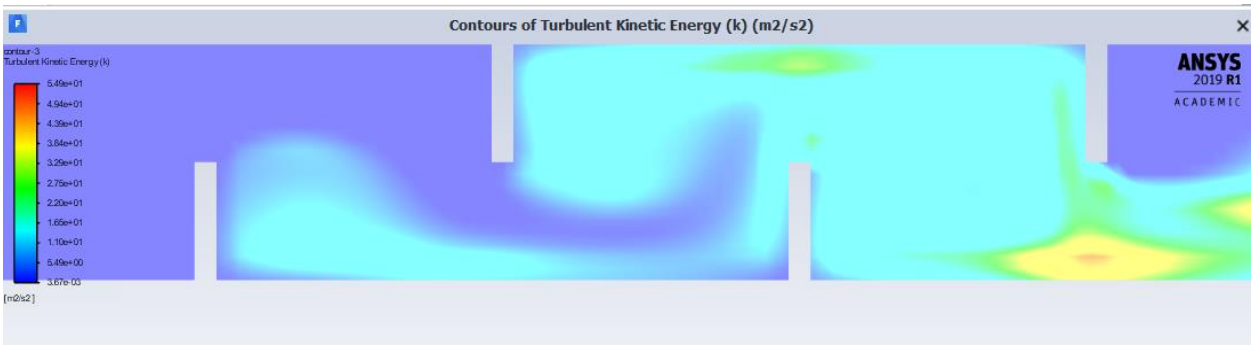

(e)

Figure 5.20. Contours of turbulent kinetic energy with Re 1.23*10^6

Figure (5.20), demonstrates the contour plots of turbulence kinetic energy. The figure shows that the higher value of turbulent kinetic energy occurs at the region down stream and just above the baffle. This is due to the acceleration of flow in these regions.

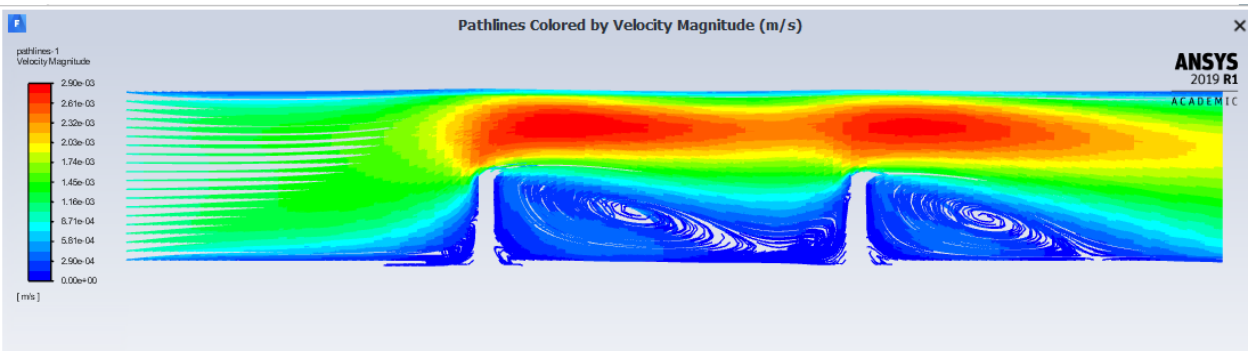

(a) Re=123

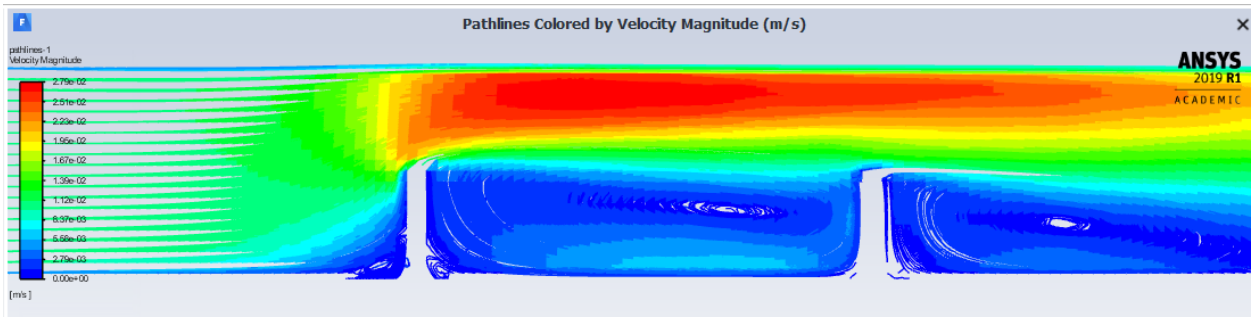

(b) Re=1230

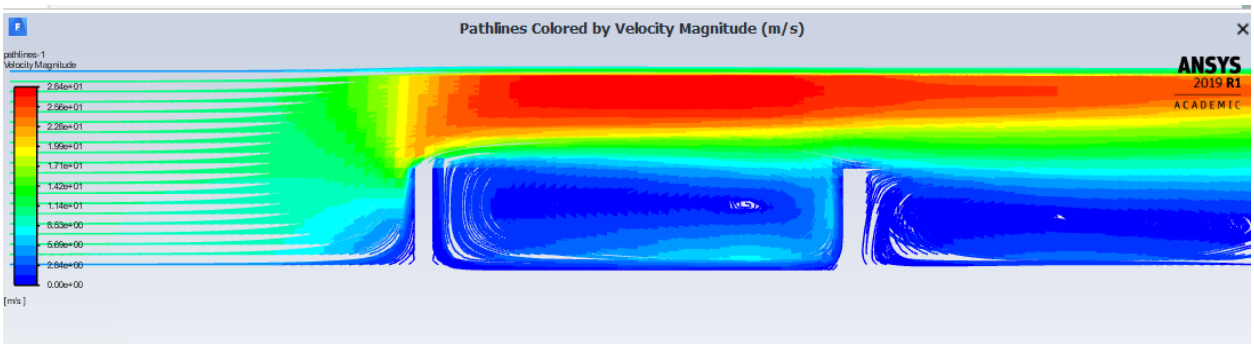

(c) Re=1.23*10^6

Figure 5.21. Effect of Reynolds number on stream line

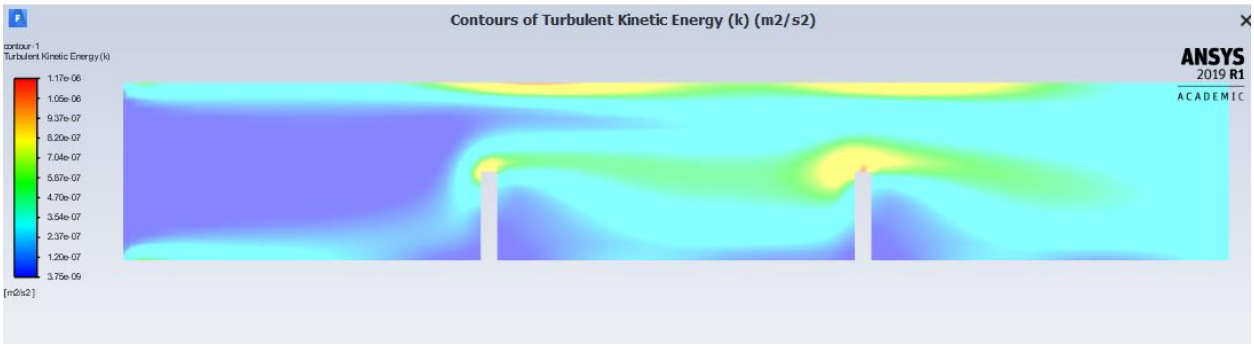

(a) Re= 123

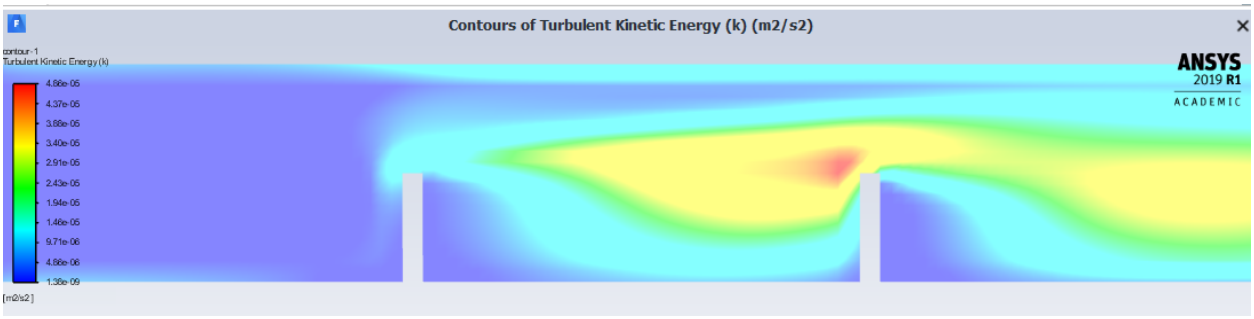

(b) Re= 1230

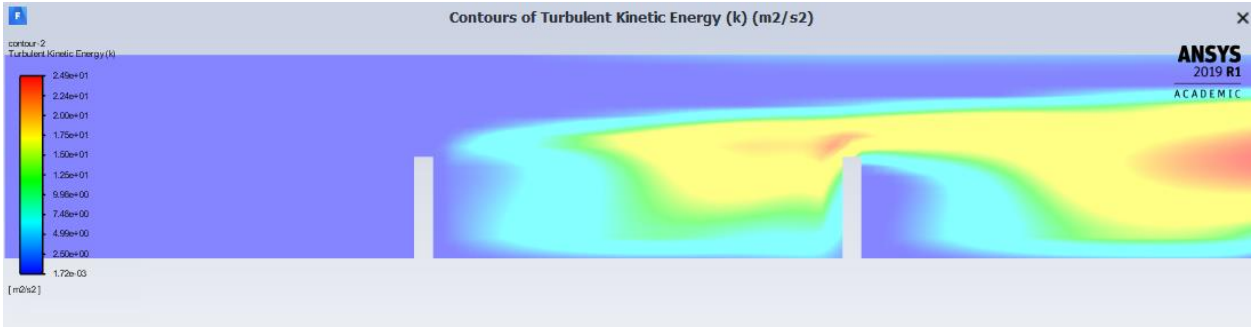

(c) Re= 1.23*10^6

Figure 5.22. Effect of Reynolds number on turbulence kinetic energy

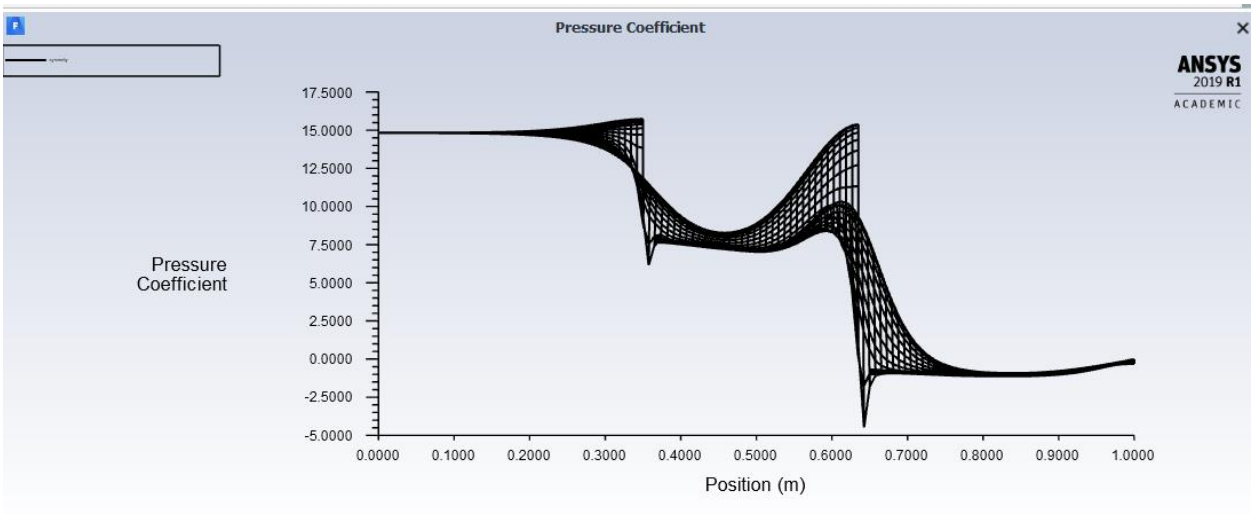

(a) cp of two staggered baffle plates

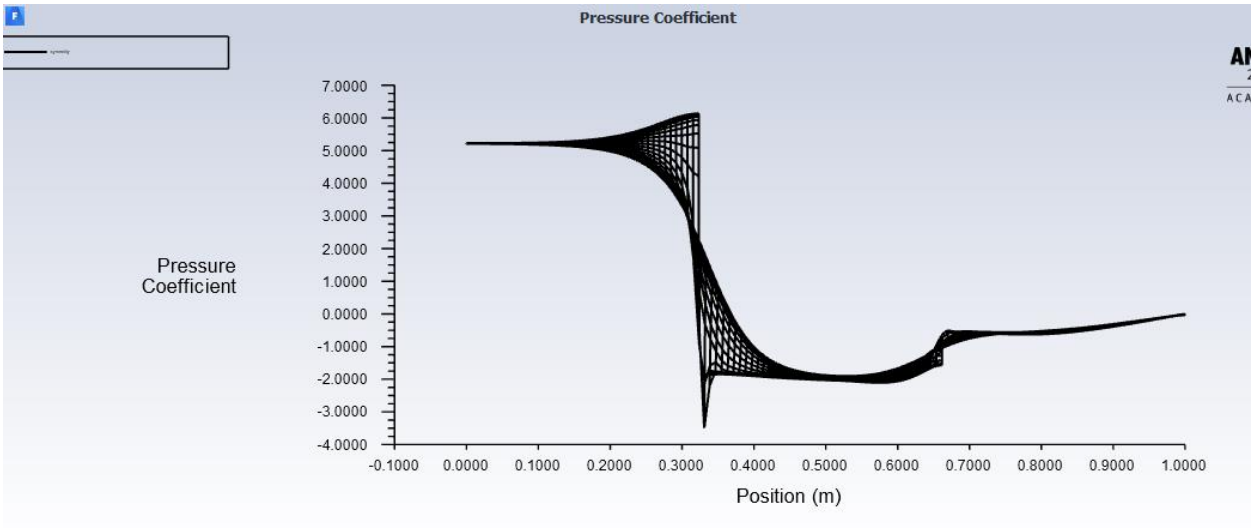

(b) cp of two inline baffles plate

Figure(5.21), shows the effect of Re on the stream wise velocity. The velocity increases with the increase of Reynolds number. This dominant in all the studied cases.Figure (5..23), exhibit the variation of pressure coefficient on the duct length for different baffle plates arrangement with a specified Reynolds number. The results shows that the pressure coefficient remains constant at the entrance and the outlet of the duct. The coefficient of pressure is increased at the first obstruction a decrease at the subsequent obstuction. With increasing the number of obstruction pressure coefficient increase. Also with the height pressure coefficient increases. The lower values near the tip of the baffles are due to high velocities in that region.

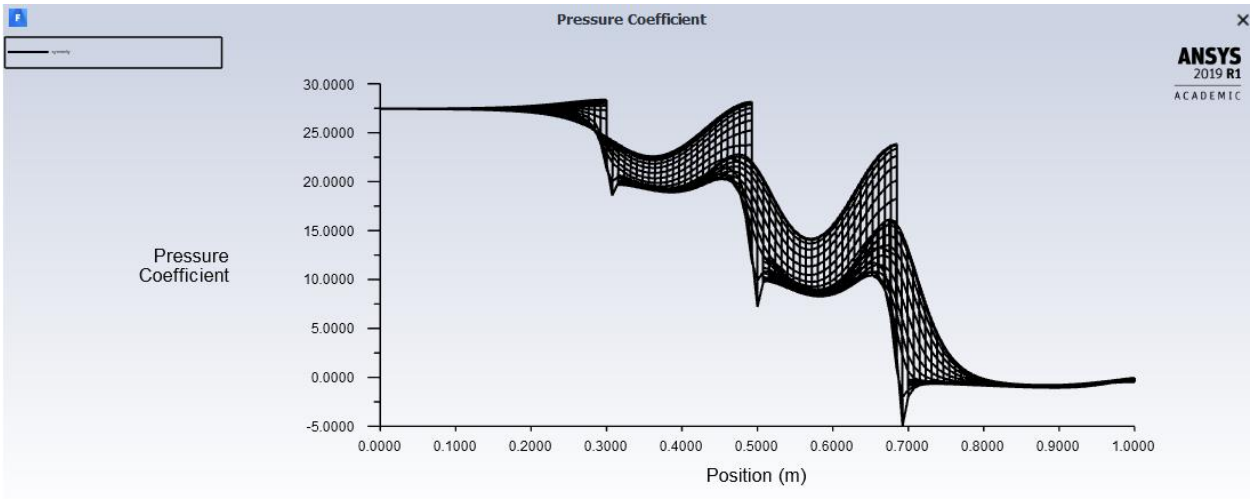

(c) cp of three staggered baffle plates

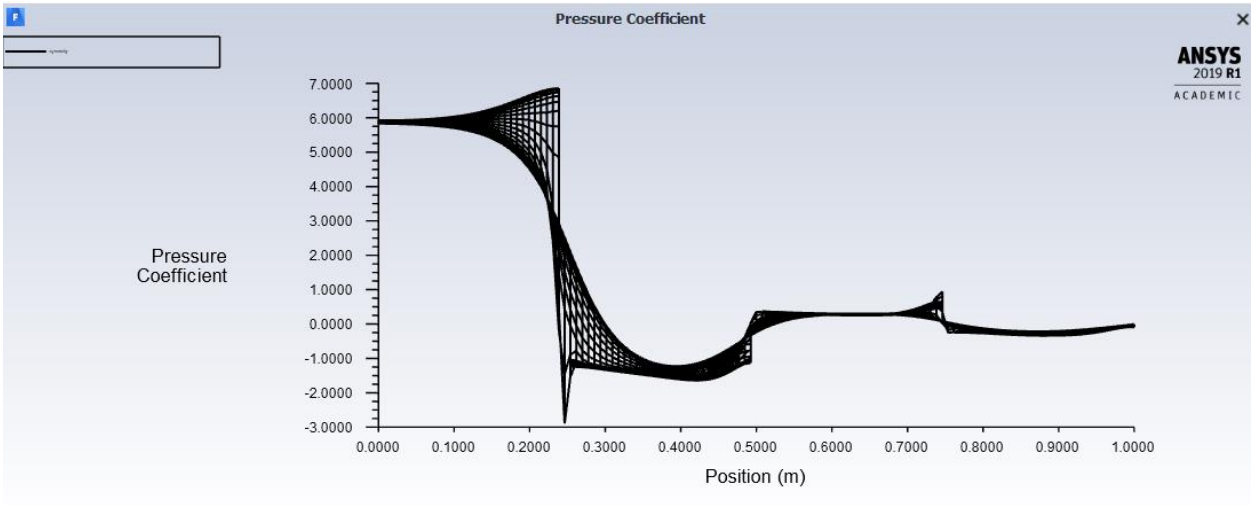

(d) cp of three in line baffle plates

Figure 5.23. variation of cp along the channel length

Figure(5.24), exhibit the variation of the surface nusselt number on the duct length for different baffle plates arrangement with a specified Reynolds number. As the figure shows, the largest value of Nu occurs at the three staggered baffles, hence the heat transfer enhancement is more than the two staggered and three baffles inline. This fact is clarified when these results are compared with the result of the flow in a duct without baffle plates.

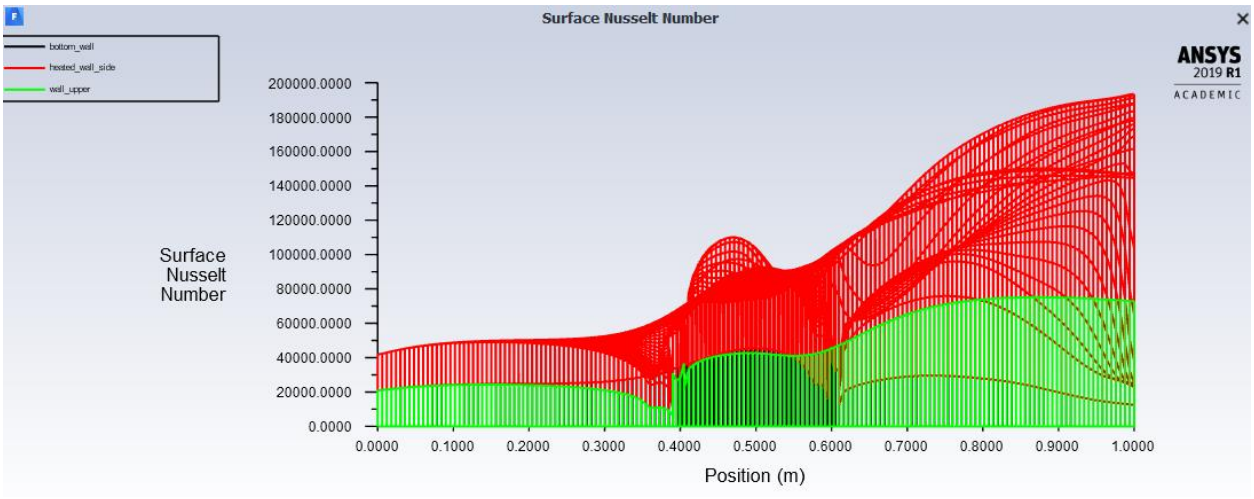

(a) Nu for two staggered baffle plates

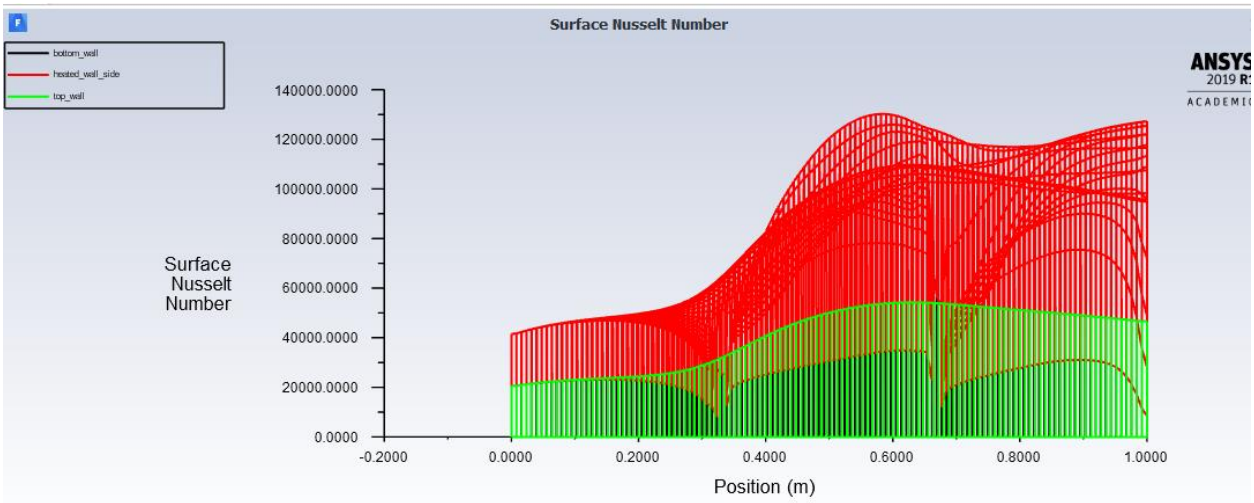

(b) Nu for two inline baffle plates

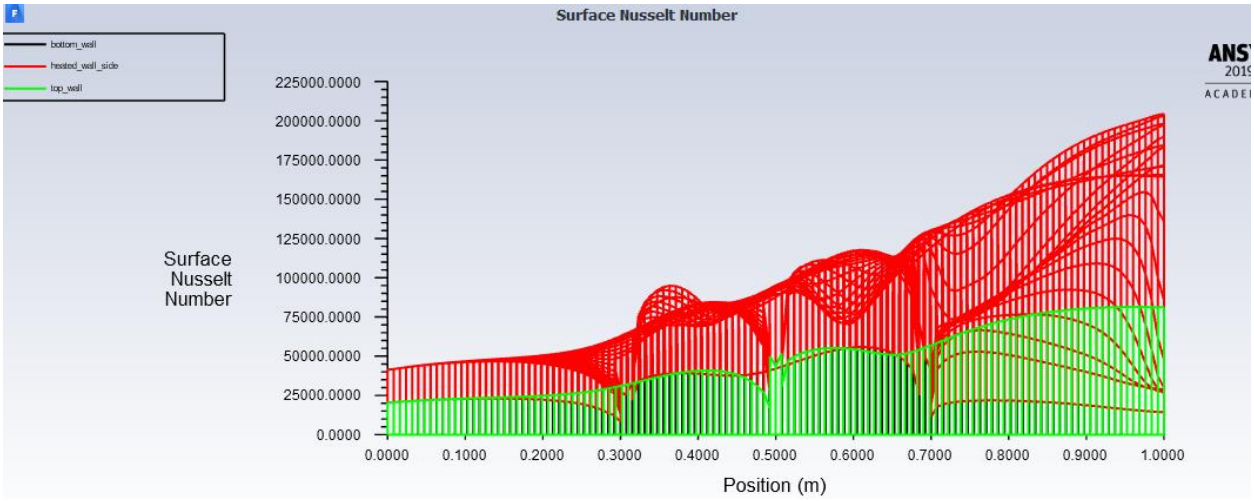

(c) Nu for three staggered baffle plates

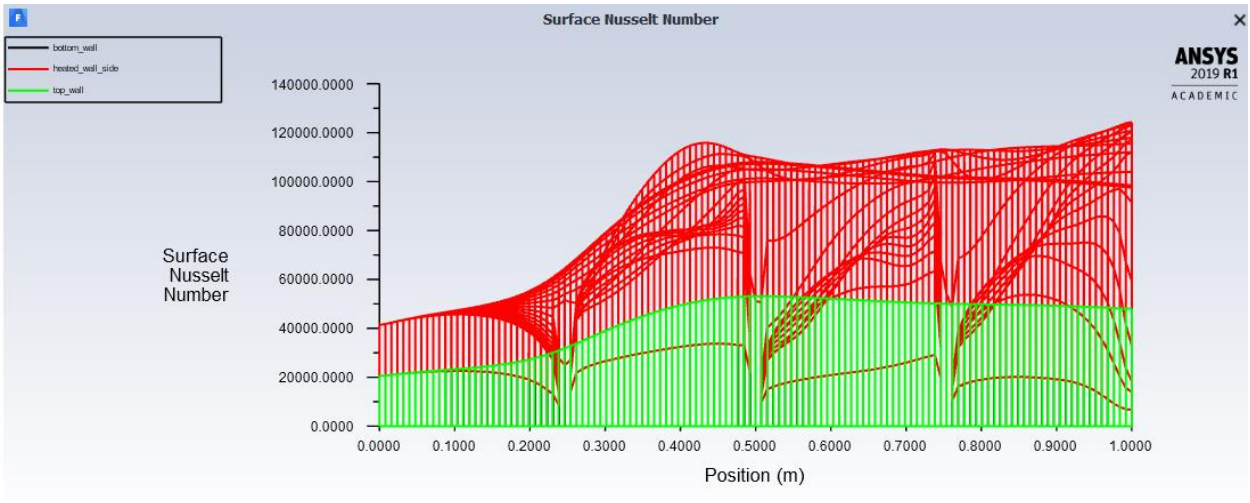

(d) Nu for three inline baffle plates

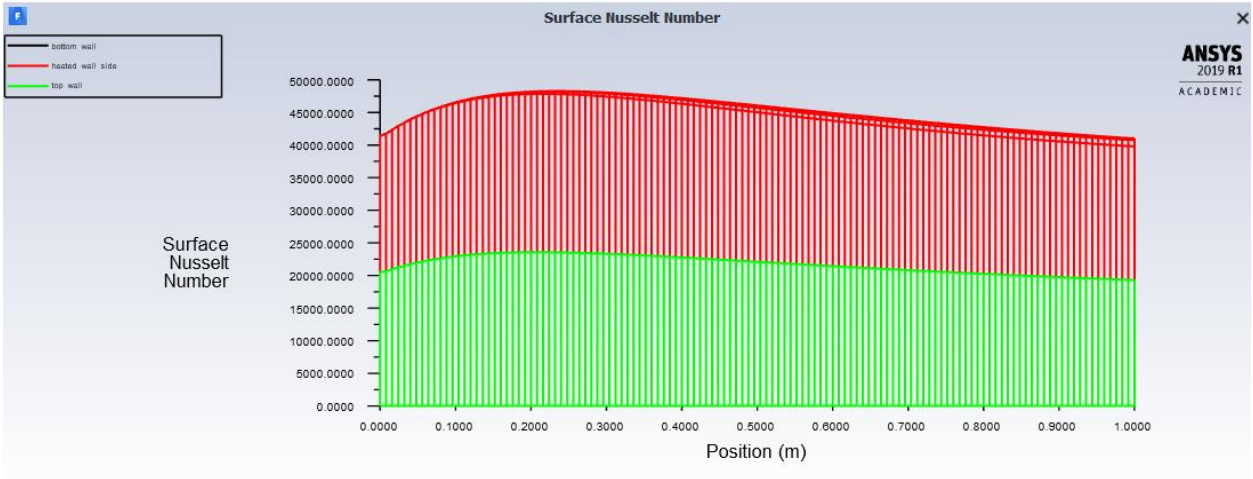

(e) Nu for duct without baffle

Figure 5.24. variation of surface nusselt along the channel length at Re=1.23*10^6

The Nu value of the flow with baffle plates is higher than that with no baffles. This enhances heat transfer. The enhancement of heat transfer is more pronounced than the momentum. The effect of Re on the local Nu values is seen in figure (5.26). The results show that the local Nu is increased with the increase of Re, because when the Re increases, the turbulence increases and recirculation region becomes stronger and consequently the heat dissipation increases.

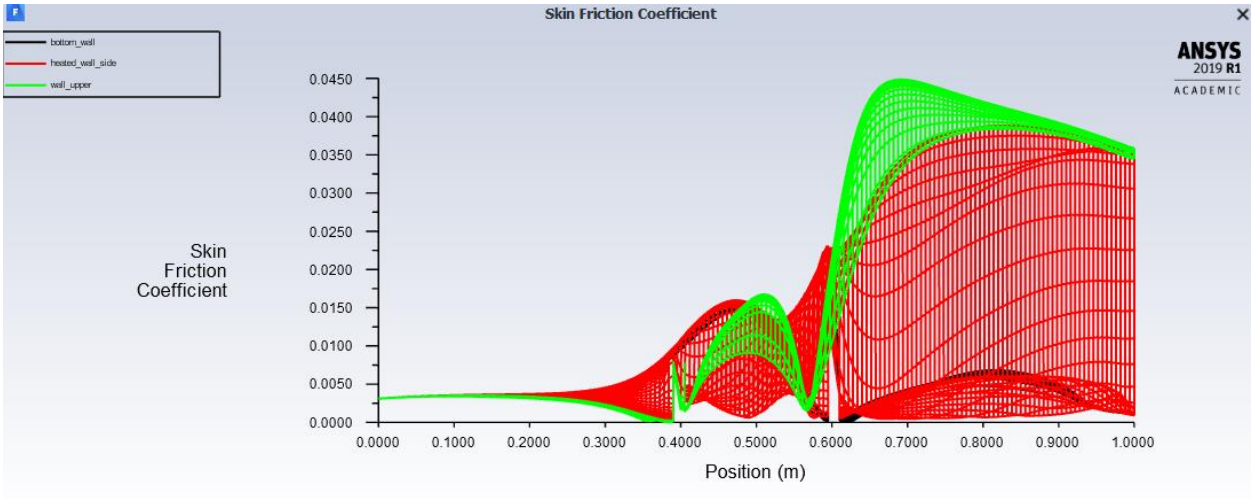

(a) the skin friction coefficient for two staggered baffle plates

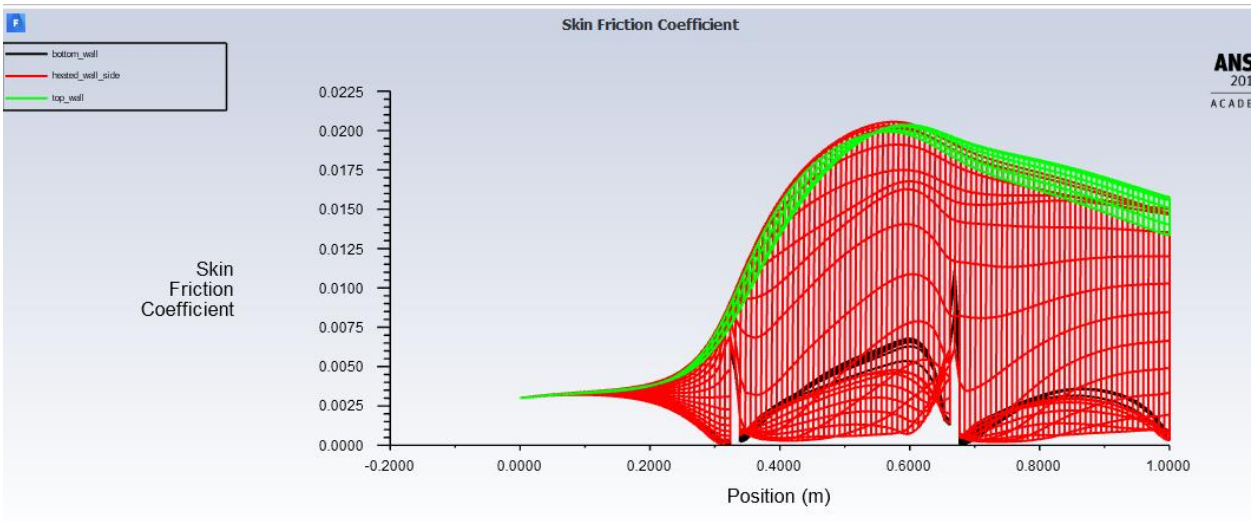

(b) skin friction coefficient for two inline baffle plates

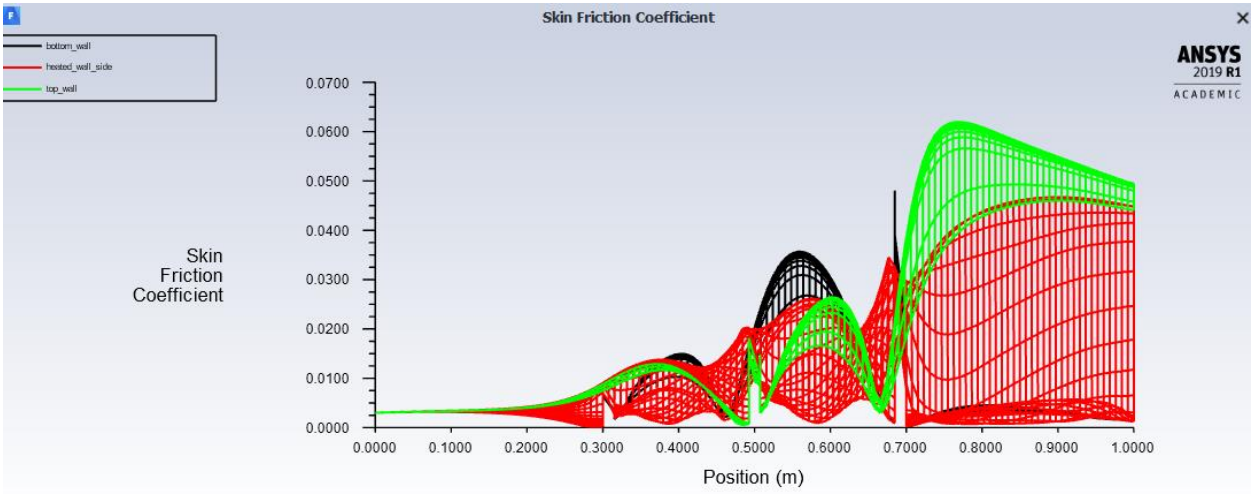

(c) the skin friction coefficient for three staggered baffle plates

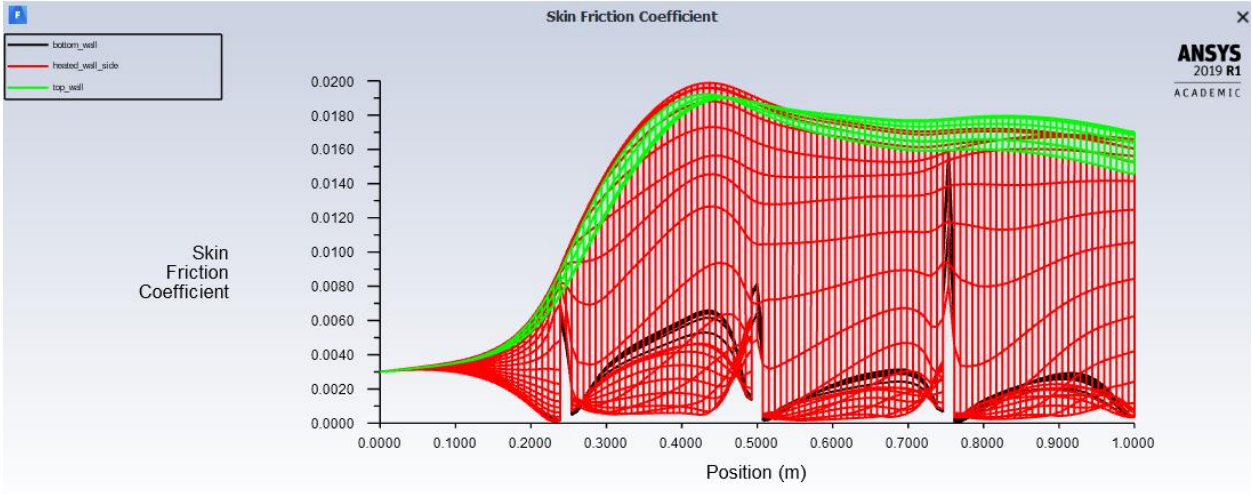

(d) skin friction coefficient for three inline baffle plates

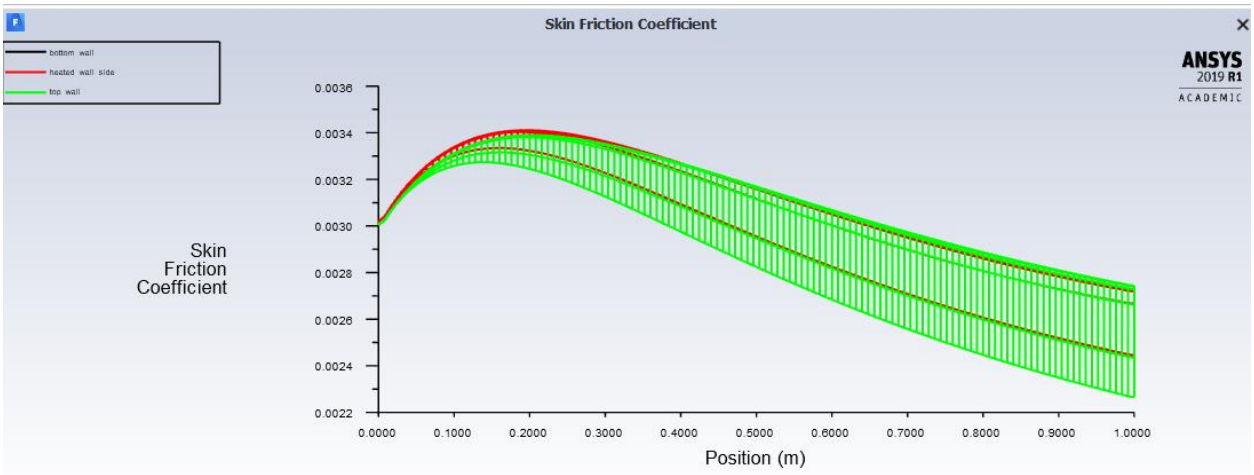

E, skin friction coefficient for duct without baffles

Figure 5.25. variation of skin friction coefficient along the channel length at Re= 1.23*10^6

Figure (5.25), exhibit the variation of skin friction coefficient on the duct length for different baffle plates arrangement with a specified Reynolds number. As the figure shows, the largest value of skin friction coefficient at the three staggered baffles, hence the drag force is more than the two staggered and three baffles inline. This fact is clarified when these results are compared with the result of the flow in a duct without baffle plates. The Figure also demonstrates that in duct without baffle the skin friction coefficient decreases in the downstream, but with the baffle its increases in the downstream. So more power is required for flow through the duct with baffles compared to duct without baffle.

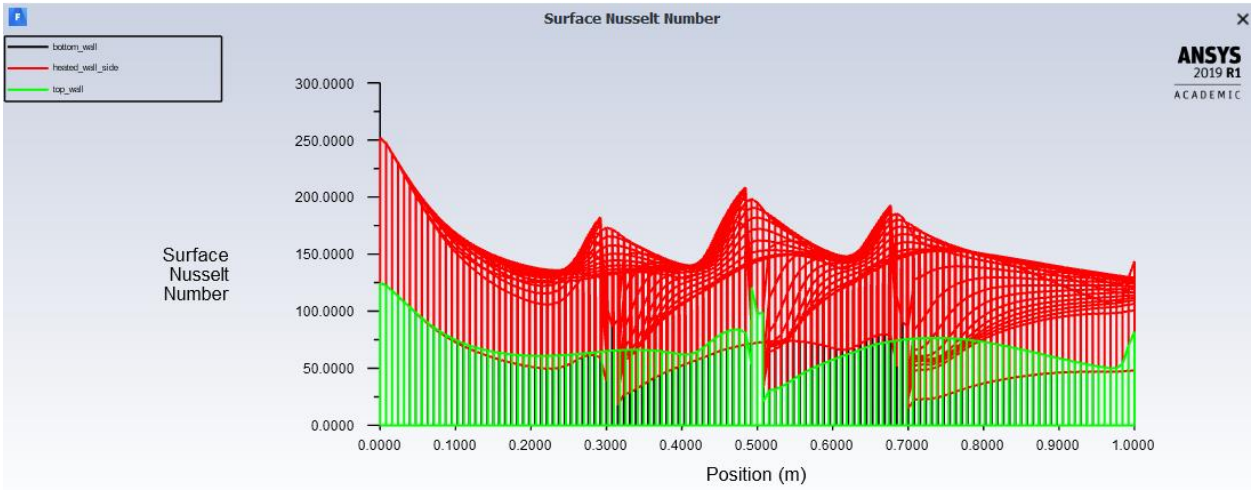

(a) Nu for three staggered baffles at Re= 123

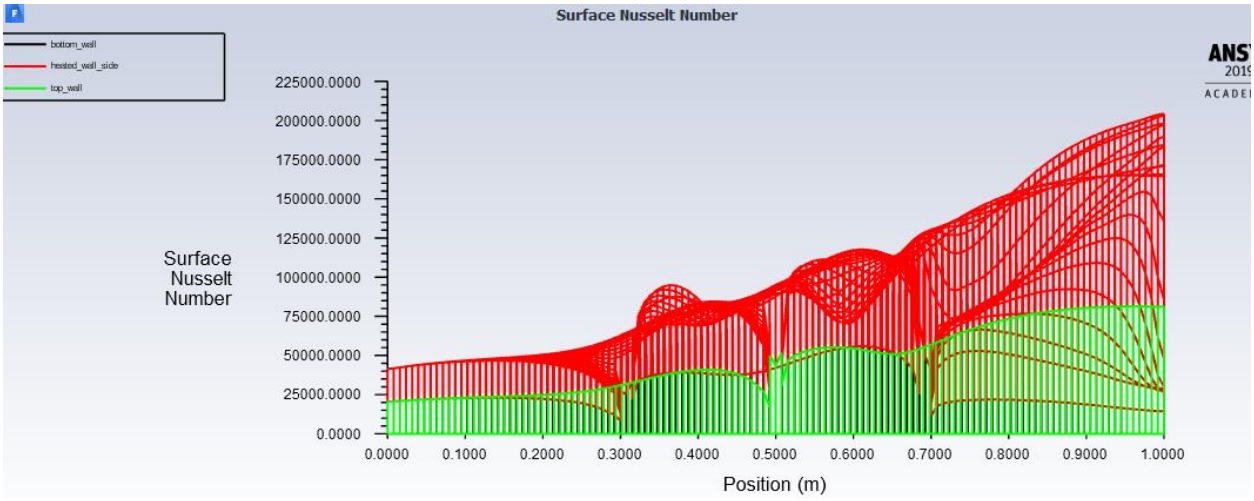

(b) Nu for three staggered baffles at Re= 1.23*10^6

Figure 5.26. variation of Nu with Reynolds number

The skin friction coefficient value of the flow with baffle plates are higher than that with no baffles. This enhances drag force and hence more power is required for flow. The effect of Re on the skin friction coefficient is seen in figure(5.27), the result shows that the skin friction coefficient is decreased with the increase of Re.

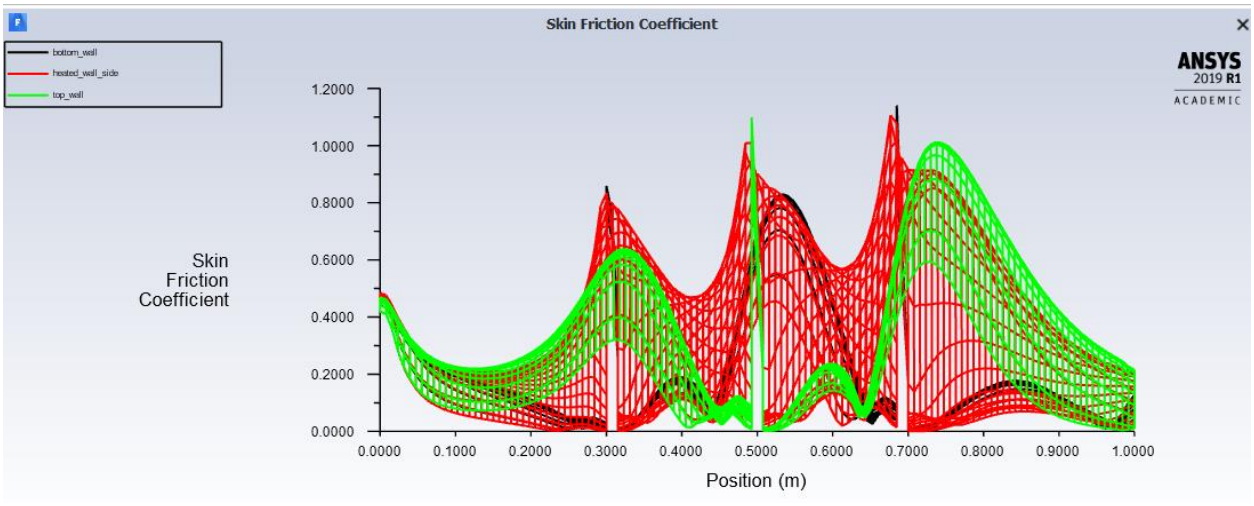

(a) Skin friction coefficient for three staggered baffles at Re= 123

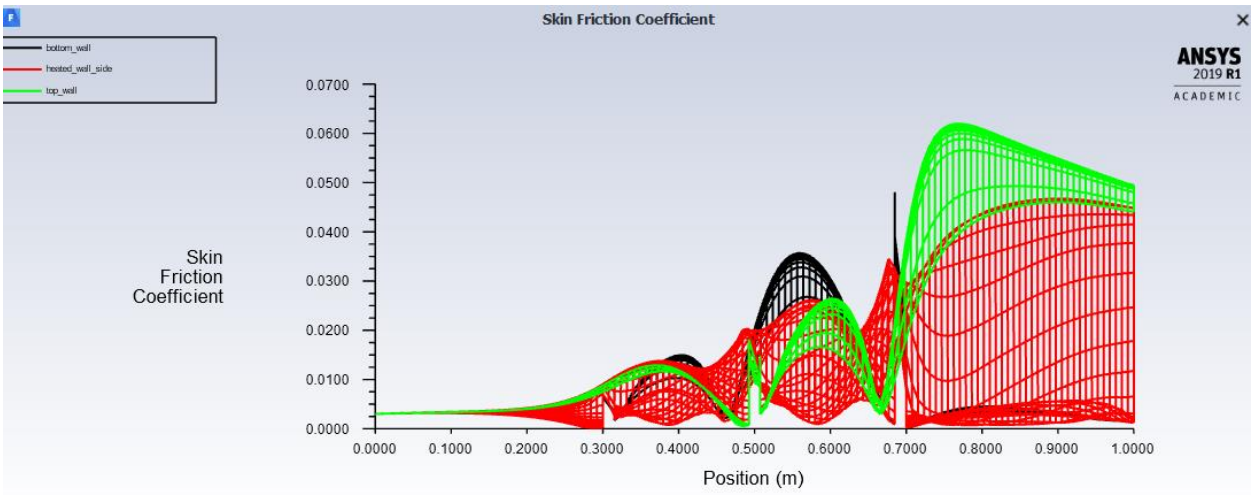

(b) Skin friction coefficient for three staggered baffles at Re= 1.23*10^6

Figure 5.27. variation of skin friction coefficient with Reynolds number

CHAPTER 6

CONCLUSION AND SCOPE OF FUTURE WORK

CHAPTER 6 CONCLUSION AND SCOPE OF FUTURE WORK

CONCLUSIONS:-

In this study the k-∈ turbulence model has been adopted to predict the details of the turbulent flow and heat transfer through a duct with backward facing step and with baffle plates. From the presented results, the following conclusions can be obtained.

It can be concluded from the comparison with the findings of present and published work that the ER affects the size of the recirculation region and the length of the reattachment point. The smaller ER leads to the smaller reattachment lengths. Also, the increase in Reynolds number increases the reattachment length and local Nusselt number. At very large Reynolds number reattachment length remains constant. with an increase in ER turbulent kinetic energy in the region downstream of flow just after step height increase. with an increase in ER results in a roughly smooth gradual change in static gauge pressure. with an increase in ER turbulent kinetic energy in the region downstream of flow just after step height increase. And with an increase in ER skin friction coefficient on the bottom wall decreases after step height in downstream of the flow.

The spacing between the baffles significantly affected the separation of the boundary layer and the recirculation zone behind the baffle. The increase Reynolds number increases the recirculation zone length and local Nusselt number, consequently enhances heat transfer. The boundary layer separation, recirculation zone and the value of Nu are influenced by baffles height and thickness. The high value of Nu is found in three staggered baffle arrangement. The standard k-ϵ model can successfully predict the characteristics of the flow and heat transfer for this type of problems.

SCOPE OF FUTURE WORK:-

In this section, we presented the scope of future work. This problem can be simulated by other turbulence models like Realizable and RNG k-epsilon model, k-omega model, SST model, Direct numerical simulation and large eddy simulation e.t.c. also one can compare all these models results. one can also use a fan and find the enhancement in momentum and heat transfer.

REFERENCES

[1] Robert M. Inman, 1967 'Heat-transfer analysis for liquid-metal flow in rectangular channels with heat sources in the fluid' National aeronautics and space administration, FEBRUARY 1967.

[2] B. E. Launder and W. M. Ying, 1972, 'Secondary flows in ducts of square cross-section' *J .Fluid Mech.* (1972), *vol.* 54, *part* 2, *pp.* 289-295.

[3] A. Melling AND J. H. Whitelaw, 1976, 'Turbulent flow in a rectangular duct, *J. Fluid Mech.* (1976), *vol.* 78, *part* 2, *pp.* 289-315

[4] A. O. Demuren AND W. RODI, 1983, 'Calculation of turbulence-driven secondary motion in non-circular ducts', *Fluid Mech.* (1984), *vol.* 140, *pp.* 189-222.

[5] J. P. Van Doormaal and G. D. Raithby**,**1984,'Enhancements of the SIMPLE method for predicting incompressible fluid flows', *Numerical Heat Transfer*,1984 vol. 7, pp. 147-163.

[6] M. Molki and A. R. Mostoufizadeh, 1988, 'Turbulent heat transfers in rectangular ducts with repeated-baffle blockages', *Int. J. Heat Mass Transfer.* 1989, Vol. 32, No. 8, pp. 1491-1499.

[7] Ravi K. Madabhushi and S. P. Vanka, 1991 'large eddy simulation on turbulence-driven secondary flow in square duct', *Department of Mechanical and Industrial Engineering, University of Illinois at Urbana-Champaign, Urbana, Illinois*, 6180I.

[8] Z.Yang and T. H. Shiht,1993,'New Time Scale Based $\kappa-\varepsilon$ Model for Near-Wall Turbulence', *AIAA JOURNAL*, 1993, Vol. 31, No. 7, July.

[9] Asmund Husert and Sedat Biringen, 1993, 'Direct numerical simulation of turbulent flow in a square duct', *J. Fluid Mech.* (1993), *vol.* 257, *pp.* 65-95 .

[10] David C. Wilcox, 1993, 'Comparison of Two-Equation Turbulence Models for Boundary Layers with Pressure Gradient' *AIAA JOURNAL,* August 1993, Vol. 31, No. 8.

[11] Fan Sixin and Lakshminarayanat Budugur, 1993 'Low-Reynolds-Number *k-*ϵ Model for Unsteady Turbulent Boundary-Layer Flows', *AIAA JOURNAL*, October 1993,Vol. 31, No.10.

[12] Menter F. R., 1994, 'Two-Equation Eddy-Viscosity Turbulence Models for Engineering Applications' *AIAA JOURNAL,* August 1994Vol. 32, No. 8.

[13] Tsan-Hsing Shih, William W. Liou, Aamir Shabbir, Zhigang Yang and Jiang Zhu, 1994, 'A new *k-*ϵ eddy viscosity model for high reynolds number turbulent flows', *Computers Fluids*, 1995, Vol. 24, No. 3, pp. 227-238.

[14] Andrew T. Thies and Christopher K. W. Tam, 1996, 'Computation of Turbulent Axisymmetric and Non axisymmetric Jet Flows Using the k-ϵ Model' *AIAA JOURNAL*, Vol. February 1996, 34, No. 2.

[15] Srinath V. Ekkad and JE-Chinhan, 1996, 'Detailed heat transfer distributions in two-pass square channels with rib turbulators', *Int. J. Heat Mass Transfer*, 1997, Vol. 40, No. 11, pp. 2527-2537.

[16] Akira Murataa, Sadanari Mochizuki, Tatsuji Takahashi, 1999, 'Local heat transfer measurements of an orthogonally rotating square duct with angled rib turbulators', *Columbia International Publishing American Journal of Heat and Mass Transfer,* 1999, 42, 3047-3056

[17] Akira Murata and Sadanari Mochizuki, 2000, 'Comparison between laminar and turbulent heat transfer in a stationary square duct with transverse or angled- rib turbulators' *International Journal of Heat and Mass Transfer,* 2001, 44, 1127-1141.

[18] K. A. M. Moinuddin, S,Hafez, P. N. Joubert and M. S. Chong, 2001'Experimental study of turbulent flow along a streamwise edge (chine)' *14th Australasian Fluid Mechanics Conference Adelaide University*, Adelaide,Australia, 10-14, December 2001.

[19] HongyiXu and Andrew Pollard, 2001,'Large eddy simulation of turbulent flow in a square annular duct'*American Institute of Physics,* VOLUME 13, NUMBER 2001.

[20] P.R. Chandra, C.R. Alexander, J.C. Han, 2003, 'Heat transfer and friction behaviors in rectangular channels with varying number of ribbed walls', *International Journal of Heat and Mass Transfer*, 2003, 46, 481–495.

[21] S.W. Chang, W.D. Morris 2003,'Heat transfer in a radially rotating square duct fitted with in-line transverse ribs', *International Journal of Thermal Sciences*, 2003, 42, 267–282.

[22] Ko, K-H .and Anand, N.K,. 2003, 'Use of porous baffles to enhance heat transfer in a rectangular channel', *International Journal of Heat and Mass Transfer*, 2003, 46 4191–4199.

[23] CUI Xiang-Zhe and KIM Kwang-Yong, 2003, 'Three-Dimensional Analysis of Turbulent Heat Transfer and Flow through Mixing Vane in A Subchannel of Nuclear Reactor', *Journal of NUCLEAR SCIENCE and TECHNOLOGY*, October-2003, Vol. 40, No. 10, p. 719–724

[24] C.M. Winkler, Sarma L. Rani and S.P. Vanka,2004,'Preferential concentration of particles in a fully developed turbulent square duct flow', *International Journal of Multiphase Flow,* 30 (2004) 27–50.

[25] Karwa Rajendra, Maheshwari B.K., Karwa Nitin, 2005, 'Experimental study of heat transfer enhancement in an asymmetrically heated rectangular duct with perforated baffles', *International Communications in Heat and Mass Transfer,* 2005, 32, 275–284.

[26] Lei Wang and BengtSunden, 2005, 'Experimental investigation of local heat transfer in a square duct with continuous and truncated ribs', *Experimental Heat Transfer*, 2005, 18:179–197.

[27] Hussien Al-Bakhit and Ahmad Fakheri,2005, 'Numerical simulation of heat transfer in simultaneously developing flows in parallel rectangular ducts' *Applied Thermal Engineering*, 26 (2006) 596–603.

[28] Chu-Wei Lin, 2006, 'Experimental study of thermal behaviors in a rectangular channel with baffle of pores', *International Communications in Heat and Mass Transfer*, 2006, 33, 985–992.

[29] Gaurav Sharma and Denis J. Phares, 2006, 'Turbulent transport of particles in a straight square duct' *International Journal of Multiphase Flow*, 32 (2006) 823–837.

[30] Markus Uhlmann, Alfredo Pinelli, Genta Kawaharaand Atsushi Sekimoto,2007'Marginally turbulent flow in a square duct' *J. Fluid Mech.* (2007), vol. 588, pp. 153–162.

[31] Abraham J.P., Sparrow E.M. and Tong J.C.K., 2008, 'breakdown of laminar pipe flow into transitional intermittency and subsequent attainment of fully developed intermittent or turbulent flow', *Numerical Heat Transfer*, Part B, 54: 103–115, 2008.

[32] Gustavo Adolfo Ronceros Rivas, EzioCastejon Garcia and Marcelo Assato, 2008, 'Turbulent flow simulations in a square-duct using nonlinear and reynolds stress models' *Instituto Tecnológico de Aeronáutica, São José dos Campos*, SP, Brasil, Outubro, 20 a 23, 2008.

[33] Honore Gnanga, Hassan Naji and GilmarMompean,2009, 'Computation of a three-dimensional turbulent flow in a square duct using a cubic eddy-viscosity model', Science Direct, C. R. Mecanique 337 (2009) 15–23.

[34] Zhu Zuo-jin, 2009, 'Direct numerical simulation of turbulent flow in a straight square duct at Reynolds number 600' *Science Direct, Journal of hydrodynamics*, 2009, 21(5):600-607.

[35] Michael Fairweather and Jun Yao, 2009, 'Mechanisms of Particle Dispersion in a Turbulent, Square Duct Flow', *American Institute of Chemical Engineers AIChE* J, 55:1667–1679, 2009.

[36] Zuojin Zhu, Hongxing Yang, Tingyao Chen, 2010, 'Numerical study of turbulent heat and fluid flow in a straight square duct at higher Reynolds numbers', *International Journal of Heat and Mass Transfer*, 2010, 53 356–364.

[37] Pongjet Promvonge, Wayo Changcharoen, Sutapat Kwankaomeng, Chinaruk Thianpong, 2011, 'Numerical heat transfer study of turbulent square-duct flow through inline V-shaped discrete ribs', *International Communications in Heat and Mass Transfer*, 2011,38, 1392–1399.

[38] Ahmed M. Bagabir, Jabril A. Khamaj, Ahmed S. Hassan, 2013,'Numerical Study of Turbulent Periodic Flow and Heat Transfer in a Square Channel with Different Ribs', *Journal of Applied Mathematics and Physics*, 2013, 1, 65-73

[39] Hamidou Benzenine, Rachid Saim , Said Abboudi, and Omar Imine , 2013, 'Numerical analysis of a turbulent flow in a channel provided with transversal waved baffles', *THERMAL SCIENCE*: Year 2013, Vol. 17, No. 3, pp. 801-812.

[40] Kamel Benoumessad, Ilhem Kriba, Ali Fourar and Abdelbaki Djebaili, 2014, '3D simulation of velocity profile of turbulent flow in open channel with complex geometry'. *Eight International Conference on Material Sciences (CSM8-IMS5)* Physics Procedia 55 (2014) 119 – 128.

[41] Hao Zhang, F. Xavier Trias, AndreyGorobets, Yuanqiang Tan and AssensiOliva, 2015, 'Direct numerical simulation of a fully developed turbulent square duct flow up to $Re_\tau = 1200$' *International Journal of Heat and Fluid Flow*, 54 (2015) 258–267.

[42] Benzenine Hamidou , Saim Rachid, Abboudi Said, Imine Omar,2016, ' Convective Thermal Analysis of a Turbulent Flow in a Pipe with Two and Three Corrugated Baffles Arranged in Overlap', *Columbia International Publishing American Journal of Heat and Mass Transfer,* 2016, Vol. 3 No. 6 pp. 382-395: 27, 605-563.

[43] Branislav D. Stankovic, Sr|an V. Belosevic, Nenad D. Crnomarkovic, An-drijana D. Stojanovic, Ivan D. Tomanovic, and Aleksandar R. Milicevic,2016, 'Specific Aspects of Turbulent Flow in Rectangular Ducts' *Thermal science*, Year 2016, Vol. 20, Suppl. 6, pp. S1-S16.

[44] A. Vidal, R. Vinuesa, P. SchlatterandH.M. Nagib , 2017, 'Influence of corner geometry on the secondary flow in turbulent square ducts', *International Journal of Heat and Fluid Flow,* 67 (2017) 69–78.

[45] Sujit K. Bose, 2017, 'An estimation of turbulent secondary flow resistance in rectangular ducts from a flow model',*International Journal of Fluid Mechanics Research*, 44(5):375–385 (2017).

[46] Benzenine Hamidou, Saim Rachid, Abboudi Said, Imine Omar,2018,'Comparative study of the thermo-convective behavior of a turbulent flow in a rectangular duct in the presence of three planer baffles and/or corrugated(wave)', *Journal of Engineering Science and Technology,* Vol. 13, No. 1 (2018) 035 – 047.

[47] Patankar, S. V., 1980, "Numerical Heat Transfer and Fluid Flow," ***Taylor and Francis Publisher***.